BACTERIAL UPTAKE MECHANISM OF PEPTIDES INVESTIGATED BY STEERED MOLECULAR DYNAMICS SIMULATIONS

by

İhsan Ömür Akdağ

B.S., Chemical Engineering, Boğaziçi University, 2009

Submitted to the Institute for Graduate Studies in
Science and Engineering in partial fulfillment of
the requirements for the degree of
Master of Science

Graduate Program in Computational Science and Engineering

Boğaziçi University

2011

ACKNOWLEDGEMENTS

It was an outstanding experience to work on this project. The most and initial thanks should be given to my thesis supervisor, Assist. Prof. Elif Özkırımlı Ölmez, for her supports and helps during the entire project.

Then I would like to thank my thesis committee members Prof. Pemra Doruker and Assoc. Prof. Berna Sarıyar Akbulut for their participations in the project and for their evaluations.

I would like to thank Pınar Kanlıkılıçer and Ahmet Özcan for their help in the starting of the project. I would also thank my lab-partners, Burcu Özkaya, Celal Ceylan, Ayşe Ezgi Akkaya, Aslıgül Doğan, Seval Aladağ, Simay Yalaz, Deniz Menekşedağ and Begüm Alaybeyoğlu for their friendship, kind motivation and encouragements.

My last but not least thanks should go to my mother Mehpare Atınç, my father Kamil Ömer Akdağ and my brother Gülhan Can Akdağ for their ever-lasting encouragement and support.

TUBITAK Project No. 108M644, Project No. 109M229 and BAP Project No. 09HA504P are gratefully acknowledged for the funding.

ABSTRACT

BACTERIAL UPTAKE MECHANISM OF PEPTIDES INVESTIGATED BY STEERED MOLECULAR DYNAMICS SIMULATIONS

β-lactam antibiotics provide defense against bacterial infections, but the misuse of antibiotics has led to the emergence of bacteria with immunity. One of the major mechanisms of this immunity is bacterial production of the β-lactamase enzyme which inhibits antibiotics. In order to overcome the inhibition and regain defense against bacteria, development of peptide inhibitors based on β-lactamase inhibitor protein (BLIP) have gained increased attention. The bacterial uptake potential of the designed BLIP based peptide was investigated using steered molecular dynamics simulations. Two peptides were used in the simulations. The BLIP based peptide has the sequence HAAGDYYA. The second peptide is the BLIP based peptide (LLIILHAAGDYYA) with the residues LLIIL added to the N terminus to enhance bacterial uptake. The SMD simulations were repeated with different spring constants, pulling velocities and reaction coordinates to optimize the simulation conditions. It was found that no obvious distinction could be made for different spring constants for the first set, while the second set favored smaller spring constant. The first peptide passed the membrane more easily when it was pulled faster, but the second peptide had shown almost no difference. When both peptides were pulled from their N terminus, the force applied to and the work done on the peptides reached their maximum values. A third set of simulations were performed on the cell penetrating peptide pVEC (LLIILRRRIRKQAHAHSK) and its mutants to analyze their cellular uptake mechanism on a residue basis. Previously the independent mutations on the 1^{st}, 2^{nd} and 14^{th} residues, and scrambling and reversing the sequence of the pVEC peptide found to make the cellular uptake harder. However, the simulations showed that scrambling the sequence , mutation of the 14^{th}, the 1^{st} and the 2^{nd} residues enhanced the uptake in descending order.

ÖZET

PEPTİTLERİN BAKTERİ HÜCRESİNE ALINIM MEKANİZMASININ YÖNLENDİRİLMİŞ MOLEKÜLER DİNAMİK SİMÜLASYONLAR İLE İNCELENMESİ

β-laktam antibiyotikleri, bakteriyel enfeksiyonlara karşı tedavi amaçlı kullanıldılar ancak bu antibiyotiklerin gereksiz kullanımı bakterilerin bağışıklılık geliştirmesine yol açtı. Bu bağışıklılığın en temel yollarından biri antibiyotikleri inhibe eden β-laktamaz enzimini sentezlemek oldu. Bu inhibisyonu yenmek ve bakterilere karşı tekrar savunma kazanmak için β-laktamaz enzimini inhibe eden protein (BLIP) temelli peptit geliştirmek dikkat çekti. Tasarlanan BLIP temelli peptidin bakteriye alım potansiyeli yönlendirilmiş moleküler dinamik (SMD) simülasyonlar ile incelenmiştir. Simülasyonlarda iki peptit kullanıldı. BLIP temelli peptidin amino asit dizisi HAAGDYYA'dır. İkinci peptit ise bakteriye alınımı arttırmak üzere peptidin N ucuna LLIIL kalıntıları eklenmiş BLIP temelli peptittir (LLIILHAAGDYYA). SMD simülasyonları farklı yay sabitleri, çekme hızları ve çekme yerleri ile simülasyon koşulları optimize etmek üzere tekrarlandı. İlk peptit ile yapılan simülasyonlarda farklı yay sabitleri arasında belirli bir ayrım yapılamadı. Buna karşın ikinci peptidin küçük yay sabiti ile çekilmesi daha avantajlı bulundu. İlk peptit hızlı çekildiğinde zardan daha kolay geçebildi. İkinci peptidin ise hızlı ya da yavaş çekilmesi herhangi bir farklılık göstermedi. Her iki peptit de N uçlarından çekildiğinde peptide yapılan iş ve uygulanan kuvvet maksimum oldu. pVEC isimli (LLIILRRRIRKQAHAHSK) bir hücre-delen peptidin ve onun mutantlarının, bunların hücresel alınım mekanizmasını kalıntı tabanlı olarak incelemek için simülasyonları koşturuldu. pVEC peptidinin birinci, ikinci ve on dördüncü kalıntıların mutasyonlarının, kalıntı dizisini karıştırmanın ve kalıntı dizisini tersine çevirmenin hücresel alınımı zorlaştırdığı önceden belirtildi. Ancak simülasyonlar, kalıntı dizisini karıştırmanın, on dördüncü, birinci ve ikinci kalıntıların mutasyonunun, azalan sırayla, alınımı arttırdığını gösterdi.

TABLE OF CONTENTS

LIST OF FIGURES

LIST OF TABLES

LIST OF SYMBOLS

a_i	Acceleration of the particle I
$b - b_o$	Distance from equilibrium that the atom has moved
$\vec{F}$	Force applied
F_i	Force exerted on the particle I
R_{min}	Lennard-Jones radius
q	Partial atomic charge
K_b	Bond force constant
K_{UB}	Force constant
K_θ	Angle force constant
K_φ	Impropers force constant
$K\phi$	Dihedral force constant
m_i	Mass of the particle i and
n	Multiplicity
$\vec{n}$	Direction of pulling
$\vec{r}$	Actual position of the SMD atom
$\vec{r}_0$	Initial position of the SMD atom
r_i	Atomic coordinates of the particle i
$r_{1,3} - r_{1,3,o}$	Distance between the 1,3 atoms in the harmonic potential
t	Time
U	Potential energy

v	Pulling velocity
V	Potential energy
α	Alpha
Å	Angstrom
ε	Lennard-Jones well-depth
$\varphi - \varphi_o$	Out of plane angle
ϕ	Dihedral angle
δ	Phase shift
$\theta - \theta_o$	Angle from equilibrium between 3 bonded atoms

LIST OF ACRONYMS/ABBREVIATIONS

μM	Micromolar
1PB	1,4-diphenyl-2-butene
A	Alanine
Ala	Alanine
AMP	Antimicrobial peptide
Arg	Argenine
Arg_9	Polyargenine
Asp	Aspartic acid
Aβ	Amyloid-β
BLIP	Beta-Lactamase Inhibitory Protein
C	Carbon
C17	7-[(3-chlorobenzyl)oxy]-2-oxo-2H-chromene-4-carbaldehyde
C18	7-[(3-chlorobenzyl)oxy]-4-[(methylamino)methyl]-2H-chromen-2-one
CbnB2	Carnobacteriocin B2
CD	Circular dichroism
Chol	Cholesterol
CL	Cardiolipin
com	Center of mass
CPP	Cell-penetrating peptide

D	Aspartic acid
DMPC	1,2-Dimyristoyl-*sn*-Glycero-3-Phosphocholine
DMPG	1,2-Dimyristoyl-*sn*-Glycero-3-[Phospho-*rac*-(1-glycerol)]
DOPC	1,2-dioleoyl-sn-glycro-3-phosphocholine
DOPG	Dioleoylphosphatidylglycerol
DOPS	Dioleoylphosphatidylserine
DPPC	1,2-dipalmitoyl-sn-glycro-3-phosphocholine
DPPC	Dipalmitoylphosphatidylcholine
DPPE	Dipalmitoylphosphatidylethanolamine
DPPG	Dipalmitoyl phosphatidyl glycerol
D-pVEC	D-enantiomer of pVEC
DSC	Differential scanning calorimetry
DSPC	1,2-Distearoyl-*sn*-Glycero-3-Phosphocholine
DSPG	1,2-Distearoyl-*sn*-Glycero-3-[Phospho-*rac*-(1-glycerol)]
EDTA	Ethylenediaminetetraacetic acid
ESBL	Extended-spectrum beta-lactamase
FOH	Farnesol
fs	Femtosecond
G	Glycine
H	Histidine
H	Hydrogen
His	Histidine
I	Isoleucine

IL	Indolicidin
Ile	Isoleucine
ISN	1H-indole-2,3-dione (isatin)
K	Lysine
K	Potassium
k	Spring constant
kcal	Kilocalorie
kDa	Kilodalton
L	Leucine
LJ	Lennard-Jones
Lys	Lysine
M	Molar
MAO B	monoamine oxidase B
MAP	Multiple antigenic peptide
MD	Molecular dynamics
mg	Milligram
MLV	Multilamellar vesicles
N	Nitrogen
ns	Nanosecond
OAK	Oligomer of acyllysine
P	Phosphorus
PE	Phosphodylethanolamine
PG	Phosphatidyglycerol

PME	Particle mesh Ewald
pmol	Picomole
pN	Piconewton
POPC	1-palmitoyl-2-oleoyl-sn-glycero-3-phosphocholine
POPE	1-Palmitoyl-2-oleoyl-*sn*-glycero-3-phosphoethanolamine
POPG	1-Palmitoyl-2-Oleoyl-*sn*-Glycero-3-Phosphocholine
ps	Picoseconds
PTD	Protein transduction domain
pVEC	Vascular endothelial-cadherin protein
Q	Glutamine
R	Arginine
RM1	N-methyl-1(R)-aminoindan
Rt	Retention time
S	Serine
S.A.R	Structure-activity relationship
SAG	(S)-(+)-2-[4-(fluorobenzyloxybenzylamino) propionamide]
Ser	Serine
SM	Sphingomyelin
SMD	Steered molecular dynamics
Tat	Trans-activating transcriptional activato
TM	transmembrane
TOCL	Tetraoleoylcardiolipin
vdW	van der Waals

vel	Velocity
VMD	Visual molecular dynamics
Y	Tyrosine
ΔPMF	Potential of mean force

1 INTRODUCTION

1.1 β-Lactamase Inhibitory Protein

1.1.1 β-Lactam Antibiotics

β-lactam antibiotics were first introduced in the medical science in the years of World War II. They are most widely antibiotics in the treatment of bacterial infections since they have high effectiveness, low cost, ease of delivery and minimal side effects. They target the transpeptidase enzymes of bacteria. These enzymes are responsible for cell wall synthesis in bacteria. The purpose of this bacterial cell wall which is called as cross-linked peptidoglycan layer is to preserve cell shape and rigidity. β-lactam antibiotics inhibit the bacterial transpeptidases by forming a lethal covalent pennicilloyl-enzyme complex. Therefore, a weakly cross-linked peptidoglycan layer is formed making the growing bacteria vulnerable to cell lysis and death [1]. The bacterial cell becomes permeable to water, so it takes up fluid and lyses [2].

The first β-lactam antibiotic was Penicillin G (benzylpenicillin) (Figure 1.1). The distinctive structural feature of the β-lactam antibiotic is its highly reactive four-member β-lactam ring [2]. In Figure 1.1, the β-lactam ring is shown by dotted circle.

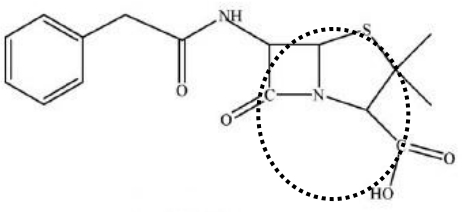

Figure 1.1. The chemical structure of the Penicillin G β-lactam antibiotic [2]. The β-lactam ring is encircled.

1.1.2 β-lactamases

The activity of β-lactams against bacteria is hindered by three primary mechanism of resistance: (i) the production of enzymes that degrade the antibiotic before it reaches the appropriate target site, (ii) the alteration of the antibiotic target site and (iii) the prevention of access of the antibiotic to the target by way of altered permeability or forced efflux. The most common mechanism is the first stated one. The enzymes that inhibit the β-lactam antibiotics are the β-lactamases. The β-lactamases provide important antibiotic resistance to their bacterial hosts by hydrolysis of the amide bond of the four-membered β-lactam ring [1].

β-lactamases are categorized based on similarity in amino acid sequence which is named as Ambler classes A, B, C, and D [3]. They are also classified according to the substrate-inhibitor profile named as Bush-Jacoby-Medeiros groups 1, 2, 3, and 4 [4]. TEM-1 and SHV-1 are the β-lactamases of interest of this work. These two types of β-lactamases are both in Class A according to the molecular and in Group 2 according to the functional classification (Table 1.1). They are the beta-lactamases usually found in E. coli and K. Pneumoniae [4].

Table 1.1. β-lactamase classification scheme I [2].

Ambler classification system		
class A	penicillinases	TEMs, SHVs, PC1, CTX-Ms, SME-1, KPC-1
class B	metallo-beta-lactamases (zinc)	IMP-1, VIM-1, Ccr A
class C	cephalosporinases	AmpCs, CMY-2, ACT-1
class D	oxacillinases	OXA-1

Table 1.2. β-lactamase classification scheme II [2].

Bush-Jacoby-Medeiros classification		
Group 1	cephalosporinases	AmpCs, CMY-2, ACT-1, MIR-1
	hydrolyze extended-spectrum cephalosporins; clavulanate resistant	
Group 2	all clavulanic acid susceptible	
2a	Penicillinase	PC1 from S. aureus
2b	broad-spectrum penicillinase	TEM-1, SHV-1, TEM-2
2be	ESBLs	SHV-2, TEM-10, CTX-Ms
2br	inhibitor resistant	TEMs, IRTs TEM-30, TEM-31
2c	carbenecillin hydrolyzing	PSE-1
2d	oxacillin hydrolyzing	OXA-10, OXA-1
2e	cephalosporinases inhibited by clavulanate	FEC-1
2f	carbapenemases	KPC-1, SME-1
Group 3	metallo-beta-lactamases	IMP-1, VIM-1, Ccr A
	hydrolyze imipenem, inhibited by EDTA, resistant to clavulanate	
Group 4	Miscellaneous	

1.1.3 β-Lactamase Inhibitory Protein (BLIP)

There are two principle ways to hinder the hydrolytic action of the β-lactamases: (i) finding inhibitors of β-lactamases and (ii) finding a new β-lactam antibiotic. In this work, the first option was chosen. Some of the main inhibitors used in clinic are clavulanic acid,

sulbactam, and tazobactam. Some of the new antibiotics are ceftabiprole and doripenem [2].

In this work, the first option was chosen. The cellular transport of a new β-Lactamase Inhibitory protein (BLIP) was the objective of this work. Especially TEM-1 was the enzyme that was aimed to be inhibited. Therefore, the TEM-1 β-lactamase and BLIP complex (1JTG.pdb) [5] was chosen as the complex to be studied. The 45 to 52 residues of chain B of the complex was extracted and referred as the BLIP based peptide. The cellular transport of the BLIP based peptide, modified BLIP-based peptide and a cell penetrating peptide were the aim of this work.

1.2 Cell-penetrating Peptides (CPPs)

The hydrophobicity of the cellular membranes makes them impermeable for most peptides, proteins and oligonucleotides [6]. This means that many hydrophilic compounds, including drugs and drug candidates, are unable to reach their targets since they cannot spontaneously cross lipid membranes [7]. Microinjection, electroporation, liposomes and viral vectors are insufficient strategies for drug delivery since they have low efficiency, poor specificity, poor bioavailability and extensive toxicity. Endocytosis is an alternative mechanism; however, proteins engaging in this mechanism stay enclosed within endosomes [6]. Thus delivery agents are necessary to transverse the lipid membranes and cell-penetrating peptides are these agents which either cross the membranes alone or carry other molecules while they are crossing the membranes.

Cell-penetrating peptides (CPPs) are positively charged (cationic) peptides which are relatively short with less than 30 amino acids [7, 8]. They in general are amphipathic; however, they do not have an obvious common sequence or structural motifs [7]. Sequences of some of the common CPPs are shown in Table 1.3. They penetrate cell membranes in an energy and receptor independent mechanism [8]. These penetrations occur via either electrostatic interactions or hydrogen bonding [9-12]. The spontaneous penetration of CPPs into the membranes is done by the carpet model, through transient

pores, through the formation of inverted micelles, local electroporation and direct insertion of the unfolded peptide into the membrane [7, 8].

Table 1.3. Sequences of some common CPPs [11].

Origin	**Name**	**Sequence**	**amino acid**
Protein Transduction Domain (PTD)	Tat	GRKKRRQRRRPPQ-NH_2	13
	Penetratin	RQIKIWFQNRRMKWKK-NH_2	16
	EB1	LIRLWSHLIHIWFQNRRLKWKKK-NH_2	23
	pVEC	LLIILRRRIRKQAHAHSK-NH_2	18
	Retro-pVEC	KSHAHAQKRIRRRLIILL-NH_2	18
	M918	MVTVLFRRLRIRRACGPPRVRV-NH_2	22
	M1073	MVTVLFRRLRIRRASGPPRVRV-NH_2	22
Model Peptides	MAP	KLALKLALKALKAALKLA-NH_2	18
	Arg_9	RRRRRRRRR-NH_2	9
Designed Peptides	TP10	AGYLLGKINLKALAALAKKIL-NH_2	21
	MPG	GALFLGFLGAAGSTMGAWSQPKKKRKV-Cya	27
	MPG-α	GALFLAFLAAALSLMGLWSQPKKKRKV-Cya	27
	Pep-1	KETWWETWWTEWSQPKKKRKV-Cya	21
	CADY	GLWRALWRLLRSLWRLLWKA-Cya	20

Several cell-entry mechanisms might act in parallel during the cellular uptake of CPPs [10, 13]. Moreover, the cargo carried by the CPP and the location of the cargo affect the uptake mechanism. Cellular internalization of some CPPs requires uptake by endocytosis. The escape of these CPPs such as penetratin from the encapsulated unilamellar vesicle occurs only in the presence of a pH gradient [14]. Some of the cellular transportation mechanisms of CPPs are shown in Figure 1.2.

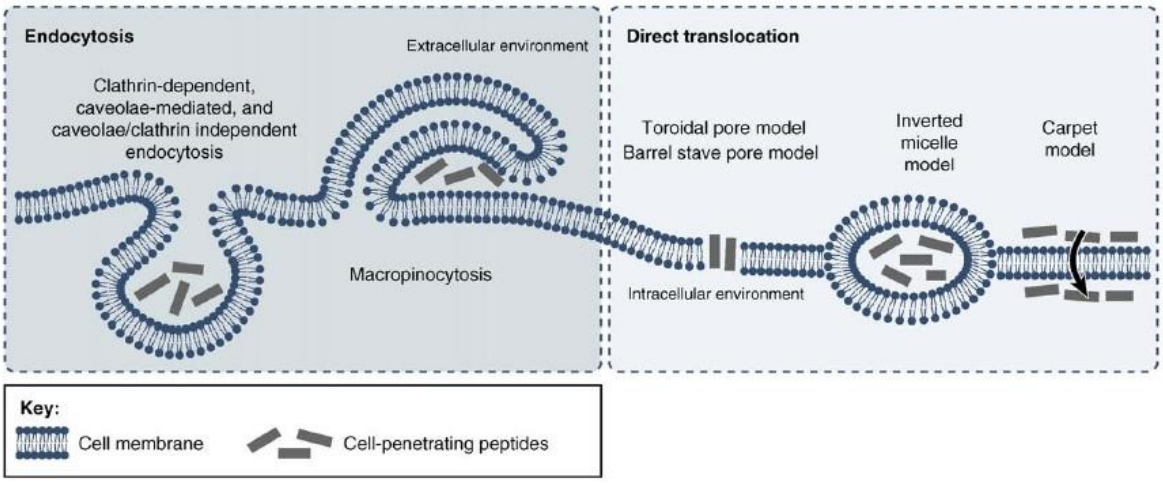

Figure 1.2. The cellular transportation mechanisms of endocytosis, macropinoctyosis, toroidal pore model, inverted micelle model and carpet model [15].

Yesylecskyy et. al studied the interaction of penetratin and Tat peptide with 1,2-dipalmitoyl-sn-glycro-3-phosphocholine (DPPC) and 1,2-dioleoyl-sn-glycro-3-phosphocholine (DOPC) bilayers. First, the spontaneous binding and aggregation of Tat peptide to the DOPC bilayer with 128 lipids was studied. Four Tat peptides were added close to one side of the membrane. A weak harmonic potential with a force constant of 30 kJ/mol/nm^2 was applied between the center of mass of each peptide and the center of the bilayer along the z axis in order to help all the peptides bound to the same monolayer. After binding, the harmonic potential was removed and the MD simulations were performed for 200 ns. Two types of systems were simulated: (i) with counterions to provide electroneutrality and (ii) without counterions. As a result, no signs of spontaneous pore formation were observed in either system. Next, binding of multiple peptides to larger bilayer patches were investigated. Eight penetratin and eight Tat peptides were added to systems having DPPC bilayer with 512 lipids separately. Again the same harmonic potential was used in order to help all the peptides bound to the same side of the membrane. Then the harmonic potential was removed and the systems were simulated for 50 ns. The peptides aggregated forming a compact cluster and the membrane started to deform. Finally, the membrane encapsulated the cluster of peptides. Finally, the pulling simulations were performed with DPPC bilayer. A single penetratin and a single Tat peptide were pulled with a rate of 10^{-4} nm ns^{-1} from the center of mass of the peptides in the direction normal to the plane of the membrane separately. Thus either peptide moved

across the bilayer forming a hydrophobic torodial-like pore. When the analyses were performed, it is stated that work is required to pull the peptide toward the center of the membrane and work is also required to pull the peptide away from the center of the membrane. The usage of PME (particle mesh Ewald) without counterions in the system can lead to distortions in the bilayer [7].

In the study of Herce and Garcia, molecular dynamics simulations of Tat protein translocating dioleoyl phosphatidyl choline (DOPC) lipid membrane were studied. The Tat peptide of this study had the sequence YGRKKRRQRRR. The molecular dynamics simulations of Tat peptides solvated in water and close to the lipid bilayer were performed on the order of 100 ns. The arginine and lysine side chains on the Tat peptides bound to the phosphate and carbonyl groups of the zwitterionic phospholipids of DOPC membrane. They occupied a region beneath the phosphate groups at the interface with the carbon chains. Then the Tat peptides sequestered phosphate groups from neighboring phospholipids and created regions on the bilayer surface that were crowded with Tat peptides and phosphate groups, as well as regions that were depleted of charged groups. This crowding of charged groups was caused by the high concentration of charges in the Tat peptide. Eight out of eleven amino acids were charged. The crowding of charged groups resulted in the attraction between the Tat peptide and phosphate groups on the layer which was closer and the phosphate groups on the layer which was far away. As a result, the bilayer became thinner with increasing Tat peptide concentration. Arginine and lysine side chains on the Tat peptide and the phosphate groups on the layer which was far away attract each other and started to penetrate the lipid bilayer. As these charged groups entered the hydrophobic lipid bilayer, water also penetrated the bilayer and solvated the charged groups. The water and phosphate penetration nucleated a water pore in the membrane. Once the pore was formed, the Tat peptides translocated across the membrane by diffusing on the pore walls. The pore closed after a few peptides translocate [8].

There are two major strategies that the CPPs carry cargo drugs. First one is making a covalent linkage of the cargo to the CPP, so a conjugate is formed by either chemical cross-linking cloning or expression of a protein fused to CPP. The second strategy is the formation of a non-covalent complex between two partners. Despite several advantages of

the conjugate method, this method has risk of changing the biological activity of the cargos. MPG and Pep family peptides (Table 1.3) are primarily amphipathic with three domais: a hydrophobic domain in N terminus, a hydrophilic lysine-rich domain and a linker domain containing proline. When the sequences of Pep family peptides are examined, it is found that there should be four cationic residues within the hydrophilic domain in order to initiate the electrostatic interactions between the peptide and the membrane components. There should charged lysine in the N terminus and proline in the linker region to provide flexibility. Both MPG and Pep family peptides spontaneously penetrate lipid-phase and insert into the natural membranes [10].

Most organism produce antimicrobial peptides (AMPs) in order to provide innate defence mechanisms against colonization and infection by microbial pathogens. It was observed that some AMPs can enter host cells without damaging the cytoplasmic membrane. Therefore, these peptides drew attraction because of their ability to translocate across the cell membrane [6]. They have relatively short sequences (≤40 residues) [12]. They are also cationic peptides typically of charge 4+ or 5+. Even though most AMPs seem to act at membrane level, their translocation into the cytoplasm is not unusual. Thus membrane-crossing AMPs can be used as templates for CPP development [6].

1.2.1 pVEC

pVEC is a CPP which is 18 amino acid long. It is derived from murine vascular endothelial-cadherin protein which functions in the physical contact between adjacent cells. It has the sequence LLIILRRRIRKQAHAHSK as also shown in Table 1.3. The N terminus of the peptide is hydrophobic, the middle part is charged and the C terminus is hydrophilic. Thus it is an amphipathic molecule. In previous cargo-carrying experiments, pVEC was able to carry some proteins and oligomers [16].

Table 1.4. Sequences and properties of pVEC and its analogues [16].

Sequence	Name	Molecular mass (Da)	Rt (min ± S.D.)	Positive charges
LLIILRRRIRKQAHAHSK	pVEC	2208.7	22.1 ± 0.2	7
ALIILRRRIRKQAHAHSK	[Ala1]pVEC	2166.7	21.1 ± 0.9	7
LAIILRRRIRKQAHAHSK	[Ala2]pVEC	2166.7	20.9 ± 0.2	7
LLAILRRRIRKQAHAHSK	[Ala3]pVEC	2166.7	21.5 ± 0.3	7
LLIALRRRIRKQAHAHSK	[Ala4]pVEC	2166.7	21.7 ± 0.2	7
LLIIARRRIRKQAHAHSK	[Ala5]pVEC	2166.7	21.9 ± 1.4	7
LLIILARRIRKQAHAHSK	[Ala6]pVEC	2123.6	23.0 ± 0.4	6
LLIILRARIRKQAHAHSK	[Ala7]pVEC	2123.6	22.0 ± 0.7	6
LLIILRRAIRKQAHAHSK	[Ala8]pVEC	2123.6	25.5 ± 0.2	6
LLIILRRRARKQAHAHSK	[Ala9]pVEC	2123.6	21.5 ± 0.8	7
LLIILRRRIAKQAHAHSK	[Ala10]pVEC	2123.6	16.3 ± 0.9	6
LLIILRRRIRAQAHAHSK	[Ala11]pVEC	2151.6	22.3 ± 0.2	6
LLIILRRRIRKAAHAHSK	[Ala12]pVEC	2151.7	21.9 ± 0.2	7
LLIILRRRIRKQAHAHSK	[D-Ala13]pVEC	2208.7	21.6 ± 0.1	7
LLIILRRRIRKQAAAHSK	[Ala14]pVEC	2142.7	21.6 ± 0.5	7
LLIILRRRIRKQAHAHSK	[D-Ala15]pVEC	2208.7	16.4 ± 0.0	7
LLIILRRRIRKQAHAASK	[Ala16]pVEC	2142.7	22.4 ± 1.0	7
LLIILRRRIRKQAHAHAK	[Ala17]pVEC	2192.7	18.5 ± 3.2	7
LLIILRRRIRKQAHAHSA	[Ala18]pVEC	2151.6	17.6 ± 1.3	6
KSHAHAQKRIRRRLIILL	retro-pVEC	2208.7	16.5 ± 4.4	7
LLIILRRRIRKQAHAHSK	D-pVEC	2208.7	16.6 ± 0.0	7
IAARIKLRSRQHIKLRHL	scramble pVEC	2208.7	10.2 ± 0.01	7

Elmquiest and coworkers carried out structure-activity relationship (S.A.R) experiments. In these experiments, each residue of the original pVEC molecule mutated to L-alanine and examined the change in the cellular uptake of pVEC into the cells. Thus defining the importance of each residue was aimed. Moreover, the cellular uptakes of the D-enantiomer of pVEC (D-pVEC) with D-amino acids, the retro-pVEC with reversed

sequence and the scramble pVEC were studied. All the pVEC analogues were shown in Table 1.4. The pVEC and D-pVEC were treated with endocyctotic inhibitors: wortmannin, nystatin, heparinase III or EIPA in order to check whether translocation of pVEC occurred via endocytosis. Also the cellular uptake of pVEC and D-pVEC in different temperatures were investigated [16].

Substitution of the first five amino acids in the N terminus of pVEC to L-alanine dropped the cellular uptake between 50 and 75% (Figure 1.3). Significant reduction was spotted in the 9^{th} and 14^{th} residues from the N terminus. The cellular uptake of the scramble pVEC reduced the most. Thus the hydrophobic N-terminus of the peptide was important for the cellular uptake [16].

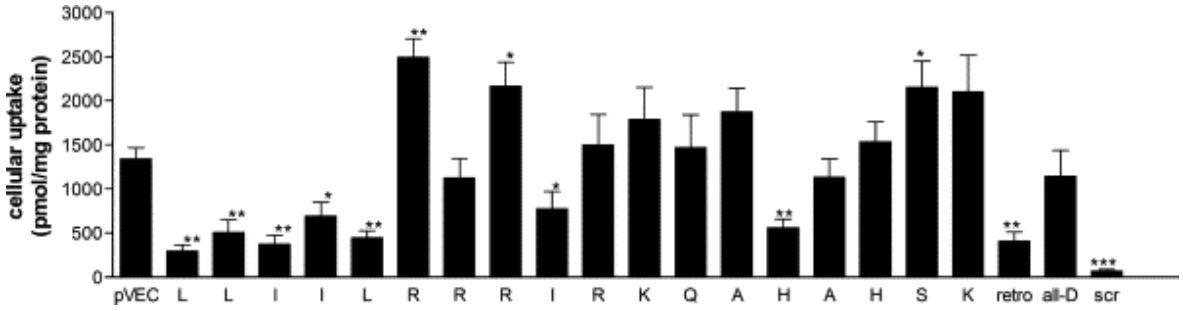

Figure 1.3. The cellular uptake values of the pVEC analogues [16].

When the effect of the endocytosis inhibitors was examined, it was seen that only wortmannin decreased pVEC uptake (by 25%). Other inhibitors had no affect on both pVEC and D-pVEC. If the affect of temperature was questioned, there was no important change was detected in the uptake when the temperature was changed from 310 K to 281 K [16].

Mäger and coworkers studied the overall cargo delivery kinetics of M918, TP10 and pVEC by quenched fluorescence assay. These CPPs are bonded with a cargo peptide by disulfide bonds. The sequences of the cargo peptide and CPPs are given in Table 1.5. The

overall delivery kinetics which are total cellular uptake and first-order rate constant of the created peptides and the endocytosis inhibitors were investigated in the study. Cargo-SS-CPP concentration was chosen as 2.5 μM which was retained high enough fluorescent signals. The inhibitors used were 10 μM chlorpromazine, 4 μM cytochalasin D, 50 nm wortmannin, and 0.4 M sucrose. As a result, the inhibitors had the strongest effect on M918-mediated uptake, whereas pVEC-mediated uptake is less affected by the inhibitors. By using sucrose or wortmannin the first-order rate constant of M918 uptake increased. Cytochalasin D did not significantly change the kinetic constants but nevertheless reduced the total uptake of M918. For the TP10 conjugate, cytochalasin D was the only inhibitor that did not significantly affect the kinetic constant of the uptake even though it increased the total uptake. Wortmannin, chlorpromazine and sucrose increased the first-order rate constants of the uptake and decreased the total uptake levels. For the pVEC conjugate it was seen that only cytochalasin D had important effect on both the kinetic constant and total uptake. The other inhibitors only affected the total uptake but not kinetic constants, except wortmannin that had no effect on both parameters. A general pattern between the kinetic constant and total uptake was seen that when the corresponding inhibitor increased the first-order rate constant, the total uptake was decreased at the same time. Lower uptake levels of the CPPs correlate with higher order rate constants. Also, when one rate limiting uptake mechanism is inhibited, other pathways may be exploited to a greater extent [13].

Table 1.5. Peptide sequences of [13].

Name	**Sequence**
Cargo	Abz-C(NPys)-LKANL-amide
TP10	AGYLLGKINLKALAALAKKIL-amide
pVec	LLIILRRRIRKQAHAHSK-amide
M918	MVTVLFRRLRIRRASGPPRVRV-amide

Eirìksdòttir *et al.* classified CPPs as into three classes: (i) protein transduction domains (PTDs), (ii) model peptides and (iii) designed peptides. These classifications were done with regard to both their biophysical properties and their ability to enter the cell. PTD

peptides are natural peptides derived from specific protein fragments with transduction abilities. Model peptides consist of amino-acid sequences that are generally based on repeat motifs or poly-residues. Designed peptides have been conceived on the basis of rational mutations or combinations between protein domains of a specific interest. In this study, both the structural state and the conformational plasticity of peptides were investigated in several distinct environments. The structural flexibility of each peptide has been evaluated by circular dichroism (CD) spectroscopy. pVEC and retro-pVEC which are PTD had random coil structure in pure water. They adopted a beta-structure in the presence of negatively charged phospholipids dioleoylphosphatidylglycerol (DOPG). No modification of structure was observed in the structure of pVEC and retro-pVEC in the presence of DOPG/DOPC mixed vesicles, only DOPC and DOPC/SM (sphingomyelin)/Chol (cholesterol) mixed vesicles. Finally, pVEC peptide is found to be poorly amphipathic [11].

1.3 Bacterial Membranes

There are two classes of bacteria: Gram positive and Gram negative bacteria. Gram positive bacteria have only one membrane, which is the cytoplasmic membrane, while Gram negative bacteria have an additional outer membrane. Both bacteria have peptidoglycan layer but the one in Gram negative is thinner. Most bacteria have zwitterionic phosphodylethanolamine (PE) as phospholipids. Especially, the Gram negative bacteria have higher content. When there is multi-domain of lipids considered, the composition generally contains PE, PG (phosphatidyglycerol) and CL (cardiolipin) [17]. Indeed, the membrane lipid composition of E. coli is 80% PE, 15% PG and 5% CL (Joanne 2009). The composition of the lipids of a membrane can vary; therefore, different sensitivities of membranes to antimicrobial compounds are expected [17].

In this work, the transition of CPPs through bacterial cell membrane was investigated. The bacterium of interest was E. coli. The software that was used to prepare the system and perform the simulations supports only two kinds of phospholipids: POPC

(1-palmitoyl-2-oleoyl-sn-glycero-3-phosphocholine) and POPE (1-Palmitoyl-2-oleoyl-*sn*-glycero-3-phosphoethanolamine). Since E. coli was the investigated bacterium and the lipid membrane composition of it is 80% PE, POPE was chosen to simulate the E. coli membrane.

In the study of Joanne and coworkers, the capacity of the selected CPPs and AMPs to reorganize binary lipid mixtures and to selectively recruit specific lipids was investigated by differential scanning calorimetry. Therefore, the studies focused on the role of electrostatic forces on the peptide/lipid interaction by using DPPC and cardiolipin vesicles. The peptides were two CPPs (Penetratin and RL16) and AMPs belonging to the dermaseptin superfamily (Drs B2 and C-terminal truncated analog [1–23]-Drs B2 and two plasticins DRP-PBN2 and DRP-PD36KF).In this study, multilamellar vesicles composed of two lipid mixtures were used to investigate the role of the electrostatic interactions and lipid bilayer fluidity on the peptide/lipid interactions. The MLVs were DMPC/DSPC or DMPG/DSPG and DMPC/POPC and DMPG/POPG vesicles. The idea behind the use of miscible binary lipid mixtures was to examine the segregation of lipids or lipid recruitment. All the peptides investigated, except RL16, interacted with the lipids, at a first level through electrostatic interactions established between the positively charged amino acids of the peptides and the negatively charged lipid head groups. Both CPPs and AMPs induced specific lipid segregation of binary lipid mixtures possessing lipid components with different phase transition temperatures. When selective lipid interactions were observed, the lipid being recruited from the binary mixture always corresponded to the one having the lowest phase transition temperature [18].

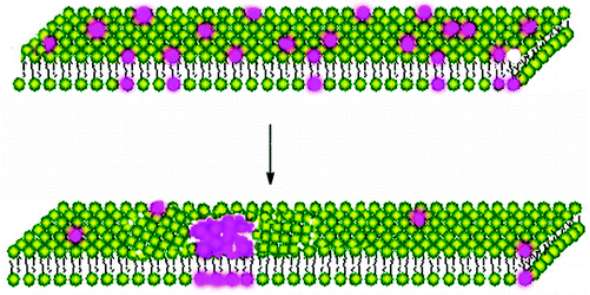

Figure 1.4. Schematic diagram of phase seperation in a membrane bilayer [19].

In the Epand and Rotem, the ability of one OAK (oligomer of acyllysine), the octamer C_{12}K-7α_8, to interact with anionic lipids and to induce lateral phase separation was demonstrated. Because of the importance of lateral phase separation for the antimicrobial action of C_{12}K-7α_8, the bacterial species that will be sensitive to the action of this compound could be predicted. Differential scanning calorimetry (DSC) was used to study phase separation between anionic and zwitterionic lipids induced by the OAK. DSC was used to obtain evidence for the promotion of lateral phase separation by starting with a mixture of two miscible lipids. If an added substance promotes lateral phase separation by binding to one of the components, it will segregate that component into a domain, leaving the rest of the membrane enriched in the second lipid component. As a result the second component will exhibit a more cooperative phase transition at a temperature closer to that of the pure lipid. The lipid mixture POPE−TOCL was chosen to demonstrate protein-induced lateral phase separation and had a broad gel to liquid crystalline phase transition centered at about 288 K. The gel to liquid crystalline phase transition temperatures of the individual lipids that comprise this mixture are 298 K and below 273 K for POPE and TOCL, respectively. Addition of C_{12}K-7α_8 produced a shift in the transition temperature of the mixture to higher temperatures and sharpened the transition. Thus C_{12}K-7α_8 bound to TOCL and left the remaining lipid enriched in POPE. This situation was demonstrated in Figure 1.4. A similar observation was made with POPE−DOPG. The mixture has a broad phase transition temperature centered at 288 K. The phase transition temperature of DOPG is also below 273 K. Again C_{12}K-7α_8 shows a larger shift of one component toward higher temperatures [19].

1.4 Recent work on Molecular Dynamics and Steered Molecular Dynamics

Molecular dynamic simulations are applied to various proteins and peptides in/on many kinds of membranes in order to reveal their behavior in lipid bilayer environments. In the study of Soliman and friends, carnobacteriocin B2 (CbnB2) peptide is simulated with a bilayer of POPG/POPE mixture initially in three different ways: The peptide is adjacent to the water-bilayer interface. The second is that the peptide is half-immersed into the bilayer and the third one is that the peptide is totally in the bilayer. The study yields

some facts that single peptides do not spontaneously penetrate lipid membranes. No hydrogen bonds form between the head groups of the membrane and the peptide when the peptide is at the surface of the membrane. However, when the peptide is immersed fully or, even, partially into the bilayer, valine, alanine and glycine form H-bonds with the bilayer. Besides, tryptophan has a crucial role when the protein positions itself near the interface. The peptide is not expelled from the hydrophobic core when partially or completely inserted. There is an activation energy barrier encountered by a peptide when it attempts to enter a bilayer from the aqueous phase. The barrier is most likely in the plane containing the polar and charged headgroups of the lipids [20].

In the work of Davis and Berkowitz, replica exchange MD simulations were performed on all-atom representations of the 42 amino acid Amyloid-β on model lipid bilayers. The results of these simulations showed that no stable secondary structure was formed by the Aβ monomer at either pH 7 or pH 5 when bound to the homogeneous DPPC or DOPS bilayers. A salt bridge between Asp23 and Lys28 was formed on the DOPS bilayer when the peptide has a net neutral charge, and the formation of the salt bridge imposed a β-hairpin like structure on the peptide. But this salt bridge was not stable and this β-hairpin like structure was not maintained because of the extensive peptide-lipid interactions. In fact, Lys28 substantially interacted with the phosphate moiety and glycerol backbone of the lipid, which stabilized protein binding to the lipid even at 502 K. As a result, the strong lipid−protein interactions which forced the tight binding of Aβ to the bilayer surface also prevented the internal interactions which would promote the secondary structure change. The β-structure formation was not because of the structuring at a monomer level but is potentially due to peptide-peptide interactions that are enhanced on the bilayer surface [21].

Killian and coworkers developed a series of synthetic tryptophan-flanked transmembrane peptides called WALP [22, 23]. White and coworkers also developed transmembrane peptides called TMs [23]. When the considered peptides were WALP and TM peptides, the insertion of WALP peptides always occured from the N terminus. Indeed, the insertion was delayed until the N terminus formed an alpha-helical conformation.

Carbonyl groups at the C terminus had larger dipole moments than the amide groups of the N terminus. Thus, desolvation at the carbonyl group of the C terminus was disfavored compared with the amide group of the N terminus [24].

The work of Babakhani and coworkers agreed with the work of Soliman et. al that tryptophan residue of the peptide had an important contribution to hydrogen bonds. Besides, the nitrogen heteroatom of the indole ring played a critical role [25]. It showed that penetration depth of the peptide into the membrane was a function of the hydrophobicity of the peptide [25]. If the thickness, order parameters, or the cross-sectional area of the membrane were dramatically changed as the peptide inserted into the membrane, then the SMD simulation was considered unrealistic [26]. When there was an increase in the number of hydrogen bonds, then it caused the peptide to localize to the interface where it had a parallel orientation. A transmembrane protein did not always present its tryptophan residues at the membrane interface [25]. And some membrane channel or gating proteins fluctuated their tryptophan residues from the interface to the membrane core [27].

Indolicidin (IL) was the peptide of interest in study of Tsai and friends [28]. In agreement with study of Soliman, this study stated that the presence of hydrophobic tryptophan residues led to its deeper insertion while positive charges were critical to the peptide's adsorption. IL was capable of killing bacteria either through distruption of the cytoplasmic membrane [29, 30] or through channel formation [30, 31]. Indolicidin diffused spontaneously from the aqueous phase to the water-lipid head group interface. Some of the residues of the peptide inserted into the hydrophobic region of the lipid bilayer. Contacts between the hydrophobic residues and the hydrophobic region of the POPC lipid bilayer occurred later than the formation of stable salt bridges. Hydrophobic contact always occurred after salt bridge formation. Despite of the results obtained for the POPC system, in which the tryptophan residues were positioned within the hydrophobic regions of the lipids, it was observed that some of the tryptophan residues were located at the water lipid interface of the POPG/POPC bilayer system. Thickness of the pure POPC lipid bilayer decreased when the peptide inserted into the hydrophobic region while the mixed POPG/POPC lipid bilayer became thinner upon the adsorption of IL at the water-lipid

interfacial region. Moreover, the tryptophan residues were critical for the disordering of the membrane. The zwitterionic POPC lipid bilayers became disordered mainly upon the insertion of IL and not upon its adsorption [28].

An antibacterial peptide 27 amino acid residues named NK-2 was investigated in work of Pimthon and coworkers [32]. The configuration that the hydrophobic face of the NK-2 towards the membrane surface stayed parallel to the membrane-water interface on PG and PE membranes [32, 33]. The electrostatic/hydrogen bonding modified the peptide-membrane affinity, which was stronger in the case of the charged DPPG bilayer than for the less charged DPPE bilayer. The peptide binding process was accelerated by the direct electrostatic interactions between positively charged amino acids of NK-2 and negatively charged groups at the membrane surface while the peptide insertion into the membrane was modulated by the hydrophobic residues [32].

The study of Lorenzo and coworkers was focused on the analyses of the system responses for spring constants and pulling-groups of steered molecular dynamics. There were two different molecules of interest: a single tryptophan residue and a pentapeptide with the sequence of WLKLL. Molecular dynamics and following steered molecular dynamics simulations were performed with these peptides separately. The peptides were initially positioned in an aqueous medium. A lipid bilayer was also positioned near the peptides. As MD simulations were performed, both peptides inserted the membranes spontaneously. The MD simulations were lasted until a molecular stable structure was reached in this medium in order to provide the initial conformational state for the SMD simulations. In SMD simulations, the molecule was pulled with constant velocity of 0.015 Å/ps and in the direction perpendicular to the membrane-water interface in order to extract the molecule from the membrane. The tryptophan residue was pulled with three different spring constants: 0.1, 0.6 and 4 kcal/mol/$Å^2$ in its SMD simulations. The pentapeptide was pulled with 0.6 kcal/mol/ $Å^2$ and with two different pulling groups: alpha carbon of the residue in the N terminus and one of the oxygen atoms from C terminus. The average local amplitude of the force response as much greater for a stiffer spring than for a softer one; the opposite occured for the local amplitudes of the center of mass. Larger local displacements and energy fluctuations were expected because softer springs exerted a less

restricted action on the system. Exceedingly large amplitude fluctuations of the force profile might have been observed if an extremely stiff spring (such as k = 4 kcal/mol/Å^2) was used. Even though the two pentapeptides followed different cell entering pathways, the main interaction which was the formation of a salt bridge between the carboxyl terminal and lysine side chain was equally seen in both cases. Additional SMD simulations were performed with half pulling velocity. As a result exit pathways and interaction forces were conserved shen the pulling velocity and the spring constant were vaired. When different pulling-groups were considered for the same conformation, different extraction pathways were followed [34].

In the study of Levtsova *et al.*, the interaction between cardiotoxin A3 peptide and POPC lipid bilayer was studied by steered molecular dynamics [35]. The toxic peptide bound to POPC which was a zwitterionic lipid. However, the results of the study showed that the toxic peptide would not bind to the membrane composed of zwitterionic lipids without auxiliary interaction. The reason of the use of SMD was that the molecular dynamics (MD) simulations required a long time for toxin to approach the membrane surface. Thus SMD was used to accelerate the process [35].

Pal *et al.* investigated the structural and dynamical properties of a poly(ethylene oxide)-poly(ethylene glycol) polymer chain at a DMPC bilayer/water interface by MD and SMD simulations. They analyzed the work necessary to penetrate the membrane by poly(ethylene oxide) and found a threshold value of work for poly(ethylene oxide) to overcome in order to penetrate the membrane. This value was calculated to be 18.6 kJ/mol [36].

Allen and Bevan studied the MD and SMD simulations of a monotopic membrane protein named as monoamine oxidase B (MAO B). They performed MD simulations of MAO B in POPC/POPE mixed bilayer and in bulk solvent. They also performed MD simulations of MAO B with its seven inhibitors. These seven inhibitors were shown in Table 1.6. After the bindings occurred, SMD simulations of unbinding of MAO B inhibitors were performed in mixed lipid bilayer and in solvent. The potential of mean

force (ΔPMF) results distinguish the active and inactive inhibitors. They found that the peak force applied during active site activity correlates strongly with inhibitor strength. The accuracy of ΔPMF measurements will increase as the replicate number increases, as the pulling constant and spring constant decrease, and the simulation time increases [37].

Table 1.6. The seven MAO B inhibitors [37].

PDB code	**Inhibitor**	**Abbr.**
1OJ9	1,4-diphenyl-2-butene	1PB
2C67	N-methyl-1(R)-aminoindan	RM1
1OJA	1H-indole-2,3-dione (isatin)	ISN
2BK3	farnesol	FOH
2V5Z	(S)-(+)-2-[4-(fluorobenzyloxybenzylamino) propionamide]	SAG
2V60	7-[(3-chlorobenzyl)oxy]-2-oxo-2H-chromene-4-carbaldehyde	C17
2V61	7-[(3-chlorobenzyl)oxy]-4-[(methylamino)methyl]-2H-chromen-2-one	C18

Wei and Pohorile studied the transport of nucleosides, ribo-adenosine and arabino-adenosine, through POPC membrane using MD simulations. Analysis of the free energy landscape, which is dependent on the orientation, inside the membrane points out that the most likely permeation mechanism of the nucleosides involves flipping of the nucleosides near the center of the membrane [38].

De Fabritiis *et al.* proposed a novel technique which was based on the use of forward-reverse steered molecular dynamics simulations in order to populate high energy regions of the potential energy surface and on the use of the Crooks fluctuation in order to obtain an estimate of the free energy barrier for ion crossing. Two sets of 25 of steered molecular simulations were performed where a K^+ ion was pulled along the *z* direction orthogonal to the pore from the pore entrance to the center (forward direction) and *vice versa* (reverse direction) taking advantage of the symmetry of the Gramicidin A pore. The pulling speed was v = 10 Å/ns for 1.7 ns each run and the spring constant was 10 kcal/mol/Å^2. Moreover, a harmonic restraining potential with k = 250 kcal/mol Å^{-2} to the center of mass of the Cα carbon atoms of the protein was applied in order to avoid the

possibility that the continuous strain on the surface of the pore produced by the pulled ion might have affected the location of the protein in the membrane. The Crooks relation was an equation that relates the work done on a system during a non-equilibrium transformation to the free energy difference between the final and the initial state of the transformation [39]. The calculations reproduced with an extremely simple protocol the results for the free energy profile obtained previously and, more importantly, allowed interpretation of the dynamic polarization of the water molecules outside the channel [40].

2 MATERIALS AND METHODS

2.1 Molecular Dynamics Simulation

Computer simulations are carried out in order to grasp the properties of assemblies of molecules in terms of their structure and the microscopic interactions between them. They bind microscopic length and time scales to the macroscopic world of the library [37]. Simulations provide details concerning individual particle motions as a function of time. Therefore, they can be used to analyze properties of model systems often more easily than experiments on the actual systems. Molecular dynamics (MD) simulation is one of the main methods used for the computational simulations of the model systems. When simulations are performed in order to examine the actual dynamics; in other words, not only to sample configuration space, but to represent the development of the system over time, molecular dynamics simulations provide the necessary information. In short, the motions and their development with time are the major interest of MD simulations [41].

MD simulations are used to calculate motions and atomic trajectories of atoms as a function of time according to Newton's second law (Equation 2.1) given by,

$$F_i = m_i a_i \tag{2.1}$$

where $F_i$is the force exerted on the particle *i*, m_i is the mass of the particle *i* and a_i is the acceleration of the particle *i*.

The force can be also expressed as the gradient of the potential energy,

$$F_i = -\nabla_i V \tag{2.2}$$

where V is the potential energy of the system.

When Equation 2.1 and Equation 2.2 are combined,

$$F_i = -\frac{dV}{dr_i} = m_i \frac{d^2 r_i}{dt^2} \tag{2.3}$$

where r_i is the atomic coordinates of the particle i and t is the time.

2.1.1 CHARMM Force Field

In order to describe the relationship of chemical structure to energy, mathematical equations are applied in theoretical chemistry. Combined with statistical mechanics, all properties of a system can be calculated with this information. However, the energy of all possible conformations of a chemical system cannot be calculated. In order to handle this problem, simple mathematical functions must be used to treat the structure-energy relationship. This method is only valid for biological molecules with a molecular weight greater than 10 kDa. This method is named as molecular mechanics or empirical force field calculations. However, the equation alone is not adequate to compute the structure-energy relationships. Parameters must be added in the mathematical equation. The empirical force field used in this study is CHARMM22 [42].

The intramolecular potential energy function is

$$\begin{aligned} V_{intra} = & \sum_{bonds} K_b(b - b_o)^2 + \sum_{angles} K_\theta(\theta - \theta_o)^2 \\ & + \sum_{torsions} K\phi(1 + \cos(n\phi - \delta)) + \sum_{impropers} K_\varphi(\varphi - \varphi_o)^2 \\ & + \sum_{Urey-Bradley} K_{UB}\left(r_{1,3} - r_{1,3,o}\right)^2 \end{aligned} \tag{2.4}$$

The intermolecular potential energy function is

$$V_{inter} = \sum_{electrostatic} \frac{q_i q_j}{r_{ij}} + \sum_{VDW} \varepsilon_{ij} \left[\left(\frac{R_{min,ij}}{r_{ij}} \right)^{12} - 2 \left(\frac{R_{min,ij}}{r_{ij}} \right)^{6} \right] \quad (2.5)$$

$$V = V_{intra} + V_{inter} \quad (2.6)$$

The first term in Equation 2.4 is the covalent bond stretching interaction where $b - b_o$ is the distance from equilibrium that the atom has moved and $K_b$is the bond force constant. The second term is associated with bond angles where $\theta - \theta_o$is the angle from equilibrium between 3 bonded atoms and $K_\theta$is the angle force constant. The third term is for the dihedral angle interaction where n is the multiplicity of the function, $\phi$is the dihedral angle, δ is phase shift and $K\phi$ is the dihedral force constant. The fourth term is associated with the impropers. $\varphi - \varphi_o$is the out of plane angle and K_φ is the impropers force constant. The fifth term is the Urey-Bradley component where $r_{1,3} - r_{1,3,o}$ is the distance between the 1,3 atoms in the harmonic potential and $K_{UB}$is the force constant.

The first term in Equation 2.5 corresponds to the electrostatics energy contribution and the second term is the van der Waals energy contribution. ε is the Lennard-Jones (vdW) well-depth. $R_{min}$is the Lennard-Jones radius and q is the partial atomic charge [42].

2.1.2 NAMD

NAMD2 is a parallel program aimed at utilizing large parallel machines in a scalable manner. The non-bonded force computations require calculation of pairwise interactions between atoms. In most common methods, a cutoff distance is used. Non-bonded interactions between atoms beyond this cutoff radius are not calculated or calculated rarely [43].

NAMD2 is written using Charm++, a parallel C++ extension that supports message-driven execution. NAMD2 uses CHARMM force fields and X-PLOR coordinate and molecular structure files. In addition to non-periodic simulations, NAMD2 can use periodic boundary conditions over any combination of the three coordinate axes. It performs cutoff simulations or full-electrostatic simulations. NAMD2 can connect to VMD, the visualization component of MDScope, to allow monitoring of and interaction with ongoing simulations.

For greater efficiency, NAMD2 allows the force field to be split into three parts based on their frequency of variation. All bonded forces (bonds, angles, dihedrals, and impropers) are considered quickly varying, non-bonded forces (electrostatics and Lennard-Jones) within a cutoff are slower, and long-range electrostatics (separated from local electrostatics by a smooth splitting function) vary on the slowest time scale [43].

2.2 Steered Molecular Dynamics Simulation

Steered Molecular Dynamics (SMD) is a simulation technique in which time-dependent forces are applied to certain atoms of a molecule [43]. Recording the applied forces and resulting positions over time gives insight into problems such as unbinding of ligands from proteins, unfolding of proteins and moving peptides.

The basic idea behind any SMD simulation is to apply an external force to one or more atoms. These atoms are called as SMD atoms. There are two types of SMD simulations: constant velocity pulling and constant force pulling [44].

In the constant velocity pulling simulation, the SMD atom is attached to a dummy atom via a virtual spring. This dummy atom is moved at constant velocity and then the force between both is measured using:

$$\vec{F} = -\nabla V \tag{2.7}$$

$$V = \frac{1}{2}k[vt - (\vec{r} - \vec{r}_0) * \vec{n}] \tag{2.8}$$

In Equation 2.7, $\vec{F}$ is the force applied and V is the potential energy. In Equation 2.8, k is the spring constant and v is the pulling velocity. t is the time. $\vec{r}$ is the actual position of the SMD atom and $\vec{r}_0$ is the initial position of the SMD atom. Finally, $\vec{n}$ is the direction of pulling.

2.3 The Simulation Systems

2.3.1 Peptide 1 – Membrane – Water System

The coordinates of the peptide of the first system is based on the crystal structure of TEM-1 beta-lactamase / beta-lactamase inhibitor protein complex (1JTG.pdb). This complex consists of four chains and the chains B and D are the chains of the beta-lactamase inhibitor protein (BLIP). The residues 45 to 52 with the sequence HAAGDYYA were extracted from chain B and set as the BLIP-based peptide (Figure 2.1).

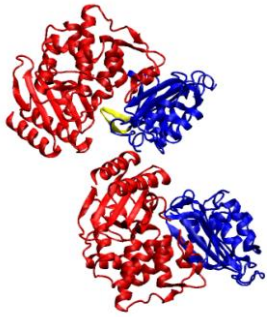

Figure 2.1. The chains A (red top), B (blue top), C (red bottom) and D (blue bottom) of TEM-1 beta-lactamase / beta-lactamase inhibitor protein complex and the peptide of residues 45 to 52 (yellow).

The membrane was created in 50 Å in x- and 50 Å in y-directions. The membrane package of the VMD membrane provides only two types of phospholipids: POPC (1-palmitoyl-2-oleoyl-sn-glycero-3-phosphocholine) and POPE (1-Palmitoyl-2-oleoyl-*sn*-glycero-3-phosphoethanolamine). Most bacteria have zwitterionic phosphodylethanolamine (PE) as phospholipids. Especially, the Gram negative bacteria have higher content. When there is multi-domain of lipids, the composition generally contains PE, PG (phosphatidyglycerol) and CL (cardiolipin) [17]. The membrane lipid composition of E. coli has been determined to be 80% PE, 15% PG and 5% CL [18]. The lipid of the membrane was chosen to be POPE in order to represent the membrane of E. coli.

Then the membrane was centered by setting the center of the membrane in the origin (0, 0, 0 coordinates) of the system. The membrane was solvated with TIP3P water molecules 40 Å in positive and negative z-direction. The water molecules in positive and negative 10 Å in z-direction were removed since this place corresponds to the inside of the membrane.

The lipid tails of the membrane were fixed and the remaining atoms (membrane atoms other than the lipid tails) and water molecules were allowed to move. The water-membrane system was minimized for 1000 steps and equilibrated for 0.5 ns. Next, the lipid tails of the membrane were also allowed to move and the system was again minimized for 1000 steps and equilibrated for 0.5 ns.

The peptide was then inserted inside the water layer which was above the membrane. The water molecules which were 2.8 Å close to the peptide were removed. All the atoms except the peptide were set to be free and the atoms of the peptide were constrained. The ‘consexp’ parameter which is the exponent to be use in the harmonic constraint energy function was set to 2. Temperature of the simulation was set to 300 K and the pressure was set to 1 atm. The simulation space partitioning parameter cutoff which is local interaction distance common to both electrostatic and van der Waals calculations was set to 12 Å. The

other simulation space partioning parameter ‘pairlistdist’ which is distance between pairs for inclusion in pair lists was set to 13.5 Å.

The ‘timestep’ parameter was set to 2.0 fs. The ‘fullElectFrequency’ parameter which is distance between pairs for inclusion in pair lists was set to 2 and the ‘nonbondedFreq’ which is timesteps between nonbonded evaluation was set to 1. The pressure control parameters: ‘useGroupPressure’, ‘useFlexibleCell’ and ‘useConstantArea’ were set to yes, yes and no, respectively.

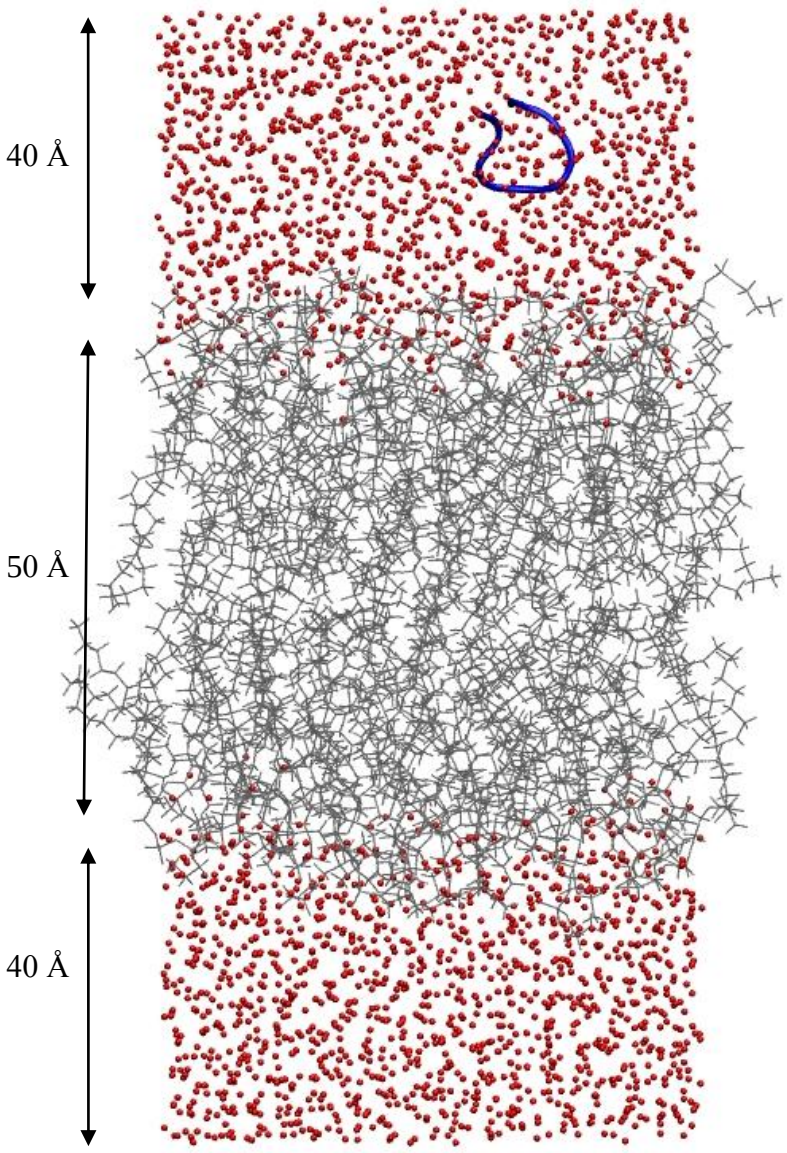

Figure 2.2. The structure of the system of water, membrane and peptide having sequence HAAGDYYA before the SMD simulation.

The ‘restartfreq’ which is the frequency of restart file generation, the ‘dcdfreq’ which is the timesteps between writing coordinates to trajectory file and the ‘xstfreq’ which shows how often to append state to XST file were all set to 1000. The ‘outputEnergies’ which is the timesteps between energy output and the ‘outputPressure’ which is the timesteps between pressure output were set to 50. The system was minimized for 1000 steps and equilibrated for 0.5 ns with the constrained peptide. Then the peptide was also left free and the system was equilibrated for 0.5 ns more.

The system composed of water, membrane and peptide was ready for SMD simulation as shown in (Figure 2.2). There are 6 SMD parameters to be entered. The first one is the SMD switch which was entered as on. Next, there is the SMDfile parameter in which the SMD atoms are labeled. In this part of the study, there were three places of pulling considered: center of mass, N terminus and C terminus. In center of mass pulling, the SMD atoms included all alpha carbon atoms of the peptide. In N terminus pulling, the SMD atom was the alpha carbon atom of the N terminus residue. In C terminus pulling, the SMD atom was the alpha carbon atom of the C terminus residue.

The ‘SMDk’ parameter, the magnitude of the spring constant was set to 7 kcal/mol/Å^2 and 10 kcal/mol/Å^2. Four different velocity values (‘SMDVel’) were used in this study: 0.0000010 Å/timestep, 0.0000050 Å/timestep, 0.0000100 Å/timestep and 0.0000300 Å/timestep which correspond to 0.50 Å/ns, 2.50 Å/ns, 5.0 Å/ns and 15.0 Å/ns, respectively (timestep was 2 femtoseconds).

The next parameter is ‘SMDDir’. The direction of the pulling is specified in this parameter. The peptide was positioned in the water layer above the membrane and it was desired to pull it in negative z-direction. The final parameter is ‘SMDOutputFreq’ which sets the frequency with which the SMD output is recorded. It was set to 10.

Temperature of the simulation was set to 300 K and the pressure was set to 1 atm. The simulation space partitioning parameter cutoff was set to 12 Å. The other simulation

space partioning parameter pairlistdist was set to 13.5 Å. The timestep parameter was set to 2.0 fs. The ‘fullElectFrequency’ was set to 2 and the ‘nonbondedFreq’ was set to 1. The pressure control parameters: ‘useGroupPressure’, ‘useFlexibleCell’ and ‘useConstantArea’ were set to yes, yes and no, respectively. The ‘restartfreq’, the ‘dcdfreq’ and the ‘xstfreq’ were all set to 1000. The ‘outputEnergies’ and the ‘outputPressure’ were set to 50.

2.3.2 Peptide 2 – Membrane – Water system

The peptide of this section had the sequence LLIILHAAGDYYAY. The coordinates of the residues of the peptide were assigned from the coordinates of HAAGDYYA peptide of the first system. The coordinates of the LLIIL part was guessed by VMD. Then the peptide was positioned in a water box. The water molecules 2.8 Å close to the peptide were removed. The atoms of the peptide were constrained and the water-peptide system was minimized for 1000 steps and equilibrated for 2 ns. Then all the atoms of the system were left free and the system was equilibrated for 2 ns further. Finally, the peptide was extracted from the water-box. This procedure was done twice in order to have peptides with two different conformations.

The membrane was created in 50 Å in x- and 50 Å in y-directions. The lipid of the membrane was chosen to be POPE in order to represent the membrane of E. coli. Then the membrane was centered by setting the center of the membrane in the origin (0, 0, 0 coordinates) of the system. The membrane was solvated with TIP3P water molecules 40 Å in positive and negative z-direction. The water molecules in positive and negative 10 Å in z-direction were removed since this place corresponds to the inside of the membrane.

The lipid tails of the membrane were fixed and the remaining atoms (membrane atoms other than the lipid tails) and water molecules were allowed to move. The water-membrane system was minimized for 1000 steps and equilibrated for 0.5 ns. Next, the lipid tails of the membrane were also allowed to move and the system was again minimized for 1000 steps and equilibrated for 0.5 ns.

The peptide was then inserted inside the water layer which was above the membrane. The water molecules which were 2.8 Å close to the peptide were removed. All the atoms except the peptide were set to be free and the atoms of the peptide were constrained. The consexp parameter was set to 2. Temperature of the simulation was set to 300 K and the pressure was set to 1 atm. The simulation space partitioning parameter cutoff was set to 12 Å. The other simulation space partioning parameter 'pairlistdist' was set to 13.5 Å.

The timestep parameter was set to 2.0 fs. The 'fullElectFrequency' was set to 2 and the 'nonbondedFreq' was set to 1. The pressure control parameters: 'useGroupPressure', 'useFlexibleCell' and 'useConstantArea' were set to yes, yes and no, respectively. The 'restartfreq', the 'dcdfreq' and the 'xstfreq' were all set to 1000. The outputEnergies and the 'outputPressure' were set to 50. The system was minimized for 1000 steps and equilibrated for 0.5 ns with the constrained peptide. Then the peptide was also left free and the system was equilibrated for 0.5 ns more.

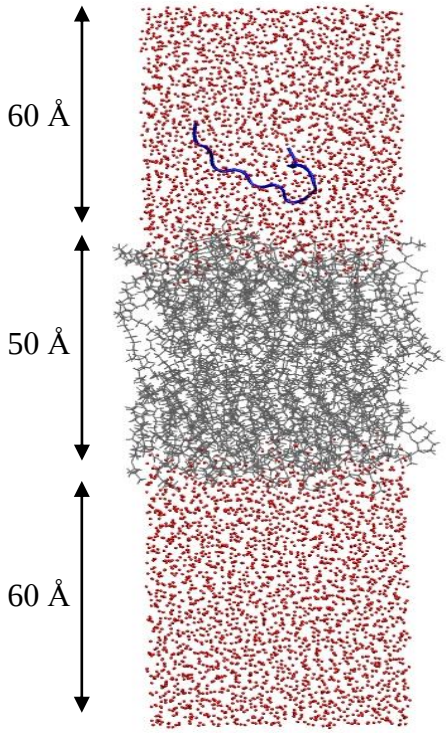

Figure 2.3. The structure of the system of water, membrane and peptide having sequence LLIILHAAGDYYA before the SMD simulation.

The system composed of water, membrane and peptide was ready for SMD simulation (Figure 2.3). The simulations were performed as described in section 2.3.1. The simulations were repeated with the 2nd conformation.

2.3.3 pVEC – Membrane – Water System

The peptide of this section was prepared manually through the VMD program. The coordinates of the residues histidine, alanine, glycine, aspartic acid and tyrosine of the peptide were assigned from the coordinates of HAAGDYYA peptide of the first system. The coordinates of the other residues were guessed by VMD.

Table 2.1. The 10 pVEC simulations with mutations on different residues.

Name	**Sequence**	**Mutated residue**	**Cellular uptake (pmol/mg protein)**
pVEC 1	LLIILRRRIRKQAHAHSK	original pVEC	1377
pVEC 2	**A**LIILRRRIRKQAHAHSK	L1A	307
pVEC 3	L**A**IILRRRIRKQAHAHSK	L2A	526
pVEC 4	LLIILRRR**A**RKQAHAHSK	I9A	789
pVEC 5	LLIILRRRI**A**KQAHAHSK	R10A	1535
pVEC 10	LLIILRRRIRKQA**A**AHSK	H14A	570
pVEC 6	LLIILRRRIRKQAHAH**A**K	S17A	2219
pVEC 7	LLIILRRRIRKQAHAHS**A**	K18A	2158
pVEC 8	KSHAHAQKRIRRRLIILL	retro-pVEC	412
pVEC 9	IAARIKLRSRQHIKLRHL	scramble pVEC	702

Next, the peptide was positioned in a water box. The water molecules 2.8 Å close to the peptide were removed. The atoms of the peptide were constrained and the water-peptide system was minimized for 1000 steps and equilibrated for 2 ns. Then all the atoms of the system were left free and the system was equilibrated for 2 ns further. Finally, the

peptide was extracted from the water-box. This procedure was repeated 10 times in order to obtain 10 pVEC peptides with different sequences (Table 2.1).

The pVEC – membrane – water system was prepared as described in Section 2.3.1.

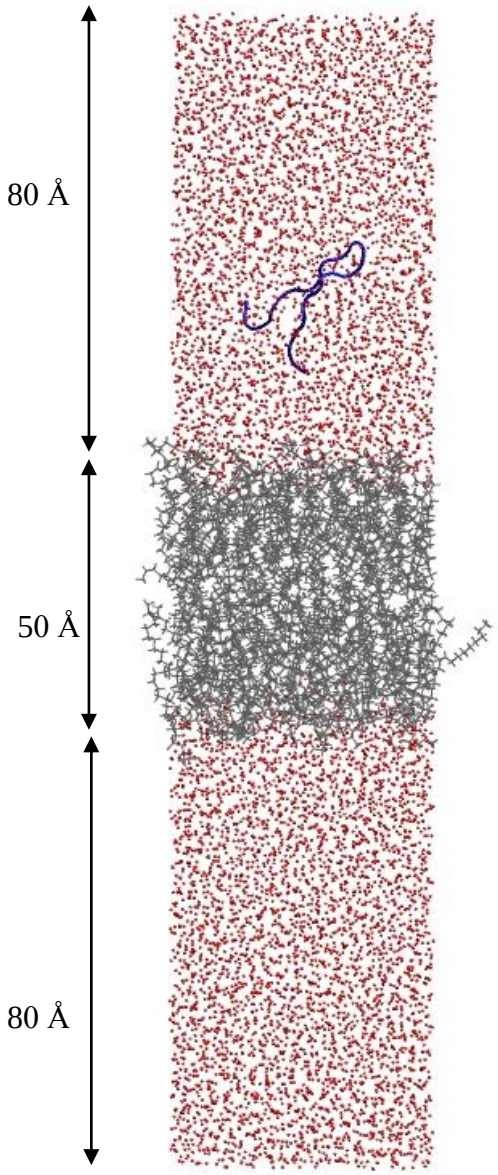

Figure 2.4. The structure of the system of water, membrane and peptide of pVEC 1 before the SMD simulation.

The system composed of water, membrane, peptide and ions was ready for SMD simulation (Figure 2.4). For these simulations, the phosphorous heads of the lipid bilayer were fixed in z-direction while they were free to move in x- and y-directions. In this part of the study, SMD atom was chosen as the alpha carbon atom of the N terminus residue. In this part, the spring constant used was set to 10 kcal/mol/$Å^2$. The velocity was set to 0.0000050 Å/timestep which correspond to 2.50 Å/ns (timestep is 2 femtoseconds).

The ‘consexp’ parameter was set to 2. Temperature of the simulation was set to 300 K and the pressure was set to 1 atm. The simulation space partitioning parameter cutoff was set to 12 Å. The other simulation space partioning parameter ‘pairlistdist’ was set to 13.5 Å. The ‘timestep’ parameter was set to 2.0 fs. The ‘fullElectFrequency’ was set to 2 and the ‘nonbondedFreq’ was set to 1. The pressure control parameters: ‘useGroupPressure’, ‘useFlexibleCell’ and ‘useConstantArea’ were all set to yes. The ‘restartfreq’, the ‘dcdfreq’ and the ‘xstfreq’ were all set to 1000. The ‘outputEnergies’ and the ‘outputPressure’ were set to 50.

3 RESULTS AND DISCUSSION

3.1 Membrane Uptake of a BLIP Based Peptide

The BLIP based peptide was chosen from the complex of TEM-1 beta-latamase / beta-lactamase inhibitor protein (1JTG.pdb). Chain B of the complex is BLIP and the residues from 45 to 52 were extracted from chain B as the peptide. The peptide had the sequence HAAGDYYA.

Steered molecular dynamics simulations were performed. The main focus of the simulations was the transition of the peptide through the phospholipid bilayer. The next significant focuses were membrane distortion and change in the peptide structure. All the atoms of the system were left free to move; in other words, there were no constraints on any atom. The simulation time was 20 ns with a desired distance to be covered as 100 Å.

The membrane was created in 50 Å in x- and 50 Å in y-directions and was chosen to be POPE. Then the membrane was centered. The membrane was solvated 40 Å in each positive and negative z-direction. The water molecules in positive and negative 10 Å in z-direction were removed. The lipid tails of the membrane were fixed and the water-membrane system was minimized for 1000 steps and equilibrated for 0.5 ns. Next, the lipid tails of the membrane were also left free and the system was again minimized for 1000 steps and equilibrated for 0.5 ns.

Table 3.1. The 9 simulations having different spring constants, velocities and places of pulling with peptide having sequence HAAGDYYA.

Simulation	**k (kcal/mol/Å^2)**	**velocity (Å/ns)**	**place of pulling**
SMD1	10	0.50	center of mass
SMD2	10	2.50	center of mass
SMD3	10	5.00	center of mass
SMD4	10	15.00	center of mass
SMD5	7	5.00	center of mass
SMD6	7	5.00	center of mass
SMD7	7	5.00	C terminus
SMD8	7	5.00	N terminus
SMD9	7	10.00	center of mass

The peptide was inserted inside the water layer which was above the membrane. The water molecules which were 2.8 Å close to the peptide were removed. The atoms of the peptide were constrained. The system was minimized for 1000 steps and equilibrated for 0.5 ns with the constrained peptide. Then the peptide was also left free and the system was equilibrated for 0.5 ns more. The system composed of water, membrane and peptide was ready for SMD simulation as shown in Figure 3.1.

In all nine simulations, the peptide (blue, cartoon representation) was initially positioned in the center of the upper water layer (red) which was 20 Å above of the top of the lipid bilayer (grey) as shown in Figure 3.1. The membrane had a thickness of 50 Å in the z direction. The same initial structure was used in all nine SMD simulations.

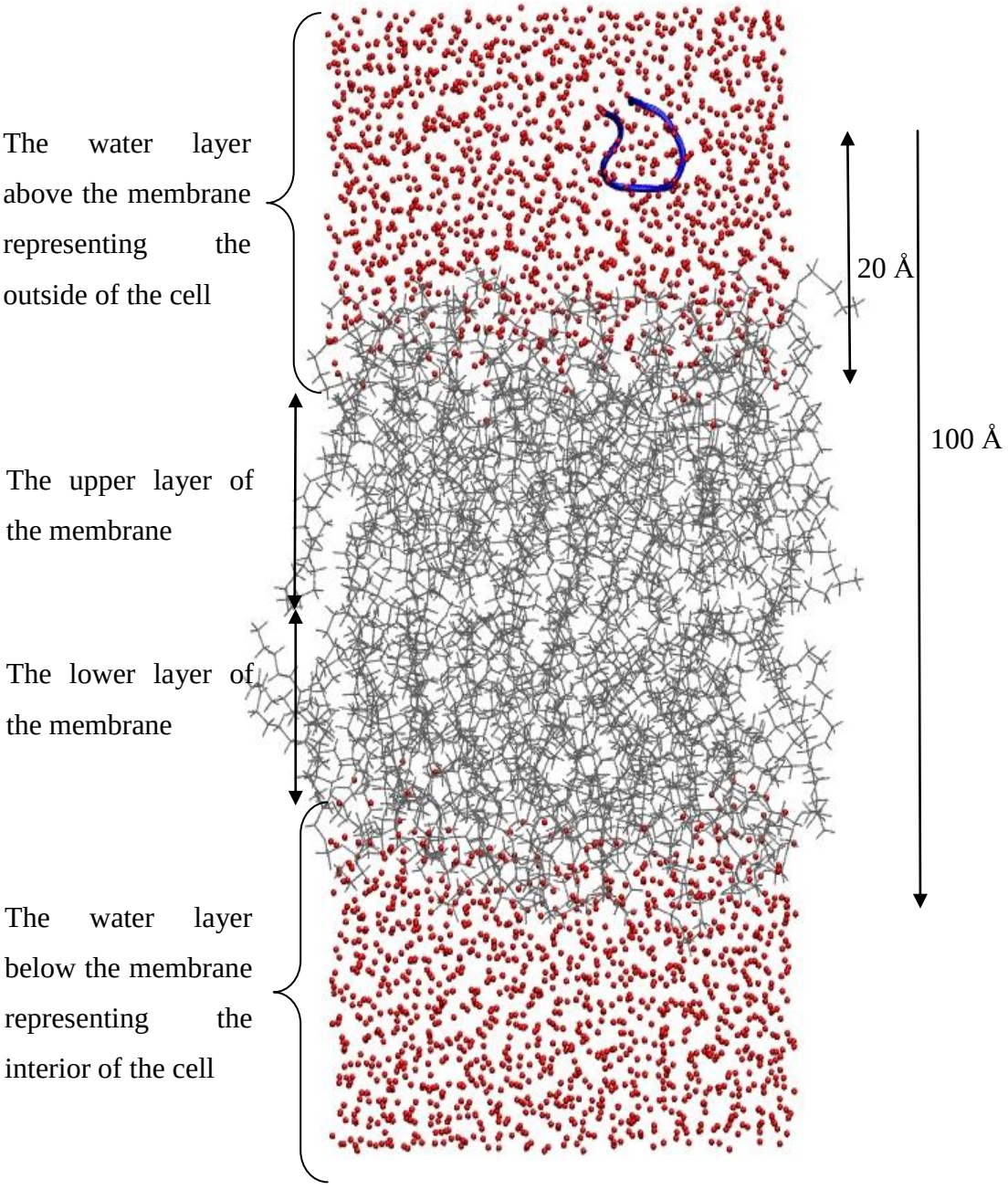

Figure 3.1. The initial structure of the system containing phospholipid bilayer (grey), peptide (blue, backbone shown) and water molecules (red sphere, oxygens shown). This same color scheme was used throughout the figures in this section.

3.1.1 The Effect of Pulling Velocity on the SMD Simulations

In the first four simulations in Table 3.1, the peptides were pulled with a spring constant of 10 kcal/mol/Å^2 from their centers of mass with velocities of 0.5 Å/ns, 2.5 Å/ns, 5.0 Å/ns, and 15.0 Å/ns.

The peptide was expected to traverse about 90-100 Å in 20 ns of the simulation time; therefore, the velocity parameter was chosen to be around 5.0 Å/ns. In order to observe the effect of the velocity on SMD simulations, the simulations were repeated with velocity values 0.5 Å/ns, 2.5 Å/ns and 15.0 Å/ns.

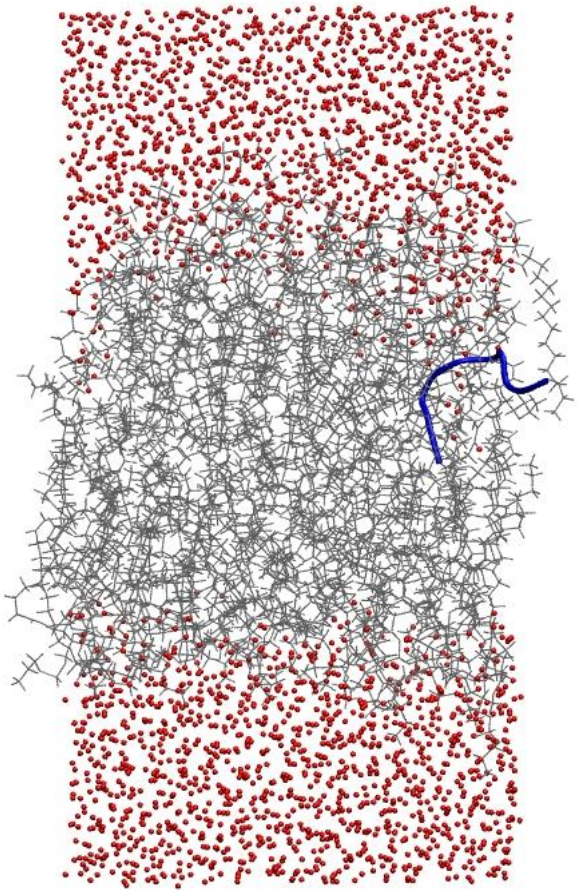

Figure 3.2. A snapshot at t = 6 ns from the SMD3 simulation (velocity = 5.0 Å/ns).

As an initial analysis, the simulations were inspected visually. At the beginning, the peptide was in the upper water layer and it was folded into a beta hairpin structure. As the SMD simulation progressed, the peptide moved in the z-direction as expected. Figure 3.2 shows a snapshot at t = 6 ns from the SMD3 simulation (v = 5.0 Å/ns). At this time, the peptide was totally immersed in the center of the membrane. The peptide assumed a different conformation than its initial state which was shown in Figure 3.1; however, it still had a folded conformation because it was pulled from its center of mass. The water molecules (red spheres) follow the peptide and go through the pore formed by the peptide.

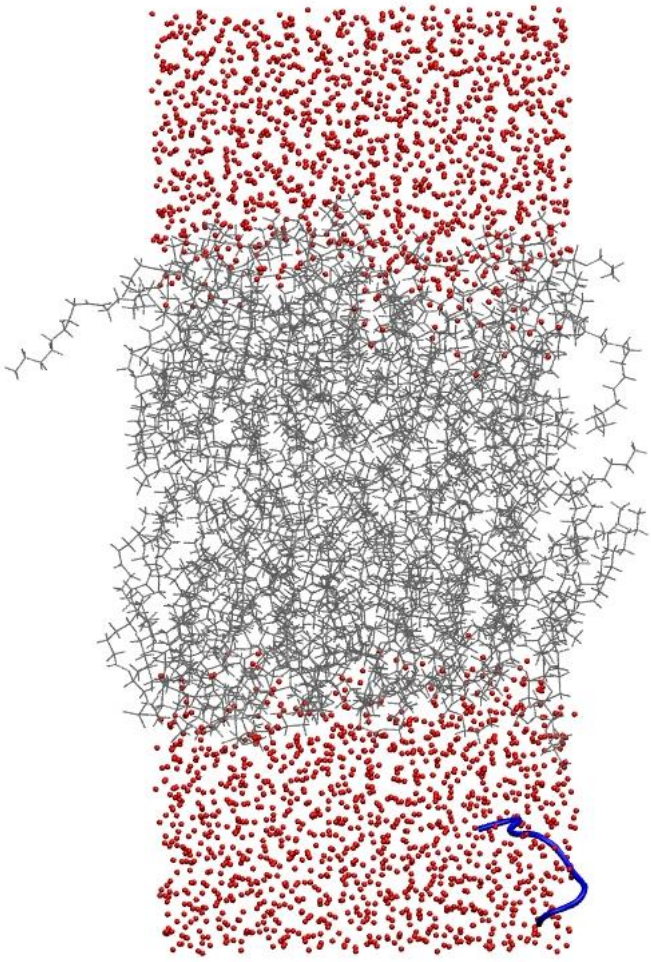

Figure 3.3. A snapshot at t = 14 ns from the SMD3 simulation (velocity = 5.0 Å/ns).

In Figure 3.3, a snapshot at t = 14 ns from the SMD3 simulation (v = 5.0 Å/ns) is shown. The peptide has left the membrane and lost its contacts with the membrane at this

time. When the peptide was compared with its structure at t = 6 ns, it had a similar folded structure. The water molecules have also left the membrane following the peptide.

After the visual inspection, the changes in the peptide, membrane and the water molecules were analyzed quantitatively.

Displacement was defined as the total change of location of the center of mass of the alpha carbon atoms of the peptide in x, y and z coordinates. The initial coordinates of the peptide, which were the same in all simulations, were chosen as the reference point. Displacement values start at 0 Å and report motion of the SMD atom (center of mass of the alpha carbon atoms) with respect to the initial coordinates of this atom.

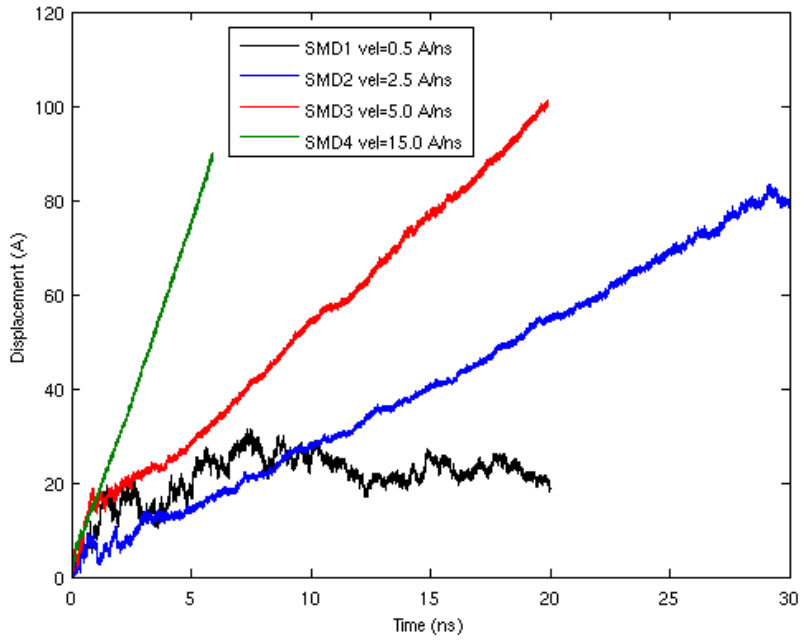

Figure 3.4. The displacements of the peptides in the simulations SMD1 (v = 0.5 Å/ns) (black), SMD2 (v = 2.5 Å/ns) (blue), SMD3 (v = 5.0 Å/ns) (red), and SMD4 (v = 15.0 Å/ns) (green). This same color scheme was used throughout the figures in this section.

Figure 3.4 shows the displacements of the peptides as a function of time for SMD1 (black), SMD2 (blue), SMD3 (red) and SMD4 (green). Initially for all cases, the peptide was in the same place, 0 Å. However, since the velocities varied, the final displacement values of the peptide altered in these simulations. The overall slopes of the plots reflected the velocities of the peptides and increased as velocity was increased.

Table 3.2. The final z and displacement values of the first four simulations.

Simulation	**Velocity (Å/ns)**	**z (Å)**	**Displacement (Å)**	**Simulation time (ns)**
SMD1	0.50	10.5	20.2	20.0
SMD2	2.50	96.8	83.5	30.0
SMD3	5.00	100.0	100.3	19.9
SMD4	15.00	88.5	90.1	5.9

Analysis of the displacement curves shows that as velocity increased, the increase in displacement became more gradual with fewer fluctuations, while when it was decreased the displacement curve acquired more fluctuations due to motion in the x-y plane. Table 3.2 shows the displacement in z and the total displacement for the four simulations at the end of the simulations. At lower velocity values, the peptide had more freedom to move in the x-y direction. When the final displacement and z values of the peptide of SMD1 were examined, the displacement was twice that of the final z value (Table 3.2). However, in the other remaining simulations, the final displacement and z values were very close to each other.

In SMD1, the peptide was pulled with a low velocity of 0.5 Å/ns. In 20 ns, it moved 10 Å in the z direction, as expected for the chosen velocity value, while its total displacement in x-, y-, z- directions was about 20 Å as shown in Figure 3.4, black curve. Up to 8 ns, the displacement of the peptide increased as expected; however, when this checkpoint was reached, the displacement curve started to decrease. In the first 8 ns, the peptide moved by 24.14 Å in the negative x-direction while it moved 3.84 Å in z-direction

also. After 8 ns, the peptide moved back to its initial position in x-direction. This movement caused the displacement curve to decrease. At the end of 20 ns, its 10 Å motion in the z-direction was only sufficient to move the peptide to the upper leaflet of the membrane.

In SMD2, the peptide traversed the membrane; however, it was unable to go out of the membrane completely at the end of 20 ns simulation time. At 20 ns the peptide was still in the membrane. Therefore, the simulation was let to run for 10 ns more. The peptide completely passed through and went out of the membrane in SMD3 when the displacement of the peptide reached 65.92 Å and SMD4 when its displacement reached 90.09 Å. The 4th simulation had the highest velocity value at 15.0 Å/ns. Since the distance the peptide needed to move was around 90-100 Å, 6 ns simulation was sufficient to complete one pass through the membrane (Figure 3.4, green curve).

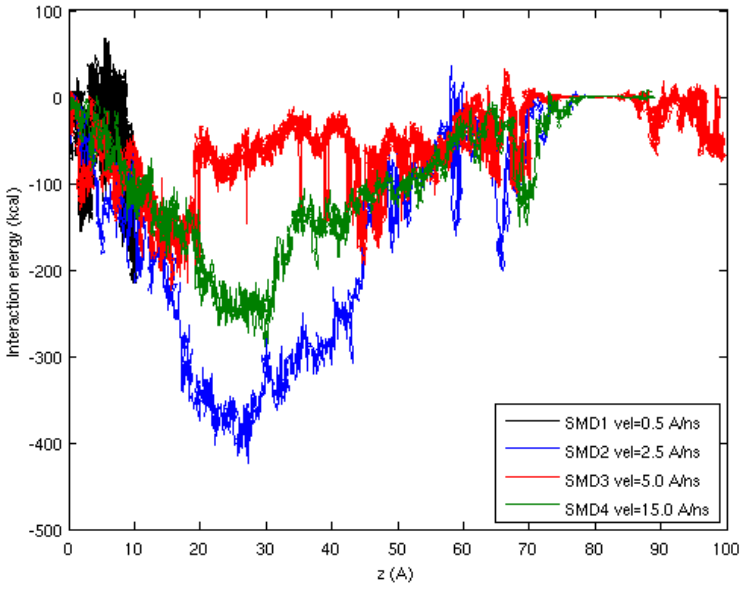

Figure 3.5. The interaction energy between the peptide and the membrane in the simulations SMD1 (v = 0.5 Å/ns) (black), SMD2 (v = 2.5 Å/ns) (blue), SMD3 (v = 5.0 Å/ns) (red), and SMD4 (v = 15.0 Å/ns) (green).

In Figure 3.5, the interaction energies between the peptide and the membrane were plotted as a function of change in z direction for the SMD atom for SMD1 (black), SMD2 (blue), SMD3 (red) and SMD4 (green). This interaction energy was the summation of electrostatic energy and van der Waals energy as calculated by the NAMD energy module in VMD. The top of the membrane corresponded to 9.8 Å, while the bottom of the membrane corresponded to 54.3 Å. As the peptide was pulled, the energy started to decrease and attained a minimum value. This minimum interaction energy value corresponded to the place where the peptide was totally immersed. As the peptide kept moving and started to go out of the membrane, the energy profile increased back to 0 kcal. When the peptide totally left the membrane, the total energy became almost stable around 0 kcal at around z = 70 Å.

The energy profiles of SMD2, SMD3 and SMD4 followed this trend since the peptide passed through the membrane and left it. When the interaction energies between the peptide and the membrane were compared, it was seen that the interaction was highest in SMD2 since it had the lowest minimum. Then the interaction of SMD2 was followed by SMD4 and SMD3 had the lowest interaction. When the energy profile of SMD1 was examined, the plot hardly started to decrease since the peptide did not go into the membrane and did not interact with the membrane.

Moreover, the electrostatic and van der Waals energies were tabulated in Table 3.3. Except for the highest energy values of SMD4, as the velocity increased, the magnitude of the minimum value of the interaction energy decreased. Indeed, it is expected that as the pulling velocity decreases, the peptide can form more favorable interactions with the membrane. The interaction energies satisfied this expectation for SMD2 and SMD3. The interaction energy profile of SMD2 (v = 2.5 Å/ns) decreased to -424.4 kcal/mol which was a much lower value than the interaction energy profile of SMD3 (v = 5.0 Å/ns) which was -224.2 kcal/mol. The interaction energy profile of SMD4 (v = 15.0 Å/ns) was -288.0 kcal/mol which is higher than the one for SMD3. From the electrostatic point of view, if there is an attraction between two objects, the electrostatic potential energy is negative. As the peptide was pulled slowly, the interaction energy attained more negative values. Thus, the expectation was also satisfied except for the values of SMD4.

Table 3.3. The highest interaction energy between peptide and membrane, and the change in the z-direction of the SMD atom.

Simulation	Velocity (Å/ns)	z (Å)	Interaction energy (kcal/mol)	Electrostatic energy (kcal/mol)	van der Waals energy (kcal/mol)
SMD1	0.50	-	-	-	-
SMD2	2.50	26.2	-424.4	-357.0	-67.4
SMD3	5.00	15.6	-224.2	-208.4	-15.8
SMD4	15.00	43.8	-288.0	-240.3	-47.7

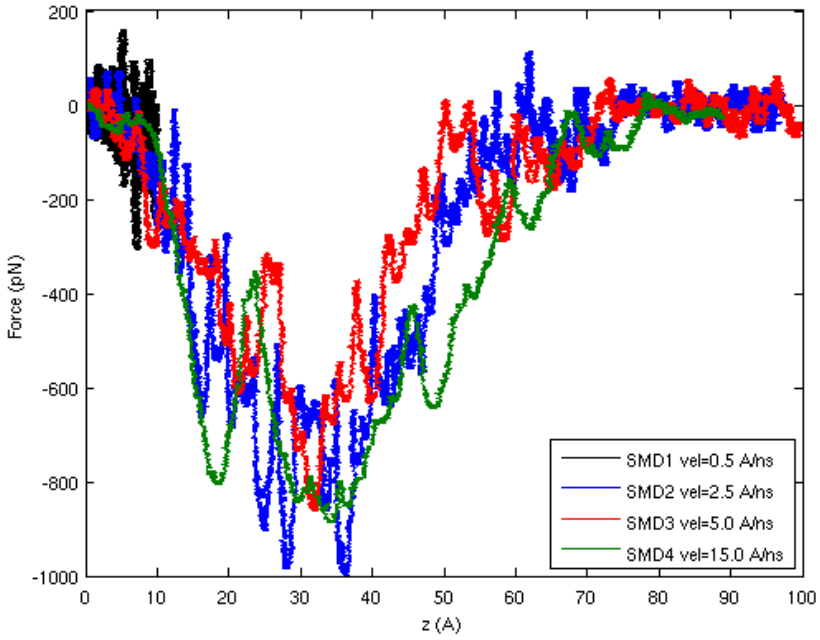

Figure 3.6. The force applied in simulations SMD1 (v = 0.5 Å/ns) (black), SMD2 (v = 2.5 Å/ns) (blue), SMD3 (v = 5.0 Å/ns) (red), and SMD4 (v = 15.0 Å/ns) (green) on the peptides. A running average is plotted for clarity.

Figure 3.6 shows the force applied in SMD1 (black), SMD2 (blue), SMD3 (red), and SMD4 (green) to the peptides. The values of the force values were negative since the force was applied in negative z direction. Similar to Figure 3.5, initial 10 Å was the water area above the membrane. Up to this point, there was not a major decrease in the curves, with

force values around 0 pN. The distance from 10 Å to 59 Å corresponded to the membrane; therefore, there were obvious decrease and increased in the plot. The maximum in negative direction was the place where the peptide was totally immersed into the membrane. After 70 Å, the force values became stable around 0 pN because the peptide had left the membrane. The force values in the water layer ($z < 10$ Å and $z > 59$ Å) were close to zero pN, suggesting that the peptide is able to move through the water layer without the application of any force.

Table 3.4 summarizes information of the distance covered in z direction, the maximum force applied to the peptide in negative z direction, and the z value at which the maximum force was applied.

Table 3.4. The distance and maximum force values of the first four simulations which differ in velocities as 0.5 Å/ns, 2.5 Å/ns, 5.0 Å/ns and 15.0 Å/ns.

Simulation	**Distance covered in z direction in 20 ns (Å)**	**Maximum force applied in negative z direction (pN)**	**z value where the maximum force is applied (Å)**
SMD1	10.5	306	7.4
SMD2	50.3	999	36.3
SMD3	100.0	863	32.0
SMD4	87.2	888	34.3

When the maximum forces applied to the peptides in negative z direction were compared, it was seen that the slowest peptide was pulled with 999 pN while the fastest one was pulled with 888 pN and the peptide of SMD3 was pulled with 863 pN which was almost equal to the fastest pulled peptide. In other words, when the velocity was lowest, the applied force value was highest. This was the result that, when the peptide was pulled with a slower velocity, a greater force was required to move the peptide through the phospholipid bilayer. However, even though similar force was required in SMD3 compared to SMD4, the work value was much higher in SMD4 (441 kcal/mol) compared

to SMD3 (293 kcal/mol) suggesting that the path taken in SMD3 followed the energy landscape more closely.

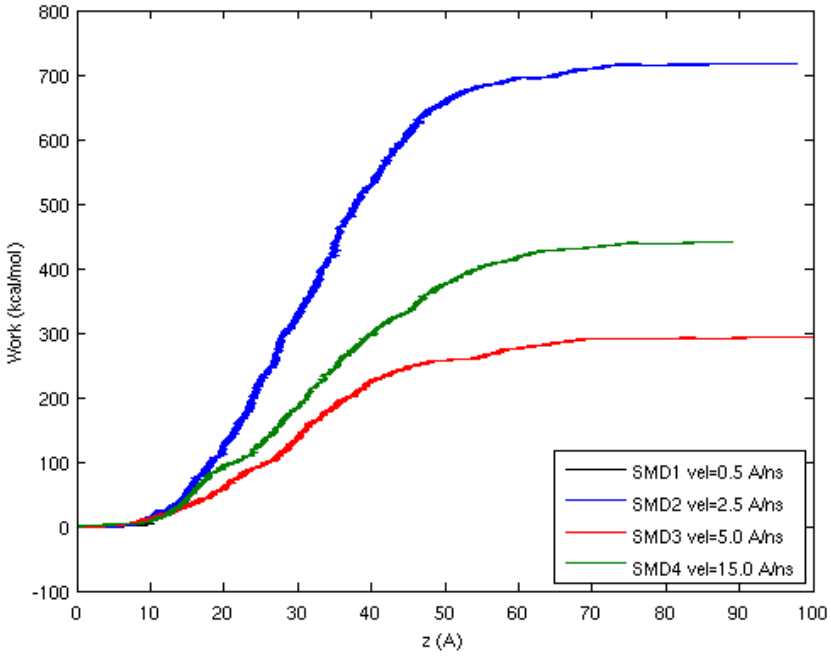

Figure 3.7. The work done in SMD1 (black), SMD2 (blue), SMD3 (red) and SMD4 (green) as a function of change in z-direction for SMD atom.

Figure 3.7 shows how work values vary for each simulation as the peptide moved. Work was calculated using Equation 3.1.

$$Work = \int F\, v\, dt \tag{3.1}$$

where F is pulling force, v is pulling velocity and dt is timestep.

In the initial 10 Å, there was no force applied to the peptide since this distance corresponded to the water area above the membrane. Therefore, there was no increase in

the work done for this region. When the peptide started to penetrate the membrane at z = 10 Å, the work done started to increase. When the peptide left the membrane, the force applied became 0 pN again and the work done reached a constant value.

Since the peptide of SMD1 had a very low velocity, the distance covered was very small. And because it did not enter the membrane, there was almost no significant increase in its force or work value. The work value increased in other simulations, with the highest work value attained in SMD2 (Table 3.5).

Table 3.5. The distance and maximum work values of the first four simulations which differ in velocities as 0.5 Å/ns, 2.5 Å/ns, 5.0 Å/ns and 15.0 Å/ns.

Simulation	**Distance covered in z direction in 20 ns (Å)**	**Maximum work done (kcal/mol)**	**z value where the maximum work is done (Å)**
SMD1	10.3	4	9.9
SMD2	50.3	717	93.6
SMD3	100.0	294	99.9
SMD4	87.2	441	88.1

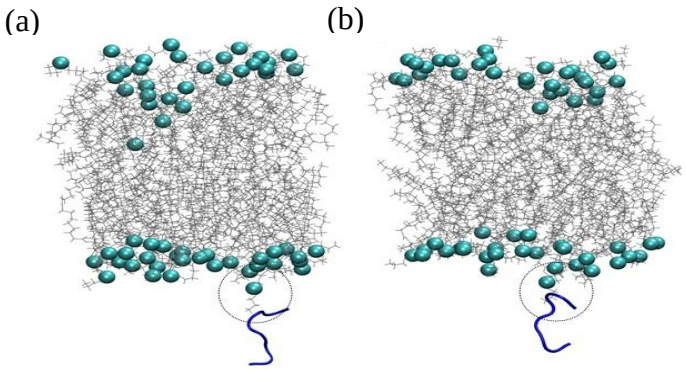

Figure 3.8. (a) The structure of SMD2 system at t = 29.3 ns. (b) The structure of SMD4 system at t = 5.9 ns. The lipid tails hanging out of the membrane are shown in the dotted circle.

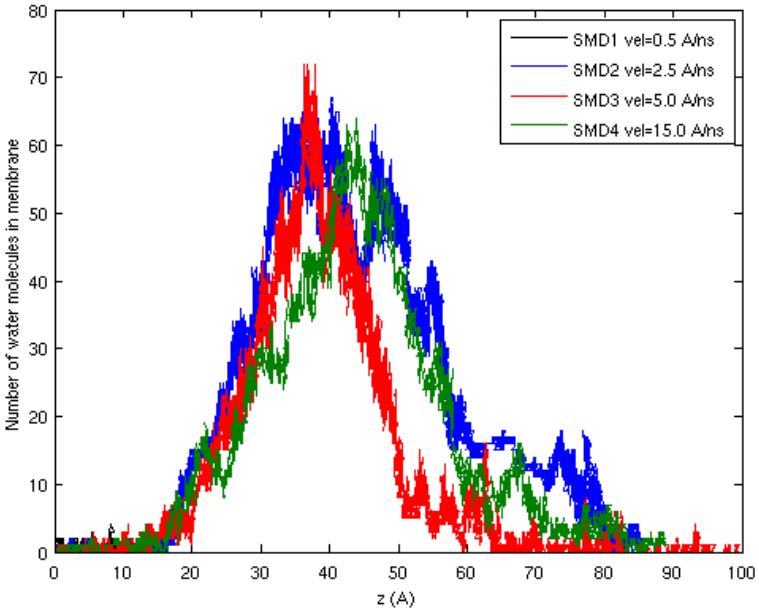

Figure 3.9. The number of water molecules present in the membranes in SMD1 (black), SMD2 (blue), SMD3 (red) and SMD4 (green) as a function of change in z-direction for SMD atom.

Insertion of the peptide into the membrane is expected to result in changes to the membrane. This disorder was first measured by the amount of water molecules moving into the membrane (Figure 3.9). The number of water molecules 10 Å above and below the middle of the membrane was counted for this analysis.

When the peptide started to insert into the membrane, the water molecules moved into the membrane with the peptide. When the peptide was totally immersed, the number of the water molecules within the membrane reached a peak and then the number of water molecules in the bilayer decreased as the peptide moved out of the membrane. Figure 3.9 shows that the peptides of SMD2, SMD3 and SMD4 accomplished the departure of the membrane. Moreover, there were almost same amount of water molecules in membrane in all the three accomplished simulations. There was no distinct change or increase in the number of water molecules in SMD1 because the peptide did not even enter the membrane.

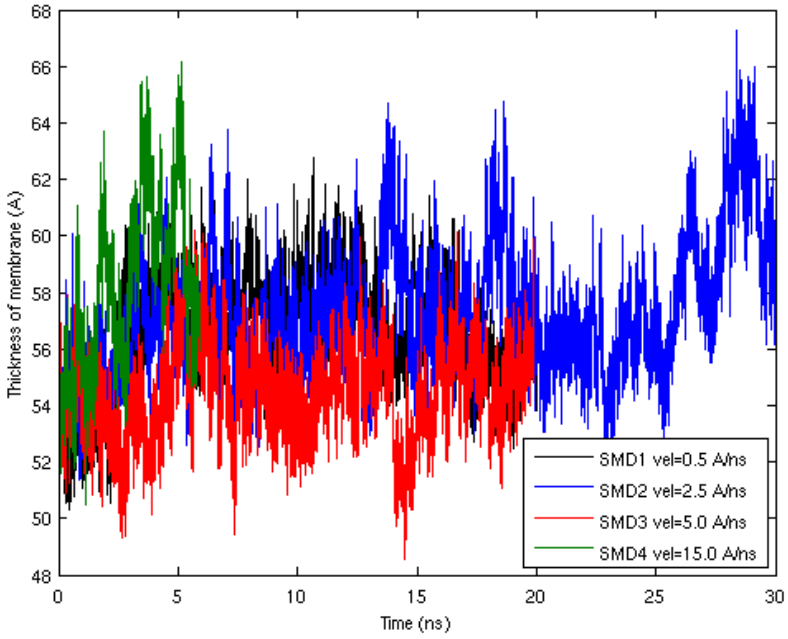

Figure 3.10. Thickness of the membranes in SMD1 (black), SMD2 (blue), SMD3 (red) and SMD4 (green) as a function of simulation time.

In Figure 3.10, the thickness of the membranes was plotted as a function of simulation time. In all simulations, except the 4-6 ns time interval of plot of SMD4 and the 26-30 ns time interval in the plot of SMD2, the thickness of the membrane, defined as the distance of the z coordinate value of the farthest atom in the bottom of the membrane from the z coordinate value of the farthest atom in the top of the membrane, stayed between 50 Å and 65 Å.

The membrane thickness does not change in SMD1, in which the peptide did not enter the bilayer. Nevertheless, the variation in membrane thickness in SMD1 could be used as a control. It also had fluctuations; therefore, the fluctuations of SMD2 and SMD3 were expected. There is a small increase in the final few ns of SMD2 because of hanging out lipid tails (Figure 3.8a). In SMD4, in the initial 4 ns interval, the thickness of the membrane was in acceptable values when it was compared with the fluctuations in SMD1. The final increase in the thickness of the membrane in SMD4 was also caused by hanging out of some lipid tails (Figure 3.8b).

When the peptide was pulled faster, there was less time for the peptide to interact with the membrane. Since there was higher interaction when the peptide was pulled slower, it required higher force to be applied in order to pass through the membrane. When the peptide was pulled out of the membrane, there was very small force to be applied. Similar to the observation that higher force was required, the work done on the peptide pulled slowly was higher than the faster ones. When the distortions on the membrane were considered, there was no obvious difference in both thickness of the membrane and the number of water molecules in the membrane.

3.1.2 The Effect of the Spring Constant on the SMD Simulations

The peptides were pulled with a velocity of 5.0 Å/ns from their centers of mass in SMD3 and SMD6. However, the peptides were pulled with different spring constants in these two simulations; the spring constant was 10 kcal/mol/Å^2 in SMD3 while the spring constant was 7 kcal/mol/Å^2 in SMD6. These two simulations were compared in order to assess the effect of the spring constant on the SMD simulations.

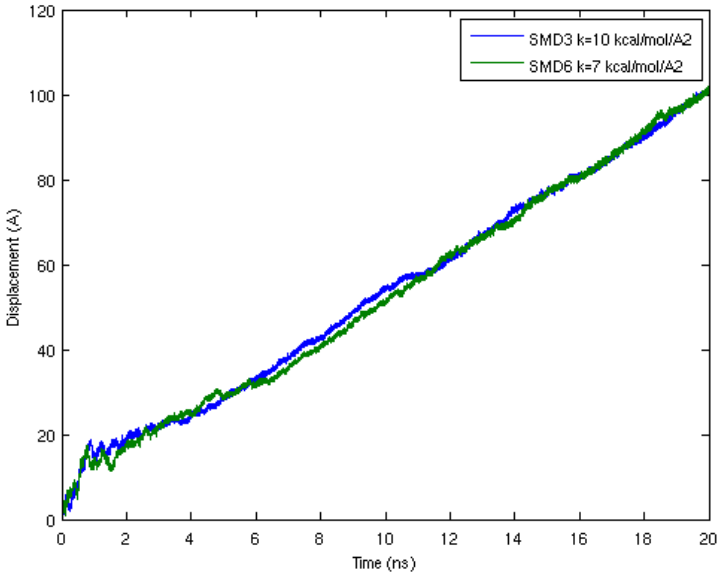

Figure 3.11. The displacements of the peptides in SMD3 (10 kcal/mol/Å^2) (blue) and SMD6 (7 kcal/mol/Å^2) (green).

Figure 3.11 shows displacements of the peptides in SMD3 and SMD6 in which different spring constants were used. Displacement was measured in x, y, z-directions. The plots of the displacements generally coincided. Since the peptides were pulled with same 5.0 Å/ns velocity, both of the peptides covered around 100 Å in 20 ns. While the peptide of SMD3 covered 101.1 Å, the peptide of SMD6 covered 101.8 Å. In both simulations, the slope was higher for the first 2 ns in which the peptide moved in both the x-y plane and z directions. After 2 ns, the peptide entered the membrane and moved only in the z-direction.

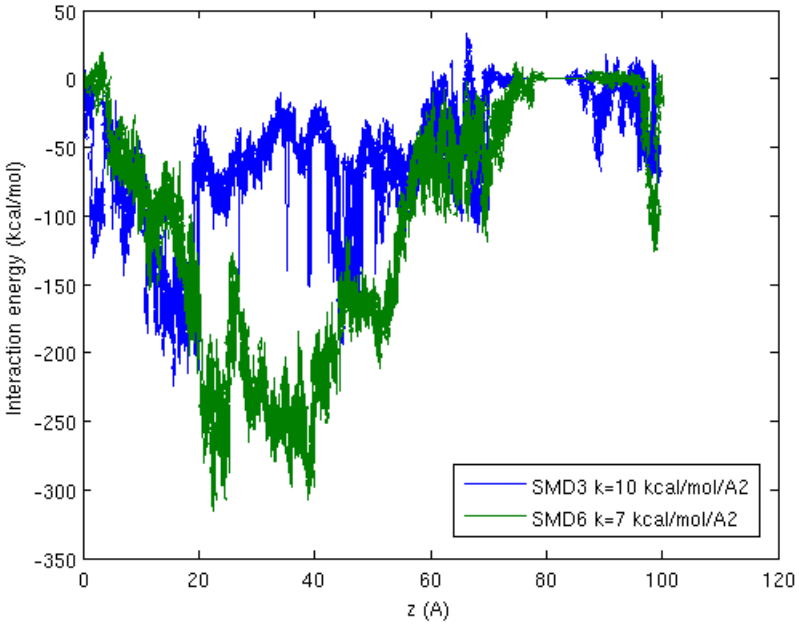

Figure 3.12. The interaction energy between the peptide and the membrane in SMD3 (blue) and SMD6 (green).

In Figure 3.12 the interaction energy between the peptide and the membrane was plotted as a function of the change in z of the SMD atom. Both simulations followed a similar interaction energy profile, starting from 0 kcal and decreasing to a minimum. After the minimum, the interaction energy increased back to 0 kcal. The minima for both curves corresponded to z = 20 Å, at which point the peptide contacts the phosphate heads of the upper leaflet. The plot of SMD6 (k = 7 kcal/mol/Å^2) had a deeper minimum of -315.2 kcal/mol than the minimum of SMD3 (k = 10 kcal/mol/Å^2) plot, which was -224.2

kcal/mol, meaning that there was a greater interaction when the spring constant was lower (Table 3.6). However, such a big interaction was not observed for the lower phosphate heads. The interaction energy increased back to 0 kcal around 80 Å since after this point, there was no membrane.

Table 3.6. The highest interaction energy between peptide and membrane, and the change in the z-direction of the SMD atom.

Simulation	**k (kcal/mol/Å^2)**	**z (Å)**	**Interaction energy (kcal/mol)**	**Electrostatic energy (kcal/mol)**	**van der Waals energy (kcal/mol)**
SMD3	10	15.6	-224.2	-208.4	-15.8
SMD6	7	22.4	-315.2	-261.7	-53.5

Lorenzo and Bisch, have shown that larger energy fluctuations were expected for softer springs [34]. They have used three different spring constant 0.1 kcal/mol/Å^2, 0.6 kcal/mol/Å^2 and 4.0 kcal/mol/Å^2 in order to drive this conclusion. The interaction energy reaches lower values and undergoes larger fluctuations but a significant difference in fluctuations could not be observed since 7 and 10 kcal/mol/Å^2 are close values.

Figure 3.13 shows force applied to the peptide in negative z direction in SMD3 (blue, 10 kcal/mol/Å^2) and SMD6 (green, 7 kcal/mol/Å^2). As the peptide moved along and touched the membrane, the force started to increase around 10 Å. The force applied reached a maximum at around z = 30 Å in SMD3 and at z = 40 Å in SMD6. The z value of the top of the membrane was 10 Å while the z value of the bottom was 55 Å. Thus both maxima in negative z direction corresponded to the inside of the membrane in where the peptide was totally immersed. The maximum applied force in SMD3 (863 pN) was greater than the maximum applied force in SMD6 (738 pN) (Table 3.7) suggesting that a higher spring constant led to an increase in the applied force. This result is in agreement with the

work of Lorenzo and Bisch who showed that larger force responses were obtained for stiff springs [34].

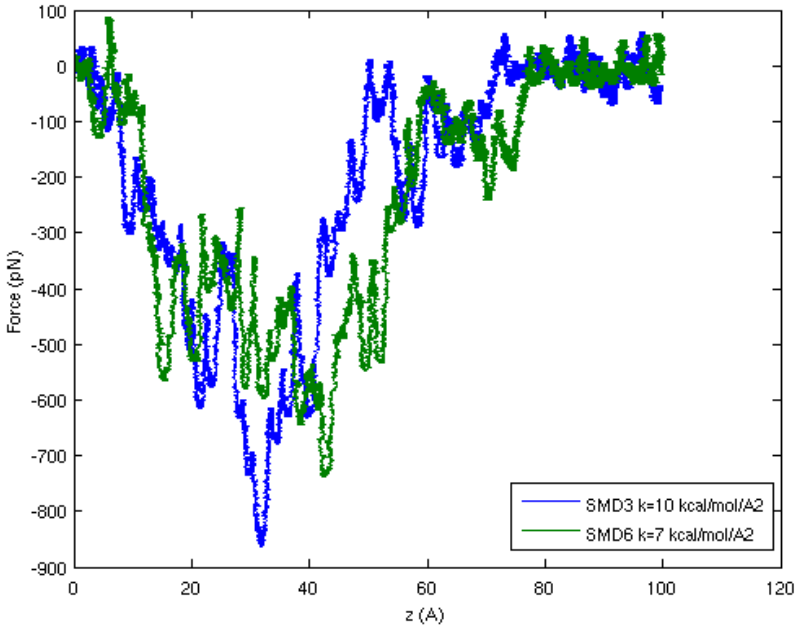

Figure 3.13. The force applied to the peptides in SMD3 (blue) and SMD6 (green) as a function of change in z-coordinates of the SMD atom. A running average is plotted for clarity.

Table 3.7. The distance covered in 20 ns, maximum force and maximum work values of the simulation systems of SMD3 and SMD6.

Simulation	**k (kcal/mol/Å^2)**	**Distance covered in 20 ns (Å)**	**Maximum force applied in negative z direction (pN)**	**Maximum work done (kcal/mol)**
SMD3	10	101.1	863 (31.9 Å)	293 (97.1 Å)
SMD6	7	101.8	738 (42.6 Å)	319 (96.9 Å)

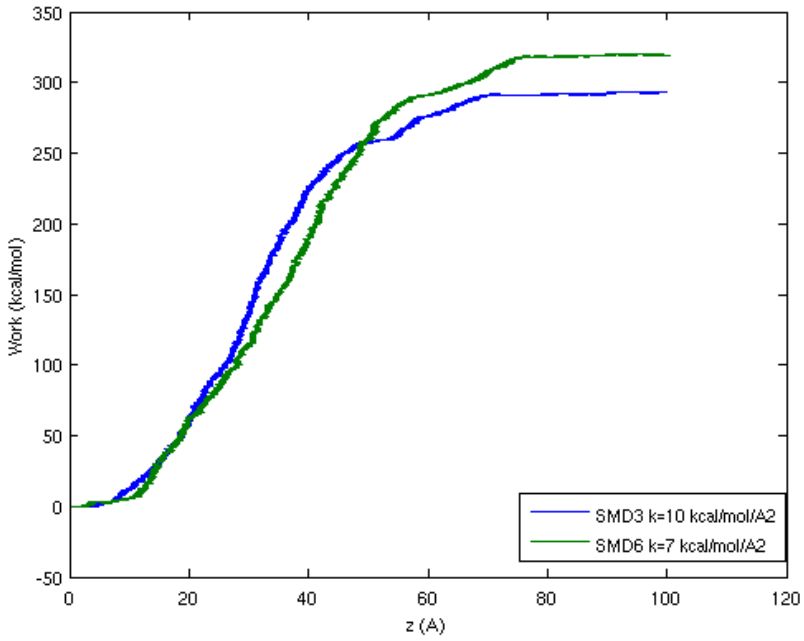

Figure 3.14. The work done on the peptides in SMD3 (blue, 10 kcal/mol/Å^2) and SMD6 (green, 7 kcal/mol/Å^2) as a function of change in z-coordinates of the SMD atom.

Figure 3.14 shows the work profile in SMD3 and SMD6 as a function of change in z-direction for the SMD atom. The work values along the entire distance were very close to each other. Up the 20 Å, the peptides had equal work values as they increased from the stable values. Then the work values of the peptide of SMD3 started to increase more than the work values of SMD6. But this difference was very small. At 50 Å, their work values became equal again and the peptide of SMD6 started to increase more. Around 75 Å, both work values reached stability. They ended up as the work values of SMD6 were greater than the ones of SMD3. Nevertheless, as seen in Table 3.7, these values were quite close to each other.

Table 3.7 (The z-values corresponding to the maximum force and maximum work values are shown in parenthesis.) shows that as the spring constant decreased, the maximum applied force in negative z direction decreased, but the maximum work done on the peptide increased. As expected, the softer spring whit the force constant 7 kcal/mol/Å^2 attained a lower maximum force value than the stiffer one (k = 10 kcal/mol/Å^2) did.

However, work values did not increase with increasing k and force even though work is the integration of F.v over time. On the contrary, work value was slightly lower at 293 kcal/mol with the stiffer force constant of k = 10 kcal/mol/Å^2 than 319 kcal/mol obtained with k = 7 kcal/mol/Å^2.

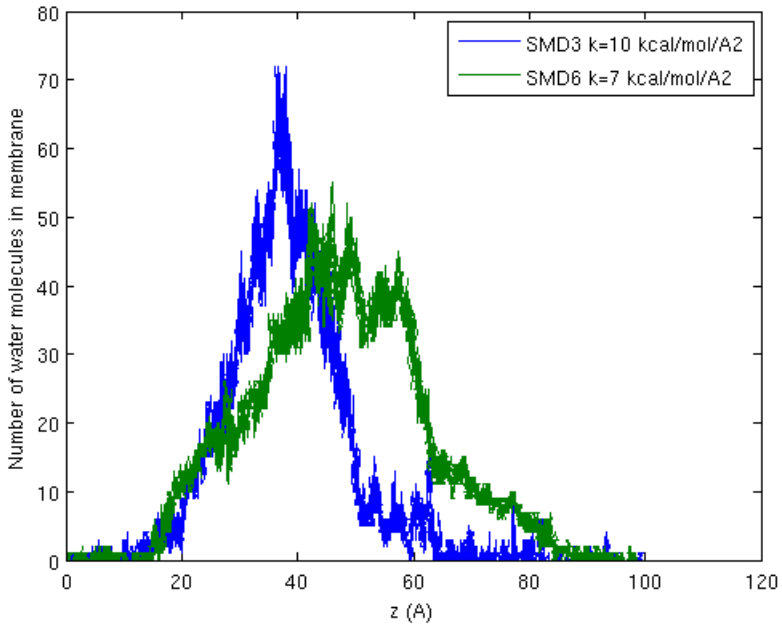

Figure 3.15. The number of water molecules present in the membrane in SMD3 (blue, 10 kcal/mol/Å^2) and SMD6 (green, 7 kcal/mol/Å^2) as a function of change in z-coordinates of the SMD atom.

In Figure 3.15, the amount of the water molecules going into the membrane was plotted. Both curves followed a similar path such that the number of the water molecules increased as the peptide contacted and inserted into the membrane, reached a maximum, and decreased as the peptide left the membrane. The peak occurred when the peptide was totally immersed in the center of the membrane. It was seen that for both simulations the peptides started to enter the membrane at the same time. However, the plot of SMD3 reached its maximum about 2 ns earlier. Moreover, plot of SMD3 decreased to zero much earlier than the plot of SMD6. Despite of this faster movement, the maximum number of water molecules in the membrane of SMD3 was much higher than the amount in the

membrane of SMD6. This meant that the distortion of the membrane was higher when the spring constant was larger.

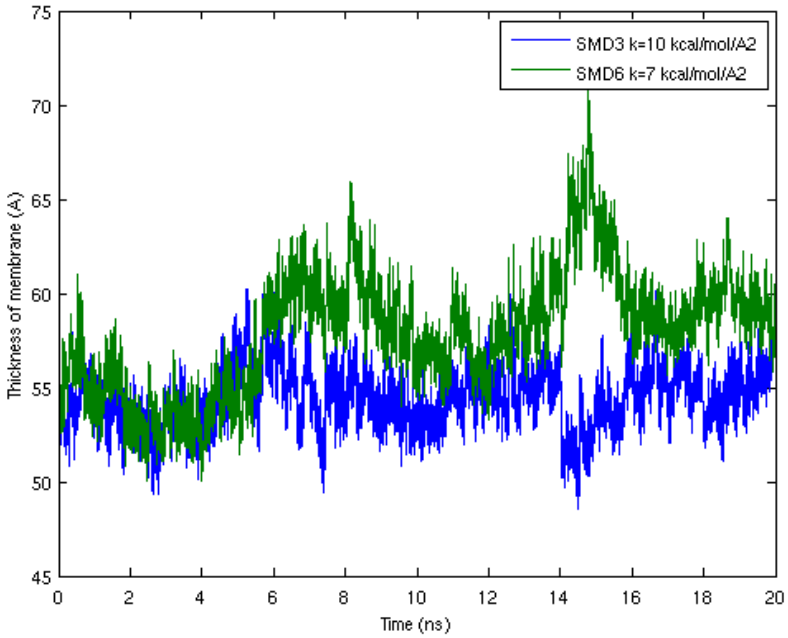

Figure 3.16. Thickness of the membranes in SMD3 (blue, 10 kcal/mol/Å^2) and SMD6 (green, 7 kcal/mol/Å^2) as a function of simulation time.

In Figure 3.16, the thicknesses of the membranes in SMD3 and SMD6 were plotted as a function of simulation time. Until 6 ns, the thicknesses did not alter much. But 6 ns corresponded to the time when the peptide was totally immersed in the membrane. After this checkpoint, the thickness of the membrane of SMD6 increased while the one for SMD3 remained the same. The thickness of membrane of SMD6 even made a huge jump at 14 ns because one lipid tail stuck to the peptide at that time and left the membrane bilayer with the peptide for about 1 ns. Then this hanging out lipid turned back to the membrane.

When the effect of the spring constant on the SMD simulation was seeked, it was shown the peptide pulled with the softer spring (k = 7 kcal/mol/Å^2) has greater interaction with its membrane. This was in agreement with the work of Lorenzo and Bisch [34] since

softer springs has larger energy fluctuations. Moreover, the force required to pull the peptide in SMD3 (k = 10 kcal/mol/Å^2) was higher. Despite, the work done on the peptide is lower in SMD3. Nevertheless, there was less amounts of water molecules in SMD6, while the water molecules were present in the membrane for a longer period in SMD6.

3.1.3 The Effect of Place of Pulling on the SMD Simulations

The peptides were all pulled with a constant velocity of 5.0 Å/ns and a spring constant of 7 kcal/mol/Å^2 in SMD6, SMD7 and SMD8. However, these peptides were pulled from different places. The peptide was pulled from its center of mass in SMD6, from its C terminus in SMD7 and from its N terminus in SMD8.

In all cases, the peptides were initially positioned at the center of the upper water side of the system which was 20 Å above of the top of the membrane. The peptides were expected to move about 90-100 Å in 20 ns; therefore, the velocity was set to 5.0 Å/ns.

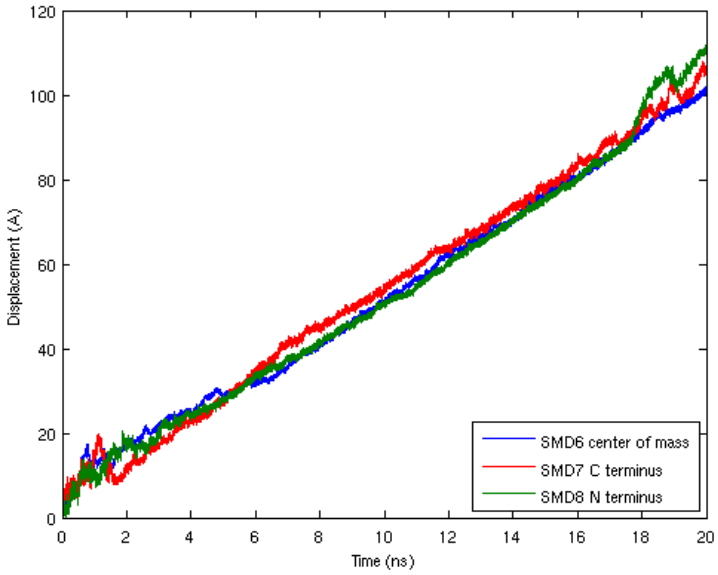

Figure 3.17. The displacements of the peptides in the simulations SMD6 (center of mass, blue), SMD7 (C terminus, red), SMD8 (N terminus, green). This same color scheme was used throughout the figures in this section.

Figure 3.17 shows the displacement of the peptide throughout the simulations. The jump in the first 1.5 ns of the simulations was due to the movement of the peptide in x and y directions while it was in water. The peptide moved 7.8 Å in negative x direction in SMD6 while the peptide made a move of 4.0 in positive x direction in SMD7. The displacement curves followed a similar trend rising all up to 100 Å. However, when the positions of the curves were analyzed, it was seen that the displacement of the peptide in SMD7 was above the others while the displacement of the peptide in SMD8 was below the others for most of the time. In SMD7, the peptide was pulled from its C terminus, while it was pulled from its N terminus in SMD8. Displacement is measured as the change in x-, y-, z-coordinates for the SMD atom, and therefore the difference in the displacement values is expected. In this section the peptide was pulled from different parts such as center of mass (SMD6), C terminus (SMD7) and N terminus (SMD8).

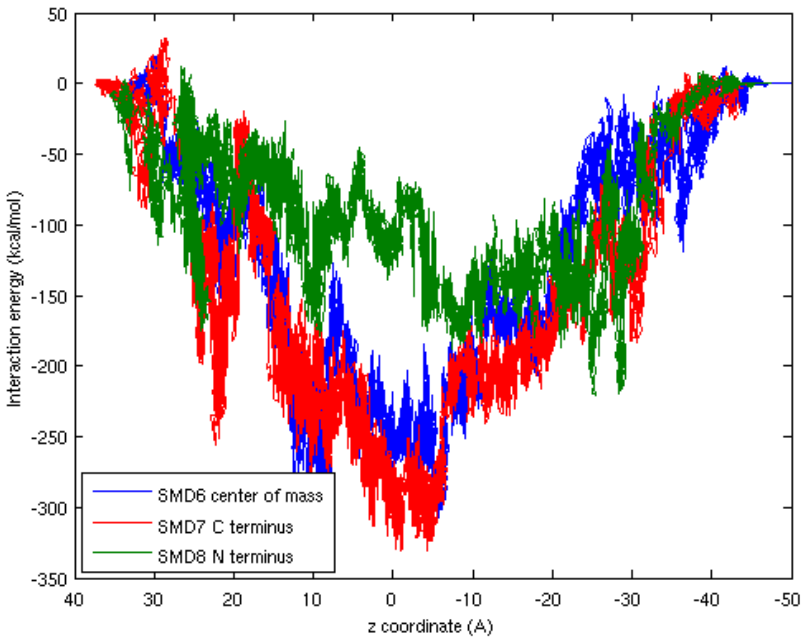

Figure 3.18. The interaction energy between the peptide and the membrane in the simulations SMD6 (center of mass, blue), SMD7 (C terminus, red), SMD8 (N terminus, green).

In Figure 3.18, the interaction energies between the peptide and the membrane were plotted as a function of z coordinate of the peptide in SMD6 (center of mass, blue), SMD7 (C terminus, red) and SMD8 (N terminus, green). The z-coordinate of the top of the membrane defined by the farthest atom of the bilayer above the center of the bilayer was 25 Å in z coordinates and that of the bottom was -25 Å while 0 Å was the center of the membrane. The interaction energy decreased with a similar slope in all simulations and reached a minimum value at around z = 0 Å except in SMD8 (N terminus). Nevertheless, the minimum of SMD6 (center of mass) which was -315.2 kcal/mol and the minimum of SMD7 (C terminus) which was -331.2 kcal/mol were very close to each other and were reached at around z = 0 Å (Table 3.8). The interaction was at maximum when the peptide was in the middle of the membrane for these two cases. However, the minimum of SMD8 was reached at z = -25 Å. The minimum of SMD8 at this point was -220.2 kcal/mol which is lower in magnitude.

Table 3.8. The highest interaction energy between peptide and membrane, and the change in the z-direction of the SMD atom.

Simulation	**Place of pulling**	**z (Å)**	**Interaction energy (kcal/mol)**	**Electrostatic energy (kcal/mol)**	**van der Waals energy (kcal/mol)**
SMD6	Center of mass	10.7	-315.2	-261.7	-53.5
SMD7	C terminus	-4.3	-331.2	-261.0	-70.2
SMD8	N terminus	-25.4	-220.2	-171.0	-49.2

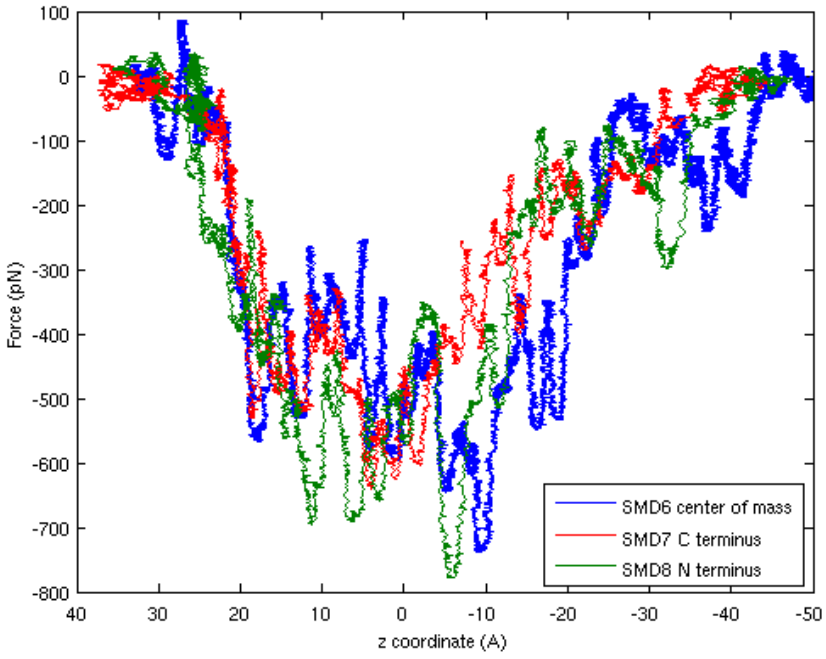

Figure 3.19. The force applied to the peptides in the simulations SMD6 (center of mass, blue), SMD7 (C terminus, red), SMD8 (N terminus, green). A running average is plotted for clarity.

Figure 3.19 shows force applied to the peptide in negative z direction in SMD6 (center of mass, blue), SMD7 (C terminus, red), SMD8 (N terminus, green). The force started to increase at around z = 20 Å since the peptide was very close to the membrane at this point. The force in SMD6 (center of mass) and SMD8 (N terminus) reached their maximum values at z = -10 Å while the maximum was reached at z = 0 Å in SMD7 (C terminus). This region between 0 and -10 Å corresponds to the region in which the peptide was totally embedded in the middle of the membrane. Therefore, the greatest force was applied when the peptide was in the middle of the membrane. The maximum force was 738 pN in SMD6 (center of mass) and 779 pN in SMD8 (N terminus). The maximum force applied was lower at 640 pN in SMD7 (C terminus) suggesting that it was easier to pull from the C terminus. As the peptide left the membrane, the applied force decreased back to 0 pN. The force values in all simulations were 0 pN at the end of the simulation when the peptide was totally away from the membrane after z = - 30 Å.

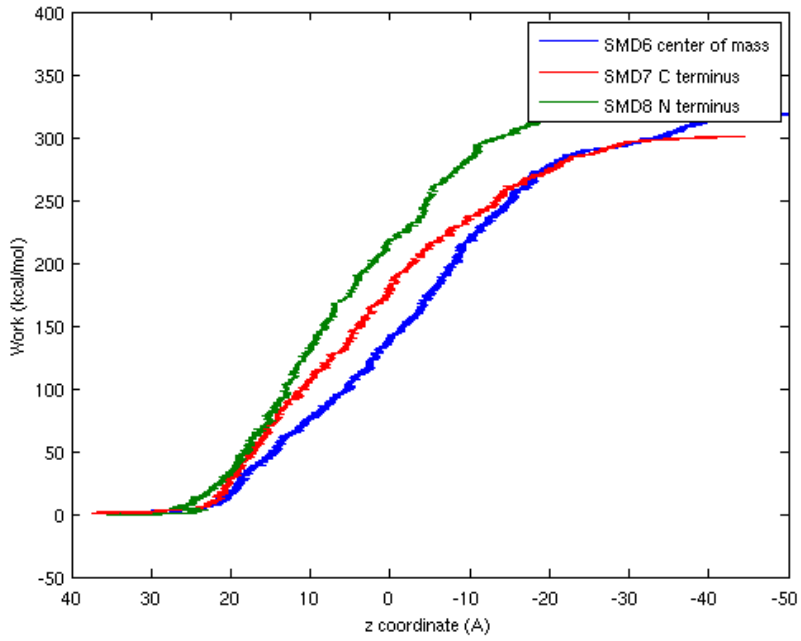

Figure 3.20. The work done on the peptides in the simulations SMD6 (center of mass, blue), SMD7 (C terminus, red), SMD8 (N terminus, green) as a function of change in z-direction for the center of mass of the alpha carbons of the peptide.

The work done on the peptide in SMD6 (center of mass, blue), SMD7 (C terminus, red), SMD8 (N terminus, green) was plotted in Figure 3.20 as a function of change in z-direction for the center of mass of the alpha carbons of the peptide. All the work values started to increase at z = 25 Å. The work curves coincided and increased together until the peptide moved out of the membrane boundary at z > -25 Å. After -30 Å, the force profiles of SMD6 (center of mass), SMD7 (C terminus) and SMD8 (N terminus) reached stable values.

Table 3.9 (The z-values corresponding to the maximum force and maximum work values are shown in parenthesis.) shows the maximum force applied in negative z direction and maximum work done. The maximum force and the total work values were lowest is SMD7, in which the peptide was pulled from its C terminus.

Table 3.9. The distance covered in 20 ns, maximum force and maximum work values of the simulation systems of SMD6, SMD7 and SMD8.

Simulation	Place of pulling	Distance covered in 20 ns (Å)	Maximum force applied in negative z direction (pN)	Maximum work done (kcal/mol)
SMD6	center of mass	100.3	738 (-9.3 Å)	319 (-49.6 Å)
SMD7	C terminus	100.9	640 (4.1 Å)	303 (-44.2 Å)
SMD8	N terminus	100.4	778.9 (-5.6 Å)	351 (-45.4 Å)

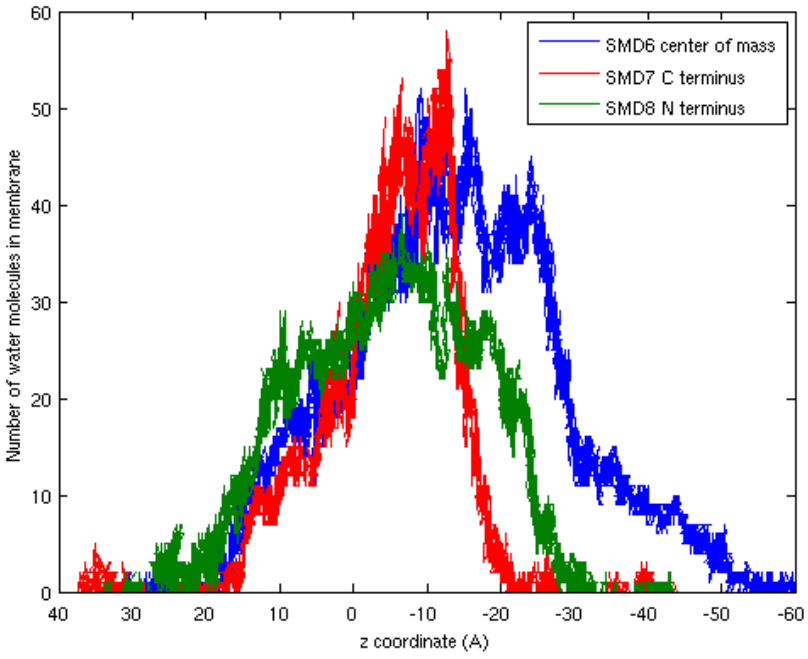

Figure 3.21. The number of water molecules present in the membrane in the simulations SMD6 (center of mass, blue), SMD7 (C terminus, red), SMD8 (N terminus, green) as a function of change in z-direction for the center of mass of the alpha carbons of the peptide.

In Figure 3.21, the number of water molecules which moved into the membrane in the SMD6 (center of mass, blue), SMD7 (C terminus, red), SMD8 (N terminus, green) was plotted as a function of change in z-direction for the center of mass of the alpha carbons of the peptide. Then the number made a maximum and decreased back to 0. The initial increase corresponded to the time when the center of mass of peptide entered the membrane, when its z-coordinate was 20 Å in SMD8 and when it was 24 Å in SMD6 and SMD7. When the peptide was totally immersed in the middle of the membrane, the number

of water molecules reached a maximum. As the peptide moved out, the number of water molecules decreased. All the three systems had their maximum number of water molecules when z was between -10 Å and 0 Å. This was the place where the peptide was totally immersed in the membrane. The maximum number of water molecules was almost equal in SMD6 (center of mass, 55 water molecules) and SMD7 (C terminus, 58 water molecules). The maximum number of water molecules in SMD8 (N terminus) was lower than the other two simulations (39 water molecules). Even though the water molecules in SMD8 entered earlier and the ones in SMD7 entered at the same time with the ones in SMD6, they left the membrane earlier when the peptide was pulled from its C terminus than when the peptide was pulled from its center of mass and N terminus.

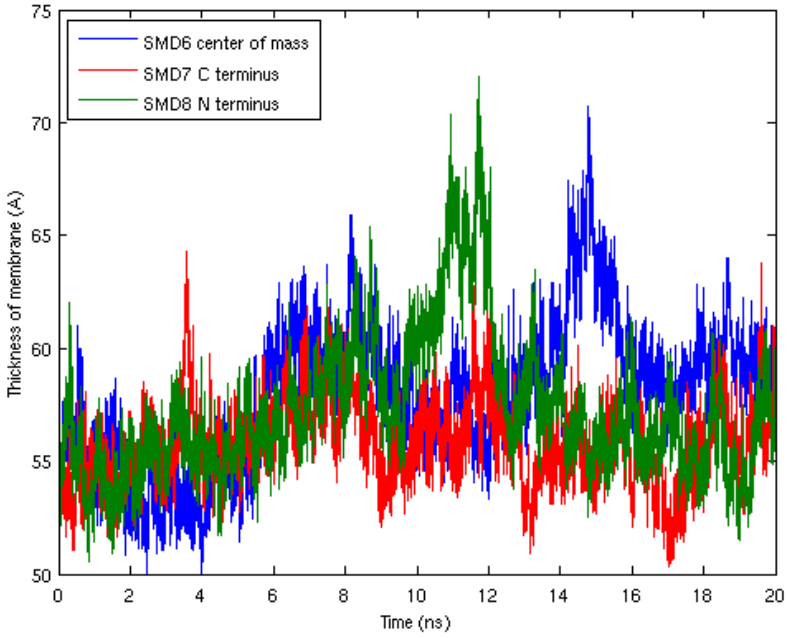

Figure 3.22. The thickness of the membranes in the simulations SMD6 (center of mass, blue), SMD7 (C terminus, red), SMD8 (N terminus, green) as a function of simulation time.

Figure 3.22 shows how the thicknesses of the membranes change during the simulations. Up to 6 ns, there seemed no obvious thickening for all the membranes. After this checkpoint, the membrane of SMD6 thickened and preserved its new thickness (59.4

Å) throughout the remaining simulation. The thickness of the membrane of SMD7 (55.8 Å) did not alter much for entire simulation. The thickness of the membrane of SMD8 was around 57.2 Å. Thus, there was not a major difference in the thickness values of the membranes.

3.2 Membrane Uptake of a Modified BLIP Based Peptide

In order to observe and analyze the passing through of a peptide with the sequence LLIILHAAGDYYAY through a model bacterial cell membrane, several steered molecular dynamics simulations were performed. The LLIIL part of the peptide is the cargo carrying part. It was extracted from the 18 amino acid long pVEC peptide. The remaining HAAGDYYAY part, of which the translocation was the aimed and explored in the previous section, is the cargo part of the peptide. In these simulations, peptides were prepared with two different conformations, namely conformations 1 and 2.

3.2.1 The Effect of the Place of Pulling on the MD Simulations with First Conformation

Three steered MD performed starting with conformation 1 were performed with different place of pulling. An additional simulation (MD4) was performed with lower speed and higher force constant, pulling the peptide from its center of mass. The change in force constant did not change the peptide transport mechanism, and therefore this simulation saved as a test for changing the pulling velocity.

The peptides of first three simulations shown in Table 3.10 were pulled with the same spring constant value 7 kcal/mol/$Å^2$ and with the same velocity of 5.0 Å/ns. However, the simulations varied in the choice of SMD atom. The peptide was pulled from its center of mass in MD1, while the peptides were from its C terminal alpha carbon atom in MD2 and N terminal alpha carbon atom in MD3. Nevertheless, the following interaction energy profiles, the force applied in negative z direction, the work done on the peptide and

the number of water molecules present in the membrane were plotted as a function of change in z coordinate values of the center of mass of the alpha carbons of the peptide.

Table 3.10. The 4 MD simulations having different spring constants, velocities and places of pulling with peptide having sequence LLIILHAAGDYYA which has the first conformation.

Simulation	**k (kcal/mol/Å^2)**	**velocity (Å/ns)**	**place of pulling**
MD1	7	5.00	center of mass
MD2	7	5.00	C terminus
MD3	7	5.00	N terminus
MD4	10	2.50	center of mass

In all cases, the peptide (blue, cartoon representation) was initially positioned in the upper water layer (red) of the system, about 50 Å from the center of the lipid bilayer (grey) as shown in Figure 3.23. The peptides were expected to move about 90-100 Å in 20 ns; therefore, the velocity parameters were set to 5.0 Å/ns. There were water molecules above and below of the membrane. The phosphate atoms of the lipid tails of the membrane were free to move in all three directions.

The system of every MD simulation tabulated in Table 3.10 had the same initial coordinates shown in Figure 3.23. The longer arrow on the right-hand side of the system representation was specific for center of mass pulling. It shows the starting point, direction and the path that the pulling is done.

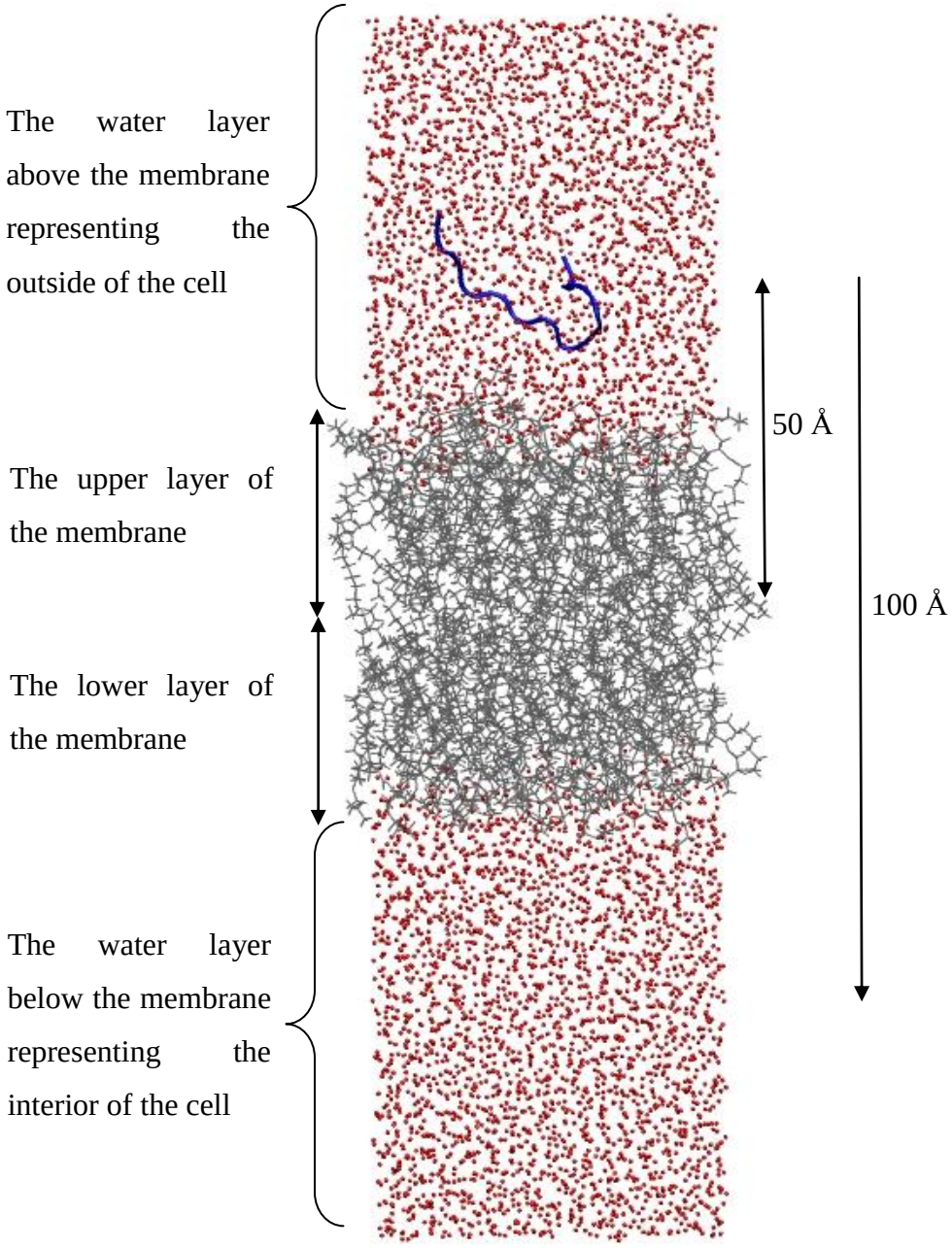

Figure 3.23. The initial structure of the system containing phospholipid bilayer (grey), peptide (blue, backbone shown) and water molecules (red sphere, oxygens shown). This same color scheme was used throughout the figures in this section.

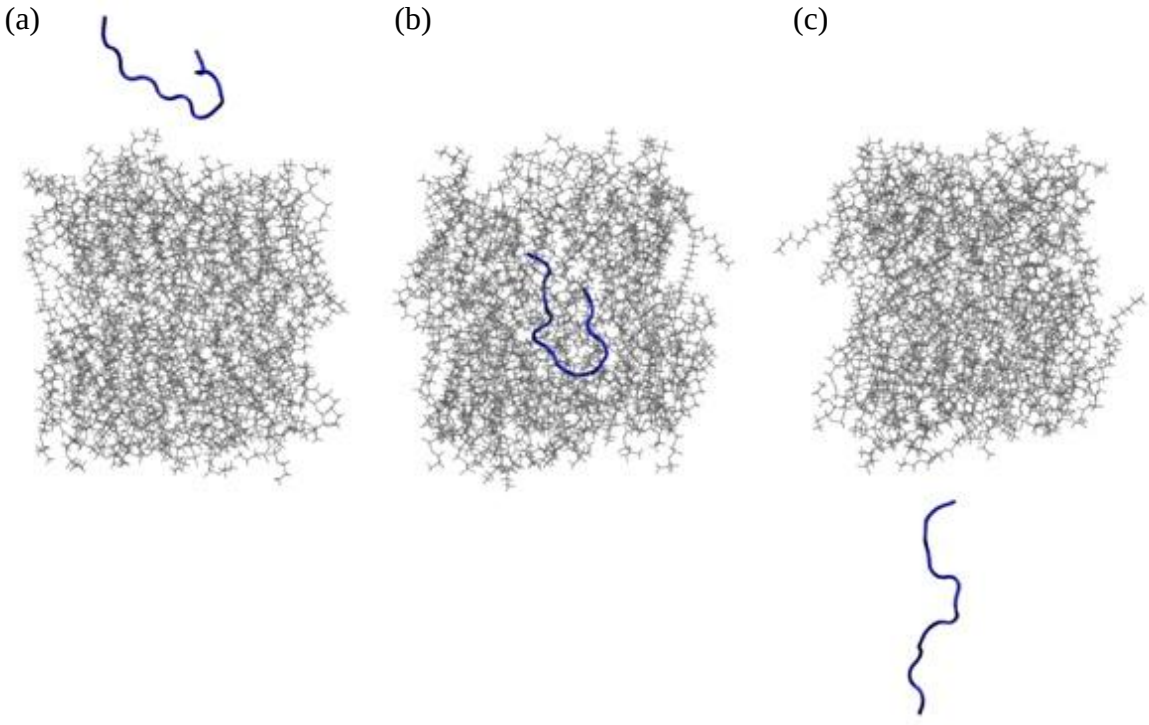

Figure 3.24. A snapshot from the MD1 simulation (k = 7 kcal/mol/Å^2, velocity = 5.0 Å/ns, center of mass pulling) system containing phospholipid bilayer (grey) and peptide (blue, backbone shown) at (a) t = 0 ns (b) t = 8 ns (c) t = 17 ns.

At the beginning, the peptide was in the upper water layer and it was folded into a beta hairpin structure (Figure 3.24(a)). As the MD simulation progressed, the peptide moved in the z-direction as expected. In Figure 3.24(b) a snapshot at t = 8 ns from the MD1 simulation (k = 7 kcal/mol/Å^2, velocity = 5.0 Å/ns, center of mass pulling) was shown. The peptide was totally immersed in the center of the membrane.

Figure 3.24(c) shows a snapshot at t = 17 ns from the MD1 simulation (k = 7 kcal/mol/Å^2, velocity = 5.0 Å/ns, center of mass pulling). The peptide totally left the membrane. Even though the peptide kept its folded structure until it reached the center of the membrane, it unfolded as the simulation continued. This unfolding continued, while the peptide was going out of the membrane. When it lost its total contact with the membrane, it was unfolded entirely. As it moved in the cytoplasm, it started to fold again.

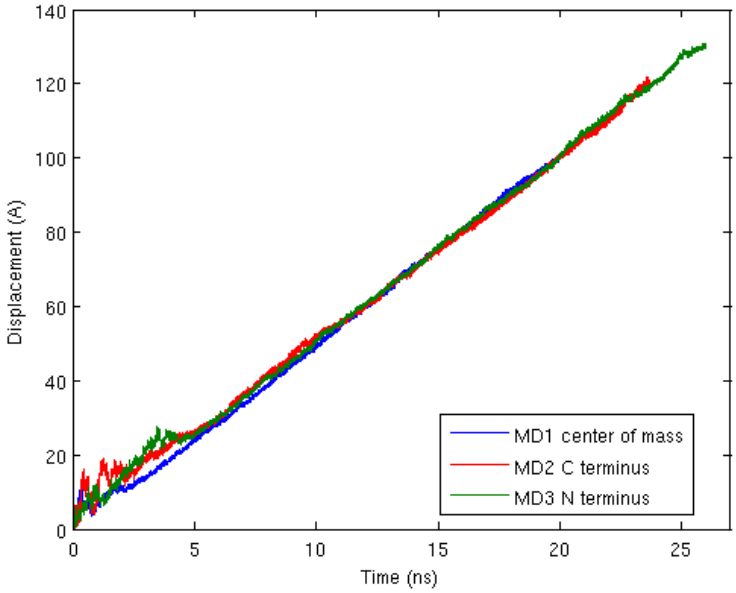

Figure 3.25. The displacements of the peptides in the simulations MD1 (center of mass, blue), MD2 (C terminus, red), MD3 (N terminus, green). This same color scheme was used throughout the figures in this section.

Figure 3.25 shows the displacement of the peptide as a function of time for MD1 (blue), MD2 (red) and MD3(green). Displacement was defined as the total change of location of the peptide in x, y and z coordinates. In other words, it was calculated as the square root of addition of squares of change of location in x, y and z coordinates. There were fluctuations and jumps in the displacement profiles of all simulations after which the displacement increased regularly. The displacement plot of MD1 had a small jump in the first 0-1 ns time interval. The displacement of the peptide of MD2 had fluctuations in 0-6 ns interval. Similarly, the plot of the displacement of MD3 had big jumps in 0-6 ns time interval. The sudden increases in MD1 were negligibly small and short compared with the others. The reasons for the fluctuations of the displacements of MD2 and MD3 were unfolding and unexpected moves of the peptides. Since the peptide was pulled from its termini in these simulations, the peptide unfolded during the first 6 ns. In addition, as the N terminal and C terminal alpha carbon atom was pulled in the z direction, the rest of the peptide rotated.

At 6 ns, the profiles of MD2 and MD3 coincided and approached to the profile of MD1. After 10 ns, all the displacement plots of all simulations coincided and became almost linear. The slopes were the same since the same velocity was applied in the simulations.

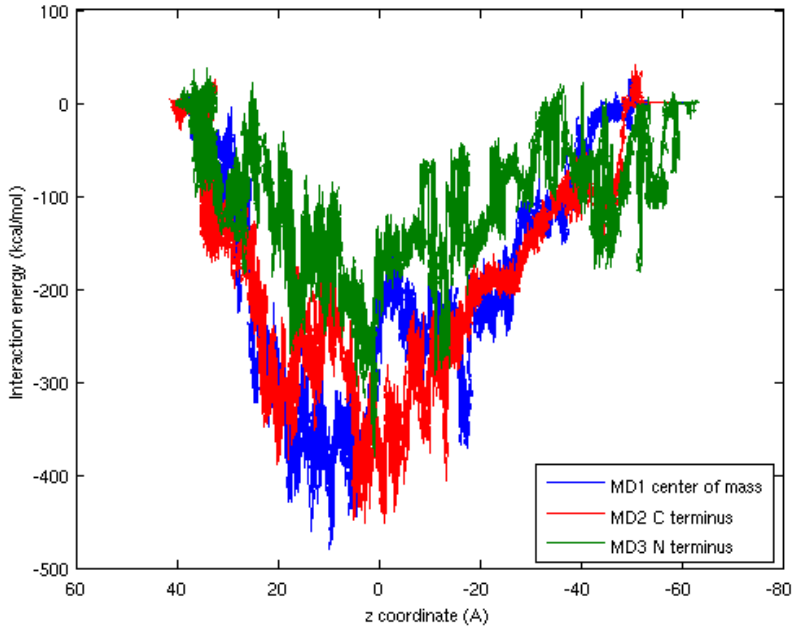

Figure 3.26. The interaction energy between the peptide and the membrane in the simulations MD1 (center of mass, blue), MD2 (C terminus, red), MD3 (N terminus, green).

In Figure 3.26, the interaction energy between the peptides and membranes was plotted as a function of change in z direction of the center of mass of the alpha carbon atoms of the peptide for MD1 (blue), MD2 (red) and MD3 (green). The top of the membrane started 25 Å in z coordinates and the bottom was -25 Å while 0 Å was the coordinate of the center of the membrane. Initially the energy was zero since the peptide and the membrane were far apart; in other words, there was no interaction. As the peptide moved into the lipid, the energy started to decrease until it reached a minimum. Most of the case, this attraction occurred when the peptide was totally immersed in the membrane where was the region between z = 20 Å and z = -20 Å. When the peptide moved out of the bilayer, the energy profile increased back to zero.

In MD1 (center of mass) and MD2 (C terminus), the slope of the decreasing energy curve was same and greater than the slope of MD3 (N terminus). With this greater slope, MD2 reached its minimum at z = 25 Å. However, for MD1 and MD3, the energy landscape reached their maxima at z = 0 Å. Even though the z coordinates of the minima differed, all of them corresponded to the membrane. The interaction was at maximum when the peptide was at the initial touch to the membrane in MD2 (z = 25 Å). And the maximum interaction in MD1 and MD3 (z = 0 Å) was in the middle of the membrane.

When the minimum values were compared, it was seen that MD1 reached -479 kcal/mol and MD2 reached -452 kcal/mol (

Table 3.11). Thus, they were very close to each other so the interaction between the peptide and the membrane were very close to each other in MD1 and MD2. The minimum of MD3 was -381 kcal/mol meaning that the interaction was less than the interactions in other two simulations. This situation was also seen in the electrostatic energies.

Table 3.11. The highest interaction energy between peptide and membrane, and the change in the z-direction of the SMD atom.

Simulation	**Place of pulling**	**z (Å)**	**Interaction energy (kcal/mol)**	**Electrostatic energy (kcal/mol)**	**van der Waals energy (kcal/mol)**
MD1	center of mass	9.7	-479.4	-372.4	-107.0
MD2	C terminus	-1.2	-451.7	-357.1	-94.6
MD3	N terminus	0.7	-380.5	-308.9	-71.6

The energy landscapes of MD1 and MD2 reached 0 kcal/mol at z = -40 Å and at z = -50 Å. Since the energies were zero, the interaction between the peptide and the membrane was diminished. Therefore, at this point, the peptide was totally out of the membrane. However, the energy landscape of MD3 was able to increase back to zero at z = -60 Å. There reason for this delay was that some lipid tails hanged to the peptide and went out of the membrane. Since there was still contact, the interaction energy had not been zero, yet.

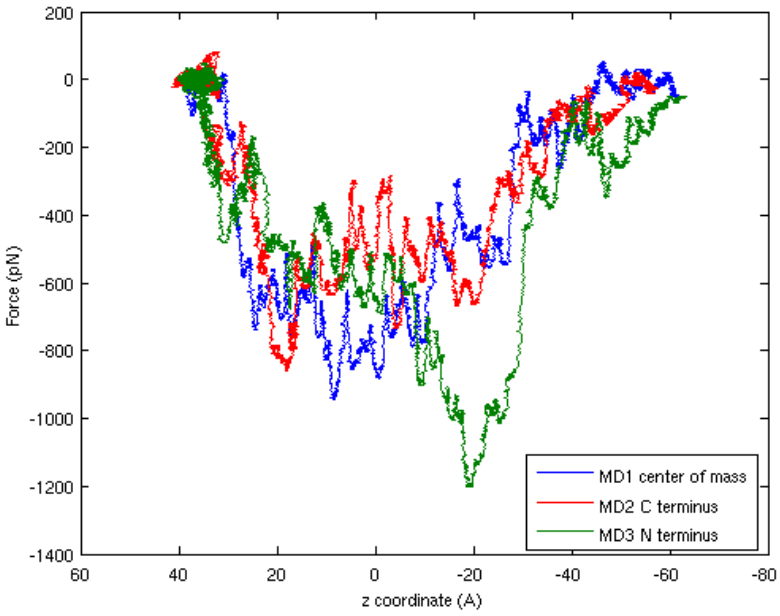

Figure 3.27. The force applied to the peptides in the simulations MD1 (center of mass, blue), MD2 (C terminus, red), MD3 (N terminus, green). A running average is plotted for clarity.

In Figure 3.27, the forces applied to the peptides in the negative z direction were plotted in MD1 (blue), MD2 (red) and MD3 (green). The top of the membrane started 25 Å in z coordinates and the bottom was -25 Å while 0 Å was the coordinate of the center of the membrane. The force started to increase as the peptide goes into the membrane. It reached maximum when the peptide was totally immersed in the center of the membrane. Finally, the force decreased back to 0 pN when the peptide was out of the membrane.

All the force profiles increased with same slope. The force curve of MD2 (C terminus) reached maximum at z = 18 Å. This location was the top of the upper layer of the membrane. The force curve of MD1 (center of mass) reached its maximum at z = 9 Å where the peptide was totally immersed in the membrane. The curve of MD3 (N terminus) reached maximum beyond the other curves at z = -19 Å. This location was close to the bottom of the lower layer, so the center of the peptide was at the bottom of the lipid. At this spot, the peptide was half immersed, half out of the membrane. When the maximum values were compared, it was seen that the maxima of MD1 (945 pN) and MD2 (859 pN)

were close to each other (Table 3.12). However, the maximum of MD3 (1203 pN) was much higher than the others. After the maximum, the curves decreased back to zero. The reason was that when the peptide was out of the membrane and had no contact to the membrane, no force was necessary to be applied to move it. However, the curve of MD3 did not totally reach back to zero since some lipid tails hanged to its peptide.

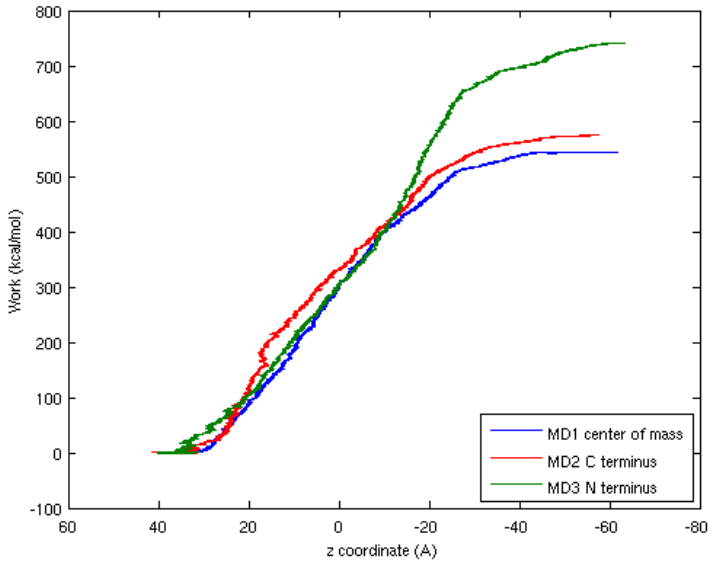

Figure 3.28. The work done on the peptides in the simulations MD1 (center of mass, blue), MD2 (C terminus, red), MD3 (N terminus, green) as a function of change in z-direction for the center of mass of the alpha carbons of the peptide.

In Figure 3.28, the work done on the peptide was plotted as a function of change in z-direction for the center of mass of the alpha carbons of the peptide in MD1 (blue), MD2 (red) and MD3 (green). The top of the membrane started 25 Å in z coordinates and the bottom was -25 Å while 0 Å was the coordinate of the center of the membrane. In all cases, the work done started from 0 kcal/mol since no force was applied to the peptide in the beginning. As the peptide started to penetrate the membrane, the work value increased, too. When Figure 3.28 was analyzed, it was seen that all the work profiles started to increase at around z = 30 Å region. All the profiles increased with similar slope and were very close to each other. Up to z = -12 Å, they increased almost coincidently. After this checkpoint, MD1 (center of mass) and MD2 (C terminus) stayed close to each other and continued

increasing with the same slope. However, the profile of MD3 (N terminus) got a greater slope and attained much higher values than the others did. MD1 and MD2 reached stable work values at z = -50 Å while MD3 did at z = -60 Å. The reason for these higher work values and delayed stability were the lipid tails in MD3. Since some lipid tails moved out with the peptide, force was being applied to the peptide. And work was still being done on the peptide of MD3 while the peptide in MD1 and MD2 left its total contact with the membrane. When the maximum work values reached were compared, it was seen that 544 kcal/mol of MD1 (center of mass) and 575 kcal/mol of MD2 (C terminus) were very close to each other, while 741 kcal/mol of MD3 (N terminus) was greater than them as seen in Figure 3.28 and Table 3.12. The reason was the hanging of lipid tails to the peptide.

Table 3.12. The distance covered in 20 ns, maximum force and maximum work values of the simulation systems of MD1, MD2 and MD3.

Simulation	**Place of pulling**	**Distance covered in 20 ns (Å)**	**Maximum force applied in negative z direction (pN)**	**Maximum work done (kcal/mol)**
MD1	center of mass	101.3	945 (-8.3 Å)	544 (-61.1 Å)
MD2	C terminus	100.4	859 (18.2 Å)	575 (-56.2 Å)
MD3	N terminus	131.0	1203 (-19.4 Å)	741 (-61.1 Å)

The maximum amount of the force applied to the peptide in negative z direction was the greatest in MD3 as seen in Table 3.12 (The z-values corresponding to the maximum force and maximum work values are shown in parenthesis.). This meant that it required greater force to pull the peptide from its N terminus. The reason for this greater force value was the deformation of the membrane. Since some lipid tails hanged to the peptide and resisted to the movement of the peptide when the peptide was out of the membrane, greater force was required to be applied on the peptide. Because of the same reasons, the work done in MD3 was the greatest of all. Higher work must have been done to move the peptide while tails were hanging to it.

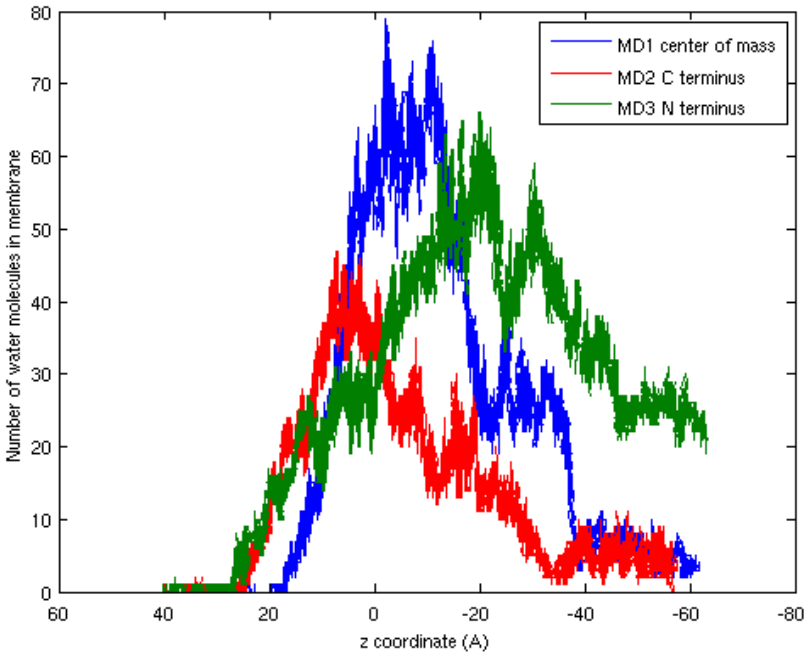

Figure 3.29. The number of water molecules present in the membrane in the simulations MD1 (center of mass, blue), MD2 (C terminus, red), MD3 (N terminus, green) as a function of change in z-direction for the center of mass of the alpha carbons of the peptide.

In Figure 3.29, the numbers of water molecules going into the membrane were shown for MD1 (blue), MD2 (red) and MD3 (green). The top of the membrane started 25 Å in z coordinates and the bottom was -25 Å while 0 Å was the coordinate of the center of the membrane. At the beginning of the preparation of the system, the membrane was centered and solvated as mentioned earlier. The water molecules in 10 Å positive and negative z directions from the middle of the membrane were removed, since the area between +10 Å and -10 Å in z direction was the inside of the membrane. Therefore, the number of water molecules in this range was counted and plotted as a function of change in z direction of the center of mass of the alpha carbon atoms of the peptide.

In all cases, the water molecules started to enter the membrane when the peptide started to penetrate the bilayer. At the beginning, there was almost no water present within the bilayer. As the peptide went into the membrane, the water also started to leak through. When the peptide was totally immersed into the membrane, the profile made a peak. Then,

as the peptide moved along and started to leave the membrane, the pore closed and water also moved out of the membrane.

However, there were some differences. The number of water molecules of MD2 (C terminus) and MD3 (N terminus) started to increase when the peptide was at z = 25 Å, while the number of water molecules of MD1 (center of mass) started to increase when the peptide was at z = 20 Å. The locations of the peptides where the maximum number of water molecules was reached also differed. The center of mass pulling MD1 and C terminus pulling MD2 had maxima at around z = 0 Å; in other words, in the middle of the membrane. But the number of water molecules in N terminus pulling MD3 kept on increasing at z = 0 Å. It reached its maximum at z = -20 Å where the peptide was very close to the bottom of the membrane. MD1 had 79 water molecules at maximum while MD2 and MD3 had 57 and 66 water molecules, respectively. Thus, MD2 (C terminus) had the lowest maximum water amount. When there were more water molecules in the membrane, there was a greater pore formed. Since the reason for the membrane existence was to enclose the cell and prevent molecules to go into the cell, when there was a larger pore, there were more water molecules going into the cell. Thus if there was greater pore, there was higher distortion. This meant that there was greater distortion in the membrane, when the peptide was pulled from its center of mass. In contrast, there was less harm to the membrane when the peptide was pulled from C terminus.

Moreover, not all the water profiles decreased back to 0. If the profile decreased to 0, it meant that the peptide totally left the membrane. This was seen in MD1 and MD2. They ended up with almost no water molecules present; however, the plot of MD3 says that there was still water present in the membrane. Therefore, it could be said that the peptides which were pulled from center of mass and C terminus accomplished to leave the membrane. The membrane of the N terminus pulled MD3 still had water when the peptide was between -40 Å and -60 Å. The first reason in that there were some lipid tails which hanged to the peptide and moved out of the membrane. Second there was a cavity left in the membrane, so the water molecules were still in it.

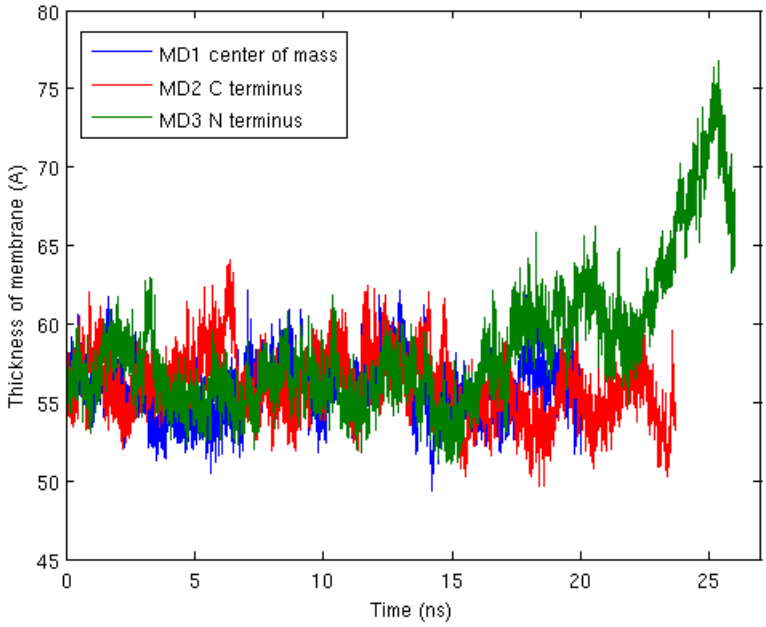

Figure 3.30. The thickness of the membranes in the simulations MD1 (center of mass, blue), MD2 (C terminus, red), MD3 (N terminus, green) as a function of simulation time.

Figure 3.30 shows the thicknesses of the membranes as a function simulation time for MD1 (blue), MD2 (red) and MD3 (green). The thickness of the membrane of MD1 (center of mass) had a mean value 55.75 Å with a standard deviation of 1.81 Å. The mean of the thickness of MD2 (C terminus) was 56.09 Å with a standard deviation of 2.12 Å while the mean of MD3 (N terminus) was 56.85 having a standard deviation of 4.39 Å. It was seen that the standard deviations of MD1 and MD2 were very close to each other and small when they were compared to MD3. This greater standard deviation was a result of moving out of lipid tails. Since thickness of the membrane was measured by calculating the minimum and the maximum z values of the membrane, the lipids out of the membrane caused this 20 Å increase.

3.2.2 The Effect of the Pulling Velocity on the MD Simulations with First Conformation

The first and fourth simulations shown in Table 3.10 were run with peptides which were pulled from their centers of mass. The peptides of MD1 and MD4 simulations pulled

with different spring constants; however, spring constant comparison was going to be done with the simulations having the second conformation.

The main variation and comparison parameter was the velocity of the peptide. There were two velocity values with which the peptides were pulled: 5.0 Å/ns and 2.5 Å/ns. In all cases, the peptides were initially positioned in the center of the upper water side of the system, about 20 Å above of the top of the membrane. In MD1, the peptide was expected to move about 90-100 Å and the velocity parameter was set to 5.0 Å/ns; therefore, 20 ns simulation was done. In MD4, the peptide was again expected to move about 90-100 Å; however, this time the velocity was set to 2.5 Å/ns and therefore the simulation was carried out for 40 ns. The displacement against time profile (Figure 3.31) showed that the slope was twice when the velocity was twice as high, as expected.

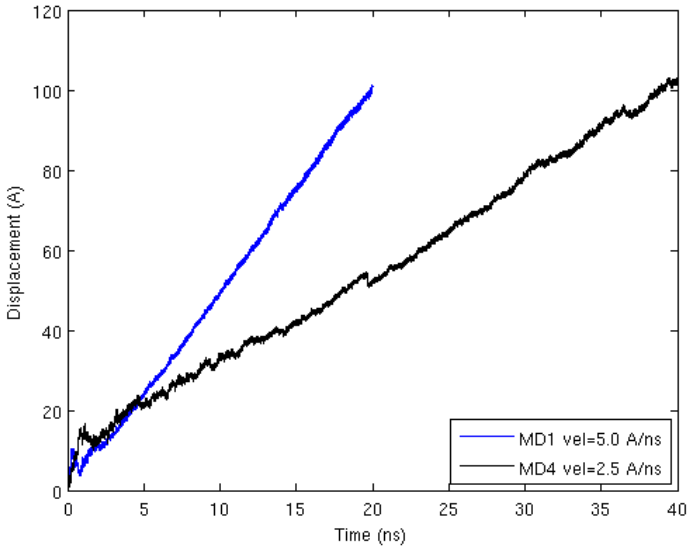

Figure 3.31. The displacements of the peptides in the simulations MD1 (v = 5.0 Å/ns) (blue) and MD4 (v = 2.5 Å/ns) (black). This same color scheme was used throughout the figures in this section.

Figure 3.31 shows the displacement of the peptide as a function of simulation time for MD1 (blue) and MD4 (black). The displacement profile of MD1 had almost no jumps

and it was linear throughout the entire simulation. In contrast, the profile of MD4 had some jumps and fluctuations. These fluctuations were caused by the unexpected moves. The force was applied in the negative z direction. However, the peptide also moved in other directions. Thus the fluctuations happened. These unexpected moves could also be seen in MD1 but since the peptide of MD4 had a slower velocity, the peptide had more time and mobility to make these moves.

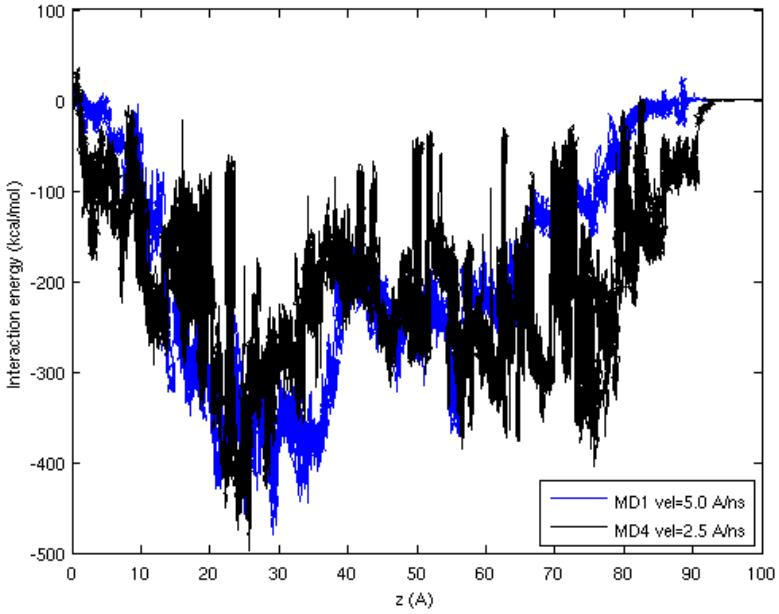

Figure 3.32. The interaction energy between the peptide and the membrane in the simulations MD1 (v = 5.0 Å/ns) (blue) and MD4 (v = 2.5 Å/ns) (black).

The interaction energies between the peptide and the membrane were plotted as a function of change in displacement in z direction in Figure 3.32 for MD1 (blue) and MD4 (black). Both of the profiles reached their minimum value when z was around 30 Å. This corresponded to the upper layer of the membrane.

Table 3.13. The highest interaction energy between peptide and membrane, and the change in the z-direction of the SMD atom.

Simulation	Velocity (Å/ns)	z (Å)	Interaction energy (kcal/mol)	Electrostatic energy (kcal/mol)	van der Waals energy (kcal/mol)
MD1	5.00	9.7	-479.4	-372.4	-107.0
MD4	2.50	19.2	-497.6	-459.9	-37.7

The interaction energy profile of MD4 made another minimum around z = 80 Å where the lower phosphate heads of the membrane were. The energy profile of MD1 made a similar but smaller dive around z = 60 Å corresponding to the lower layer of the membrane. As tabulated in Table 3.13, the highest interaction energies were almost equal in MD1 (-479.4 kcal/mol) and MD4 (497.6 kcal/mol). However, when the distribution of the interaction energies were considered, the electrostatic energy of is higher in MD1. This meant that there was greater attraction between the membrane and the peptide in MD1.

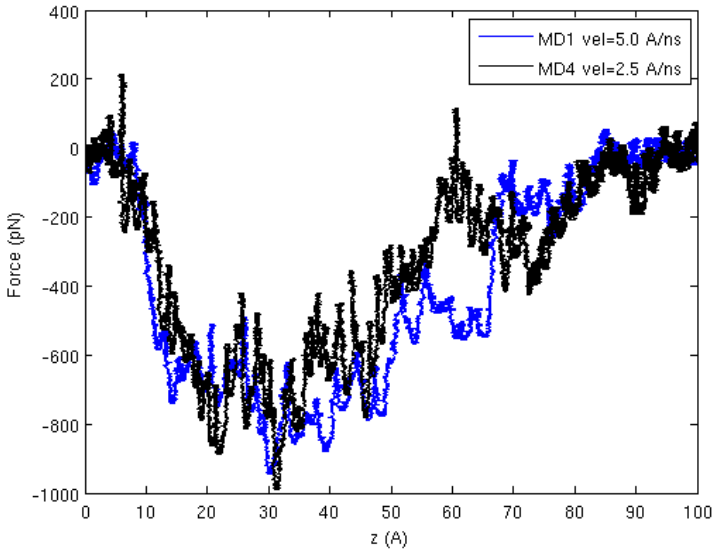

Figure 3.33. The force applied in simulations MD1 (v = 5.0 Å/ns) (blue) and MD4 (v = 2.5 Å/ns) (black) on the peptides. A running average is plotted for clarity.

The forces applied to the peptides in negative z direction for MD1 (blue) and MD4 (black) were shown in Figure 3.33. The force profiles coincided in MD1 and MD4 despite the difference in velocity. Both of the profiles started from 0 pN because the peptides were stable at the beginning. When the force was being applied to the peptide, the peptide started to move. And this force was applied in negative z direction since the desired movement was in that direction. As the peptide moved along, the force profile kept on increasing in negative z direction. Both of the profiles reached their maxima at 30 Å where the upper layer of the membrane was. In other words, when the peptide was immersed in the upper layer of the membrane, the greatest force was necessary to be applied to keep the peptide moving.

While the peptide was moving on and leaving the membrane, the applied force started to decrease to zero. At the end of the simulation, the peptide was away from the membrane; therefore, the force was 0 pN at that time.

Table 3.14. The distance covered in entire simulation, maximum force and maximum work values of the simulation systems of MD1 and MD4.

Simulation	**Displacement in all direction in entire simulation (Å)**	**Maximum force applied in negative z direction (pN)**	**Maximum work done (kcal/mol)**
MD1	101.3	945 (8.3 Å)	544 (-61.1 Å)
MD4	102.5	991 (7.4 Å)	465 (63.1 Å)

The maximum values of the force applied in negative z direction were shown in Table 3.14 (The z-values corresponding to the maximum force and maximum work values are shown in parenthesis.). It was seen that the maximum values were almost equal. Therefore, variation of the velocity parameter did not affect the maximum value and the general trend of the force necessary.

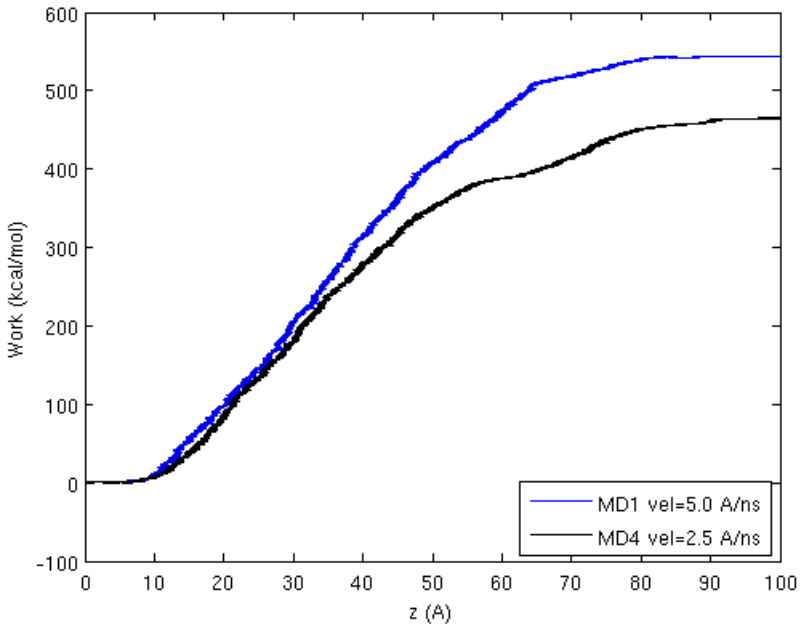

Figure 3.34. The work done in MD1 (v = 5.0 Å/ns) (blue) and MD4 (v = 2.5 Å/ns) (black) as a function of change in z-direction for SMD atom.

In Figure 3.34, the work done on the peptides of simulations MD1 and MD4 plotted as a function of change in displacement in z direction for MD1 (blue) and MD4 (black). Up to 10 Å, the work profiles were stable; in other words, there was no increasing pattern. The reason was that this region was the upper water part above the membrane. Since there was no membrane yet, no work was done on the peptide.

In both cases, the work profile started to increase in 10 Å where the membrane started. Up to 40 Å, the work profiles were very close to each other. But after 40 Å, the work profile in MD1 increased more rapidly.

Around 80 Å, the profiles of both of the simulations reached stable values. Around 80 Å the peptide was out of the membrane; therefore, no work was necessary to be done on the peptide. Moreover, as seen in Figure 3.33, the force applied to the peptide became 0 pN, so no more additional work could be done. When the maximum work values were

compared, the value in MD1 was greater than the value in MD4 as also seen in Table 3.14. Therefore, more work was done when the peptide was pulled faster.

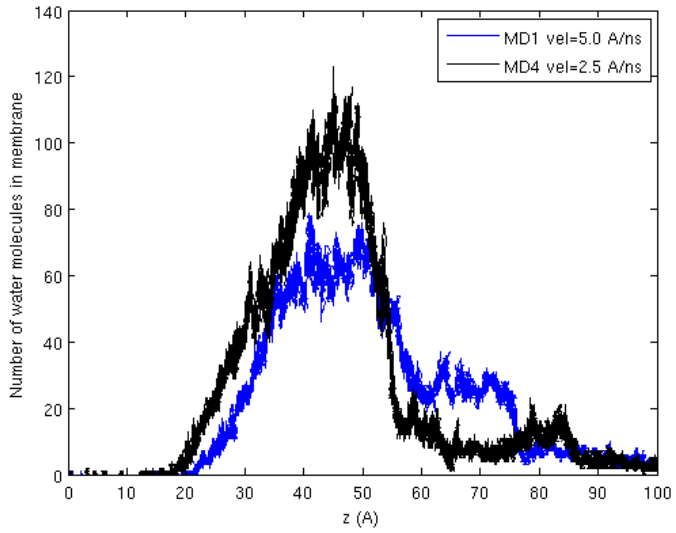

Figure 3.35. The number of water molecules present in the membranes in MD1 (v = 5.0 Å/ns) (blue) and MD4 (v = 2.5 Å/ns) (black) as a function of change in z-direction for SMD atom.

The number of water molecules in the membrane was plotted as a function of change in displacement in z direction for MD1 (blue) and MD4 (black) in Figure 3.35. There was a pattern that both of the profiles follow. The number of water molecules was zero in the beginning. Then the number increased and reached a maximum. After the maximum, the amount of water in the membrane decreased back to zero. The top of the membrane was at z = 10 Å while the bottom was at z = 67 Å. The center of the membrane was at z = 39 Å. When Figure 3.35 was analyzed, it was seen that the number of water molecules in both case started to increase at z = 20 Å. This was the place where the peptide passed the phosphate heads of the membrane and was totally immersed in the membrane. Both of the curves reached their maximum at z = 40 Å where corresponded to the middle of the membrane since the center of the membrane was at z = 39 Å.

The maximum number of water molecules was 79 in MD1 (vel = 5.0 Å/ns), while it was 123 in MD4 (vel = 2.5 Å/ns). This meant that there were more water molecules entering the membrane with the peptide as the peptide was being pulled more slowly. Therefore, higher distortion occurred when the peptide had a slower velocity because there was more time available for water molecules to fill the cavity that the peptide formed.

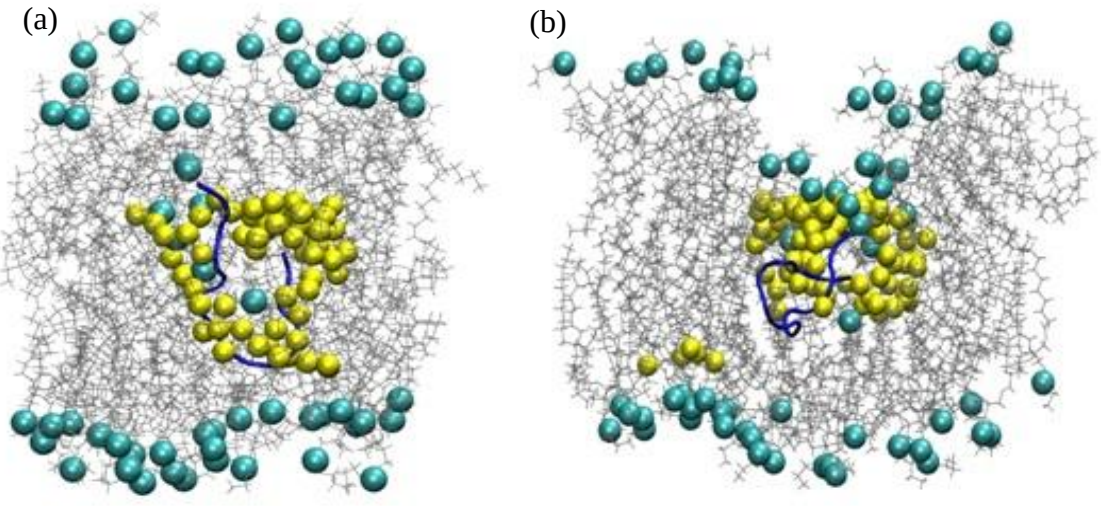

Figure 3.36. The system of water, membrane and peptide of (a) MD1 (vel = 5.0 Å/ns) at z = 39 Å and t = 8.2 ns (b) MD4 (vel = 2.5 Å/ns) at z = 39 Å and t = 16.0 ns.

In Figure 3.36, the snapshots of the systems of MD1 and MD4 were shown at time when the maximum number of water molecules was reached. The peptide was shown in NewCartoon representation and in blue color. The lipid tails of the membrane were shown in color grey and the phosphate heads were shown in cyan VDW representation. The water molecules in the membrane were shown in yellow color and VDW representation. This same color scheme was used throughout the figures in this section. As stated above, there were more water molecules in the membrane in MD4 (vel = 2.5 Å/ns) since there was a greater pore formed in the membrane and the deformation of the membrane was higher. This was seen when Figure 3.36(a) (MD1) was compared with Figure 3.36(b) (MD4). In the membrane of MD4, there was a large pore formed on the top of the peptide.

The curves of the number of water molecules shown in Figure 3.35 decreased back to zero at the same time; however, before they reached closer values to zero, there were small maxima for each case. The small maximum of MD1 (vel = 5.0 Å/ns) occurred in the region between z = 60 Å and z = 75 Å, while the small maximum of MD4 (vel = 2.5 Å/ns) occurred in the region between z = 75 Å and z = 85 Å. The reason for these maximum was the final unfolding of the peptide when it was moving out of the membrane.

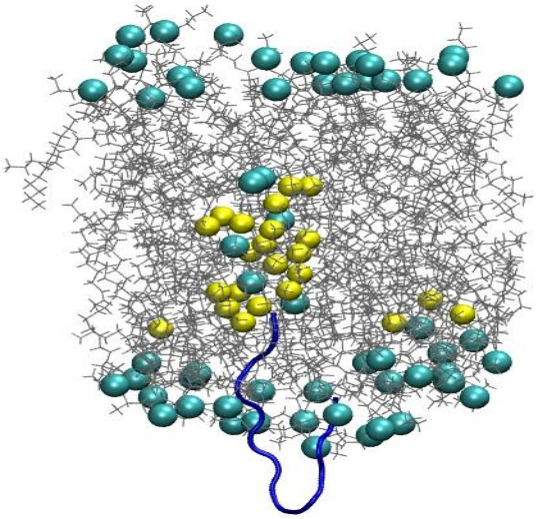

Figure 3.37. The beginning of the final unfolding of the peptide in system of MD1 (vel = 5.0 Å/ns) at z = 60 Å.

The beginning of the final unfolding of the peptide during it was leaving membrane was shown in Figure 3.37, while the end of this movement was shown in Figure 3.38. These two figures were the snapshots from the system of MD1. When the peptide was in its final unfolding, the pore that the peptide opened to leave the membrane enlarged and more water molecules entered the membrane. Thus, the small maximum of the curve occurred. Similar motion occurred in MD4.

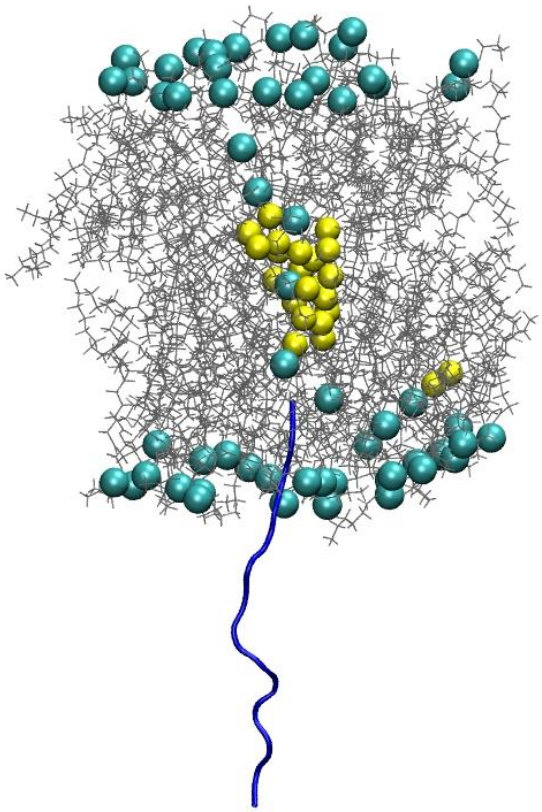

Figure 3.38. The end of the final unfolding of the peptide in system of MD1 (vel = 5.0 Å/ns) at z = 70 Å.

Figure 3.39 shows the thicknesses of the membranes as a function simulation time for MD1 (blue) and MD4 (black). Since the peptide left the membrane in 20 ns in MD1, the thickness plot of MD1 ended at 20 ns. In contrast, the peptide left the membrane in 40 ns was MD4. Thus the plot of MD4 lasted to 40 ns.

There was no major change in the thickness of the membrane of MD1. There was no lipid tail moving out of the membrane with the peptide. However, there was a huge increase in the thickness of MD4. The reason was some lipid tails. There were some lipid tails hanging out of the membrane, since they stuck to the peptide. As the simulation proceeded, the thickness almost returned to its initial values. Nevertheless, these lipid tails were the distortion of the membrane.

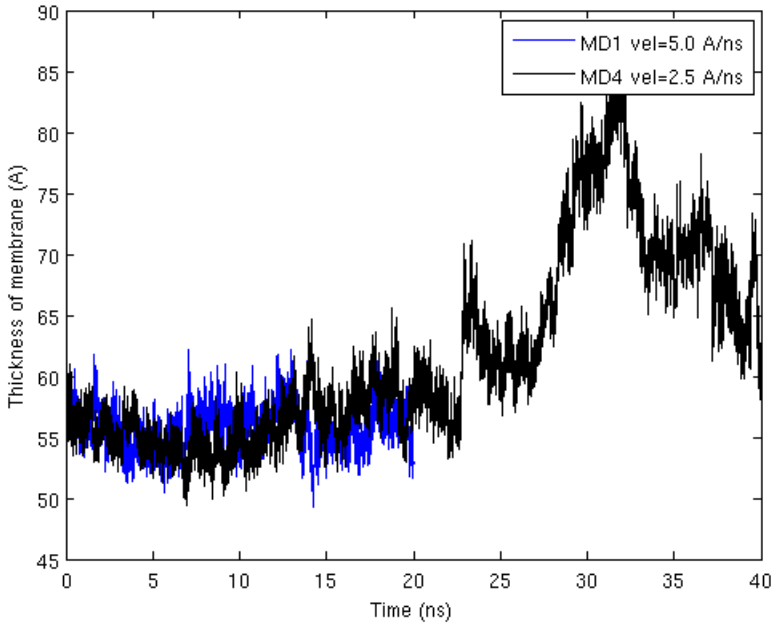

Figure 3.39. Thickness of the membranes in MD1 (v = 5.0 Å/ns) (blue) and MD4 (v = 2.5 Å/ns) (black) as a function of simulation time.

3.2.3 The Effect of Spring Constant on the MD Simulations with Second Conformation

Even though the simulations were named as MD, these simulations shown in Table 3.15 were also steered molecular dynamics simulations. These 2 simulations having the second conformation were done with same place of pulling and same velocity. The variation parameter was the spring constant; therefore, the spring constant contribution to steered molecular dynamics simulation was seeked.

Table 3.15 shows the simulations done with the peptide having second conformation. In both cases, the peptides were initially positioned in the center of the upper water side of the system which was 20 Å above of the top of the membrane. The peptides were expected to move about 90-100 Å in 20 ns; therefore, the velocity parameters were set to 5.0 Å/ns. Moreover, both of them were pulled from the center of mass. The only variation was the

spring constant. The peptide of MD5 was pulled with spring constant of 7 kcal/mol/Å^2 while the peptide of MD6 was pulled with spring constant of 10 kcal/mol/Å^2.

Table 3.15. The last 2 MD simulations having different spring constants, same velocities and same places of pulling with peptide having sequence LLIILHAAGDYYA which has the second conformation.

Simulation	**k (kcal/mol/Å^2)**	**velocity (Å/ns)**	**place of pulling**
MD5	7	5.00	center of mass
MD6	10	5.00	center of mass

The effect of spring constant on SMD simulations which were the translocation of the cargo peptide was explored in the previous section. When the spring constant was smaller, there was a greater interaction between the peptide and the membrane the work done was also higher when the spring constant was smaller, though the force necessary to pull the peptide was higher when the spring constant was higher. The number of water molecules was less with the softer spring but the molecules were present for longer period. Thus, the simulations in this chapter were performed in order to elucidate the spring constant effect further.

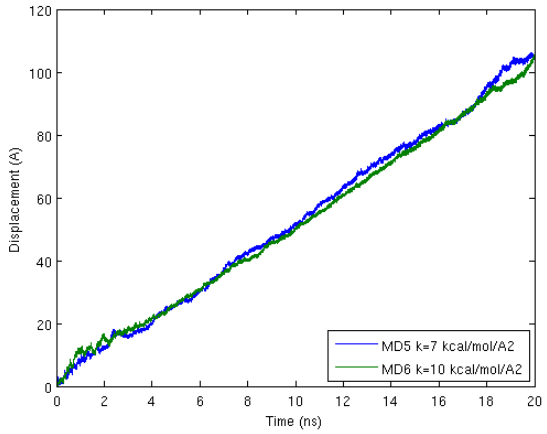

Figure 3.40. The displacements of the peptides in MD5 (7 kcal/mol/Å^2) (blue) and MD6 (10 kcal/mol/Å^2) (green).

In Figure 3.40, the displacements of the peptides having second conformation were plotted as a function of simulation time for MD5 (blue) and MD6 (green). The slopes of the displacement profiles were same since the slopes were velocities and velocities were equal. Both of the displacement profiles were almost linear. There were some minor fluctuations which could be ignored. For most of the time, the displacement profiles coincided. The final displacement values were almost same. The final displacement of MD5 was 106.0 Å while the one of MD6 was 105.6 Å.

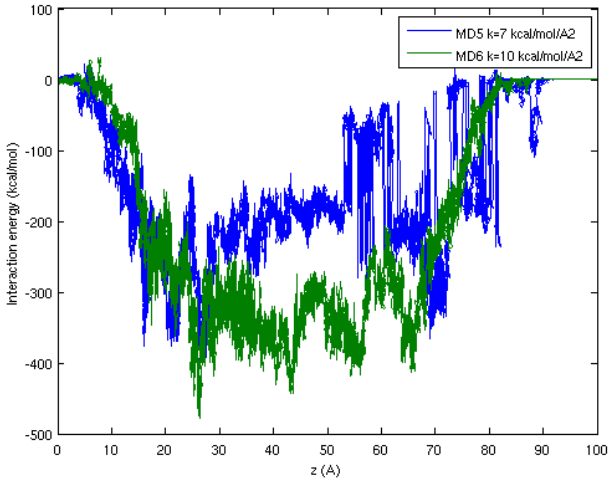

Figure 3.41. The interaction energy between the peptide and the membrane in the simulations MD5 (7 kcal/mol/Å^2) (blue) and MD6 (10 kcal/mol/Å^2) (green).

Figure 3.41 shows the interaction energy between the peptides and membranes was plotted as a function of change in z direction of the center of mass of the alpha carbon atoms of the peptide for MD5 (blue) and MD6 (green). The energy profile followed a general trend. At the beginning the profile started to decrease to a minimum value. After it reached the minimum, it fluctuated around those values for a while. Then it increased back to 0 kcal/mol.

Both of the energy profiles reached their minimum around 20-30 Å region which was the upper layer of the membrane. Both of them fluctuated in very low values from 20 Å to 70 Å. These points were the upper and lower boundaries of the membrane, respectively. Thus there was interaction between the membrane and the peptide when the peptide was inside of the membrane. Especially, when the peptide was in the upper layer, there was an important interaction for both cases.

Table 3.16. The highest interaction energy between peptide and membrane, and the change in the z-direction of the SMD atom.

Simulation	**k (kcal/mol/Å^2)**	**z (Å)**	**Interaction energy (kcal/mol)**	**Electrostatic energy (kcal/mol)**	**van der Waals energy (kcal/mol)**
MD5	7	27.4	-398.2	-296.9	-101.3
MD6	10	26.3	-477.4	-413.7	-63.7

For most of the time, the energy profile of MD6 had lower values than the energy profile of MD5 did. Therefore, the interaction was greater in MD6 meaning that there was greater interaction when the spring constant was larger. When the highest interaction energy values were compared (Table 3.16), the stiff spring (k = 10 kcal/mol/Å^2) had a greater value (-477.4 kcal/mol). This redundancy was also valid in the electrostatic energy values yielding to a greater attraction between the membrane and the peptide when the spring constant was greater.

Figure 3.42 shows the forces applied to the peptides in the negative z direction in MD5 (blue) and MD6 (green). Both of the force profiles had a similar trend. Force increased when the peptide was moving in the membrane. Then the force reached its maximum when the peptide was totally immersed. As the peptide kept on moving and went out of the membrane, the applied force decreased back to 0 pN.

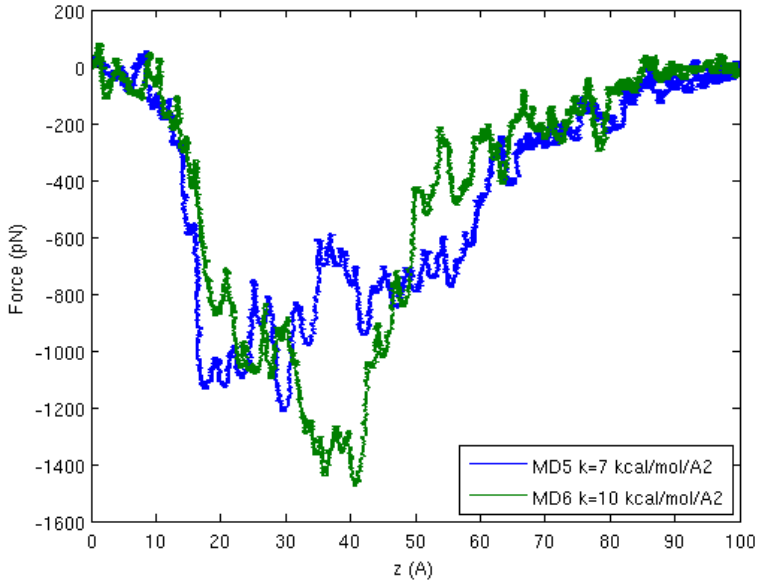

Figure 3.42. The force applied to the peptides in MD5 (7 kcal/mol/Å^2) (blue) and MD6 (10 kcal/mol/Å^2) (green) as a function of change in z-coordinates of the SMD atom. A running average is plotted for clarity.

In the first 15 Å region, since this region was the water part above the membrane, there was very small force applied for both cases. After this checkpoint, the membrane started and the applied force increased. The force applied in MD5 reached its maximum earlier than the force in MD6 did. Nevertheless, the maximum of MD6 was quite close to it. These maxima regions corresponded to the upper layer of the membrane for MD5 and center of the membrane for MD6. Then up to 80 Å, the applied force values decreased to 0 pN. After this point, the peptides left the membrane and the applied force was very close to 0 pN.

The maximum force values were tabulated in Table 3.17. It was seen that the maximum of MD6 was greater than the maximum of MD5. This meant that more force must have been applied to the peptide when the spring constant was greater.

Table 3.17. The distance, maximum force and work values of the simulations MD5 and MD6 having peptides with second conformation and different spring constants as 7 kcal/mol/Å^2 and 10 kcal/mol/Å^2, respectively.

Simulation	**Distance covered in 20 ns (Å)**	**Maximum force applied in negative z direction (pN)**	**Maximum work done (kcal/mol)**
MD5	106	1216 (29.4 Å)	638 (99.7 Å)
MD6	105.6	1476 (40.7 Å)	631 (99.7 Å)

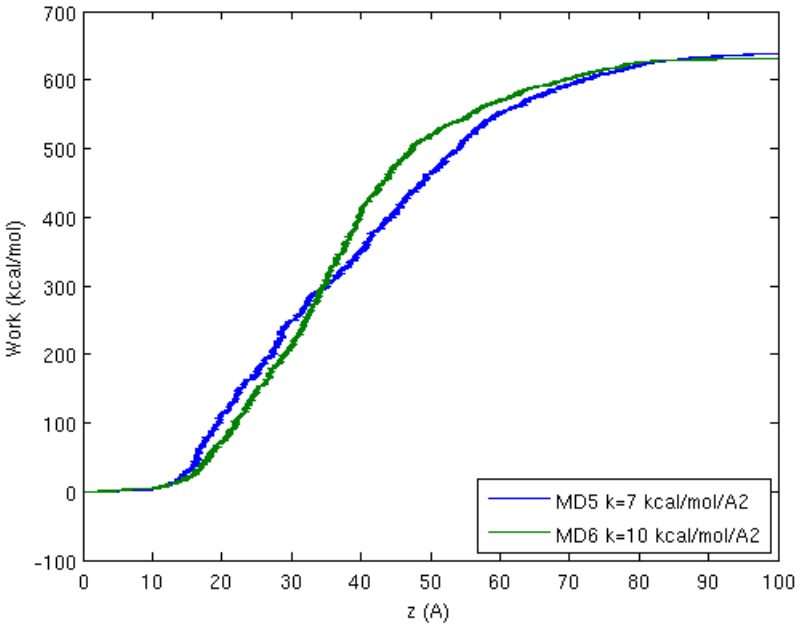

Figure 3.43. The work done on the peptides in MD5 (7 kcal/mol/Å^2) (blue) and MD6 (10 kcal/mol/Å^2) (green) as a function of change in z-coordinates of the SMD atom.

In Figure 3.43, the work done on the peptide was plotted as a function of change in z-direction for the center of mass of the alpha carbons of the peptide in the forces applied to the peptides in the negative z direction were plotted in MD5 (blue) and MD6 (green). Work values for both peptides stayed stable at 0 kcal/mol up to 15 Å. The reason was that there was no membrane in this region and thus there was no major force applied. At 15 Å, both work values started to increase as the peptide went into the membrane. The work profile of MD5 increased faster. However, around 40 Å the work profiles intersected and

the profile of MD6 started to increase faster. Nevertheless, at 80 Å the profiles coincided as the peptide left the membrane. At the end, both profiles reached almost the same value.

As also seen in Table 3.17, the maximum work done values were 638 and 631 kcal/mol for MD5 and MD6, respectively. The values were very close to each other. Therefore, there was no effect of spring constant variation on the work values.

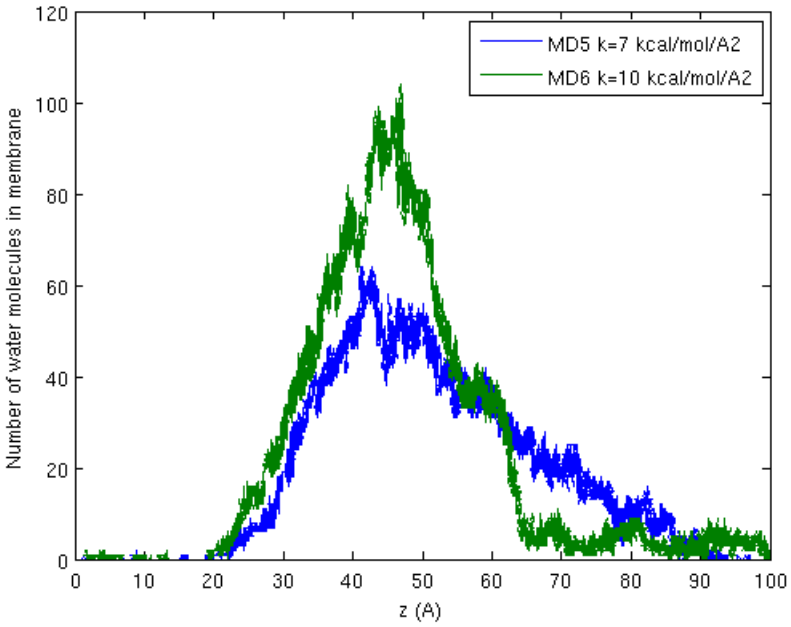

Figure 3.44. The number of water molecules present in the membrane in MD5 (7 kcal/mol/Å^2) (blue) and MD6 (10 kcal/mol/Å^2) (green) as a function of change in z-coordinates of the SMD atom.

In Figure 3.44, the numbers of water molecules going into the membrane were shown for MD5 (blue) and MD6 (green). Up to 20 Å, there was almost no increase on the water molecule number. The reason was that up to this time, the peptide came close to the membrane but did not touch it, yet. At 20 Å, the peptide started to enter the membrane. Around 45 Å the amounts of water molecules in the membranes reached a maximum. 45 Å corresponded to the time when the peptide was totally immersed in the membrane. As the

peptide kept on moving and left the membrane, the water molecules decreased. At the end the amount of the water molecules was almost zero.

When the maximum values were compared, the water present in MD6 was much higher than the water present in MD5. Even though the water profile of MD6 seemed to decrease faster, both profiles reached to zero level at the same time. There were more water molecules when the spring constant was greater. Therefore, there was a bigger distortion in the membrane when the spring constant was greater.

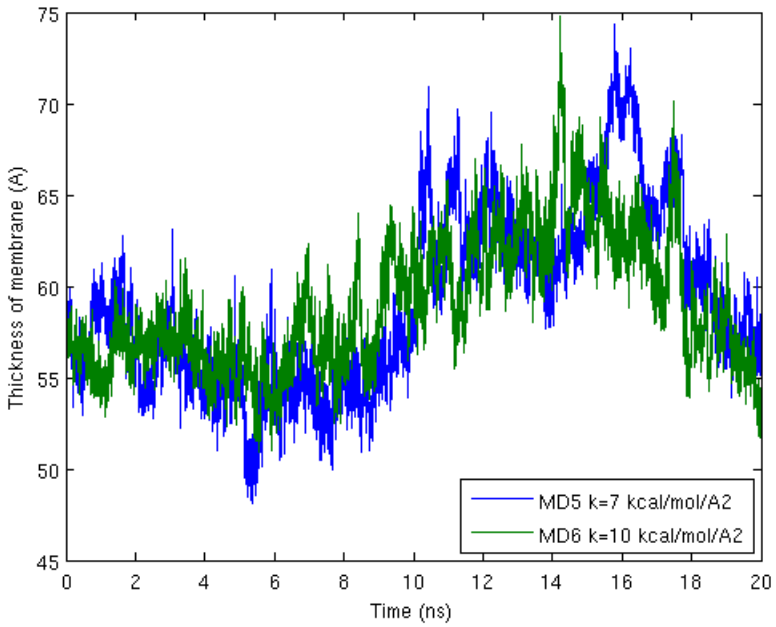

Figure 3.45. Thickness of the membranes in MD5 (7 kcal/mol/Å^2) (blue) and MD6 (10 kcal/mol/Å^2) (green) as a function of simulation time.

The thicknesses of the membranes as a function simulation time for MD5 (blue) and MD6 (green) were plotted in Figure 3.45. Up to 10 ns the thicknesses did not change much. They stayed around 55 Å. However, at 10 ns both of the membranes started to thicken. The thicknesses even raised up to 75 Å. The reason of this thickening behavior was the lipid tails. In both simulations, some lipid tails hanged to the peptide and moved out of the membrane as the peptide left the membrane. Nevertheless, when the peptide was

far away from the membrane, the lipid tails returned to the membrane. Thus the thicknesses of both membranes returned to initial values at the end.

Even though the study of Lorenzo and Bisch showed that softer springs have larger energy fluctuations [34] and the results of the previous section agreed with that finding, the interaction between the peptide and the membrane is greater for the stiff spring (10 kcal/mol/$Å^2$). The force applied to the peptide was also higher when the stiff spring was used. When the work values compared, there is no difference between the stiff and the soft (7 kcal/mol/$Å^2$) springs. Similar to the finding of the previous section, there was more water molecules in the membrane when the peptide was pulled with the stiff spring. Likewise, the water molecules stayed in the membrane longer when the spring constant is smaller.

When the results of the simulations having only the cargo peptide and the simulations having peptide with the additional cargo carrying part were compared for the spring constant, the interaction energy and work values did not agree with each other. The force results showed that greater force was necessary for the greater spring constant. However, when the distortion on the membrane was considered, even though greater number of water molecules entered the membrane when the constant was higher, they spent more time in the membrane for the softer spring. The previous results for the thickness of the membrane showed that the membrane became thicker when the softer spring was used. Therefore, when the distortion on the membrane was considered (and since other parameters did not yield an obvious difference), the spring constant was chosen to be 10 kcal/mol/$Å^2$ in the following section.

When the results for the varying place of pulling of the modified BLIP based peptide were analyzed, it was shown that there was greater interaction when the peptide was pulled either from its center of mass or C terminus. When it was pulled from N terminus, the interaction was smaller. When the force and work values for different places of pulling were considered, the C terminal pulling and center of mass pulling have equal values and these values are lower than the values of N terminal pulling. However, there were some

lipid tails hanging out of the membrane in the simulation in which the peptide was pulled from its N terminus. Thus, the higher work and force values in N terminal pulling were expected. There was less number of water molecules when the peptide was pulled from its C terminus while the number is highest in center of mass pulling simulation.

When the pulling velocities of the modified BLIP based peptide were compared, it was shown that the interaction energy and force values yielded coinciding plots. Thus there was no obvious difference for these values. The work done was higher when the peptide was pulled with 5.0 Å/ns. There were more water molecules in the membrane when the peptide was pulled with 2.5 Å/ns. The thicknesses in both simulations did not alter and were almost equal to each other.

The comparison of the results of the only cargo peptide and the peptide with additional cargo carrying part gave some idea about the addition of LLIIL part. The spring constant comparison showed that there was not an obvious agreement in the results, especially interaction energy between the peptide and the membrane and the work done on the peptide. Even though the only-cargo peptide pulled with the smaller spring constant yielded higher interactions, the condition was vice versa for the cargo carrier added peptide. When the places of pulling were considered, the only-cargo peptide favors N terminal pulling. The cargo-added peptide showed that the N terminal pulling yielded the worst results among the three; however, hanging out lipid tails affected its results. When the velocities were in consideration, there was not an obvious difference for the simulations performed with 2.5 Å/ns and 5.0 Å/ns.

3.3 Membrane Uptake of pVEC and its Mutants

pVEC was derived from the murine vascular endothelial-cadherin protein. It mediates physical contact between adjacent cells by homophilic dimerization. It is a 18 amino acid long peptide with the sequence LLIILRRRIRKQAHAHSK. The N terminus of the peptide is hydrophobic while the C terminus is hydrophilic and the middle of it is

charged. Each residue of pVEC was previously mutated to alanine and how the mutations affect the cellular uptake of the peptide was examined experimentally in order to define which part of the peptide is important for the cellular translocation. They yielded the conclusion that the N terminal hydrophobic part is crucial for translocation [16]. Moreover, retro-pVEC and scramble-pVEC are studied for comparison.

In this study, the goal was to repeat the investigation of which part of the peptide is significant for cellular translocation using molecular dynamics simulations and elucidate the mechanism of the cellular uptake of the peptide. Thus the original pVEC, seven mutants, retro- and scramble pVEC molecules were chosen to be studied.

Table 3.18. The 10 pVEC simulations with mutations on different residues.

Name	**Sequence**	**Mutated residue**	**Cellular uptake (pmol/mg protein)**
pVEC 1	LLIILRRRIRKQAHAHSK	original pVEC	1377
pVEC 2	**A**LIILRRRIRKQAHAHSK	L1A	307
pVEC 3	L**A**IILRRRIRKQAHAHSK	L2A	526
pVEC 4	LLIILRRR**A**RKQAHAHSK	I9A	789
pVEC 5	LLIILRRRI**A**KQAHAHSK	R10A	1535
pVEC 10	LLIILRRRIRKQA**A**AHSK	H14A	570
pVEC 6	LLIILRRRIRKQAHAH**A**K	S17A	2219
pVEC 7	LLIILRRRIRKQAHAHS**A**	K18A	2158
pVEC 8	KSHAHAQKRIRRRLIILL	retro-pVEC	412
pVEC 9	IAARIKLRSRQHIKLRHL	scramble pVEC	702

All the 10 pVEC simulations were shown in Table 3.18. The mutations done on the peptide were tabulated in the mutated residue column and the sequences of the peptides were also given in the sequence column. The cellular uptake values of these peptides were shown in the right column.

pVEC 1 was the peptide having the original sequence. pVEC 2 through pVEC 7 had alanine mutations close to the N terminus, the middle or the C terminus of the peptide. pVEC 8 has no mutation but the sequence is in the reverse direction and pVEC 9 has a randomly mixed sequence with the same residue composition.

First, the peptide was prepared according to the specific sequence and placed into a water box in VMD. The initial coordinates of the peptide were assigned from an existing protein. The water-peptide system was equilibrated and the peptide was extracted. Then the membrane was created and solvated in x-y directions by VMD. After solvation, the water-membrane system was equilibrated. The peptide was placed into the water molecules above the membrane. Finally, steered molecular dynamics simulations were performed.

The peptides were all pulled from the N terminus in the simulations with a spring constant of 10 kcal/mol/Å^2 and at velocity 2.5 Å/ns. There were 60 Å of explicit water molecules both above and below of the membrane. The peptide was positioned in the center of the upper water layer. The membrane had a thickness of 50 Å. Therefore, the peptide traveled 120 Å to complete the simulation within about 50 ns simulation time. Some of the simulations were extended to longer than 50 ns for the peptide to completely pass through the membrane.

In Figure 3.46 a snapshot at t = 0 ns of the simulation system which had the original pVEC was shown. The peptide was in the water layer above the membrane. The peptide was shown in NewCartoon representation and in blue color. The membrane had a thickness of 50 Å in z direction and was shown in color grey. The water molecules in the entire system were shown in red color and small VDW representation. This same color scheme was used throughout the figures in this section.

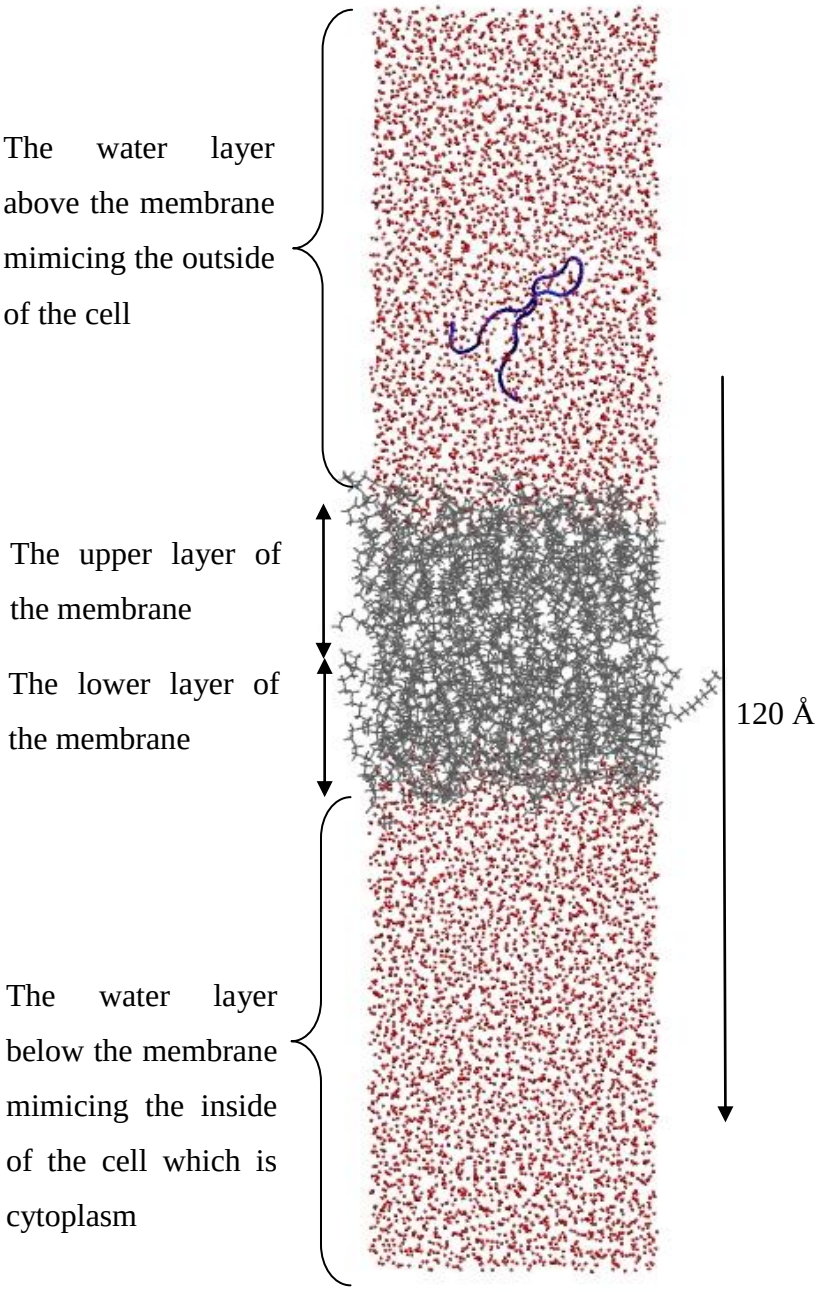

Figure 3.46. The structure of pVEC 1 (original pVEC), membrane and water system at t = 0 ns of the steered MD simulations.

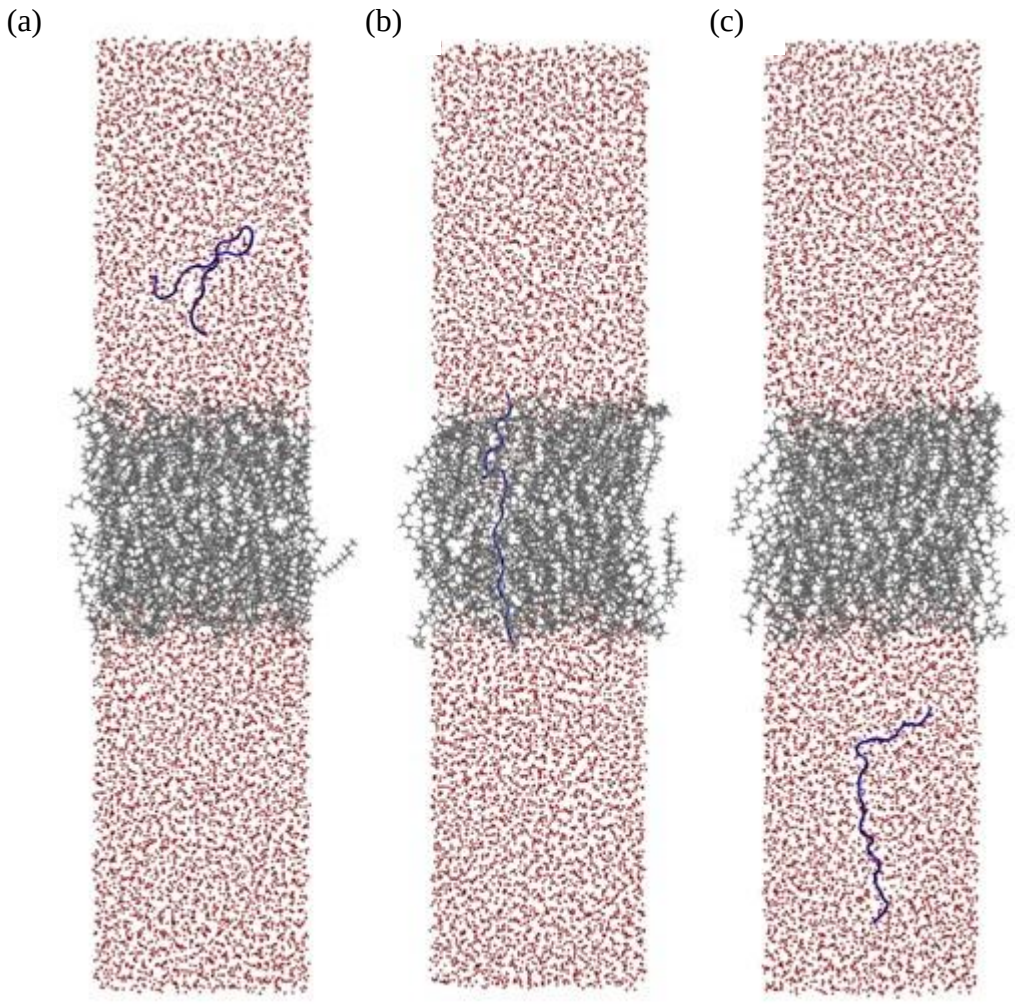

Figure 3.47. The structure of pVEC 1 (original pVEC), membrane and water system of the steered MD simulations at (a) t = 0 ns (b) t = 30 ns (c) t = 50 ns.

Figure 3.47(b) shows the system of original pVEC when the peptide was in the membrane. The pVEC peptide was totally unfolded. The N terminus of the peptide was at the bottom of the membrane while the C terminus was at the top the membrane. Figure 3.47(c) shows the system of the original pVEC when it was totally out of the membrane. The peptide was unfolded; however, it started to fold. There was no lipid tail hanging out of the membrane.

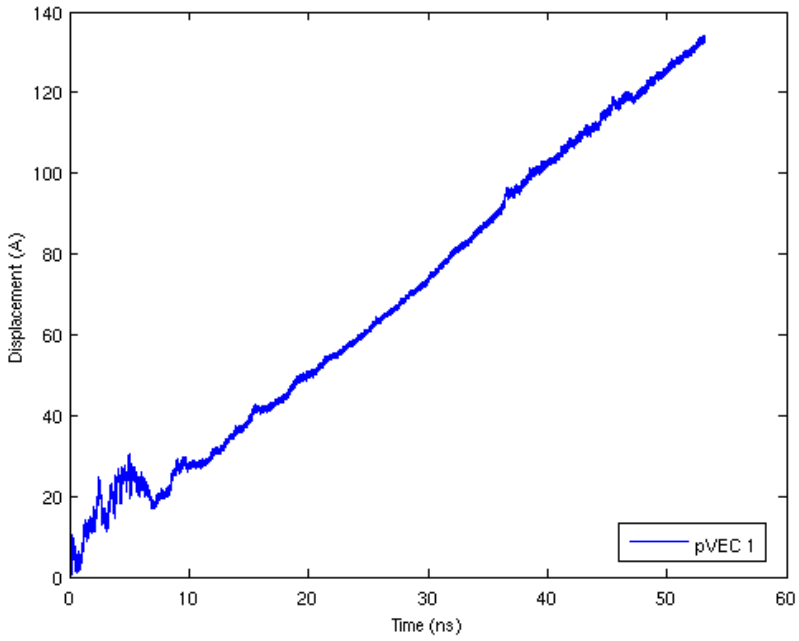

Figure 3.48. The displacement of the SMD atom of pVEC 1.

Figure 3.48 shows the displacement of the SMD atom of pVEC 1 during the simulation. In all simulations performed in this section, the SMD atom was the alpha carbon atom of the first residue in the N terminus of the peptide. In the first 10 ns of the simulation there were some fluctuations. These were caused because of the movements of the peptide in the x-y plane while it was in the upper water layer. The force was applied in negative z direction, so the expected movement was in negative z direction. The movements in other directions caused these fluctuations. In addition, the peptide extended from a more compact form as force was applied in the negative z-direction and fluctuations in the displacement of the SMD atom were observed.

After 10 ns, the displacement profile became almost linear since the unfolding was completed and the extended peptide moved in a straight line through the membrane. There were no major moves in any direction than negative z.

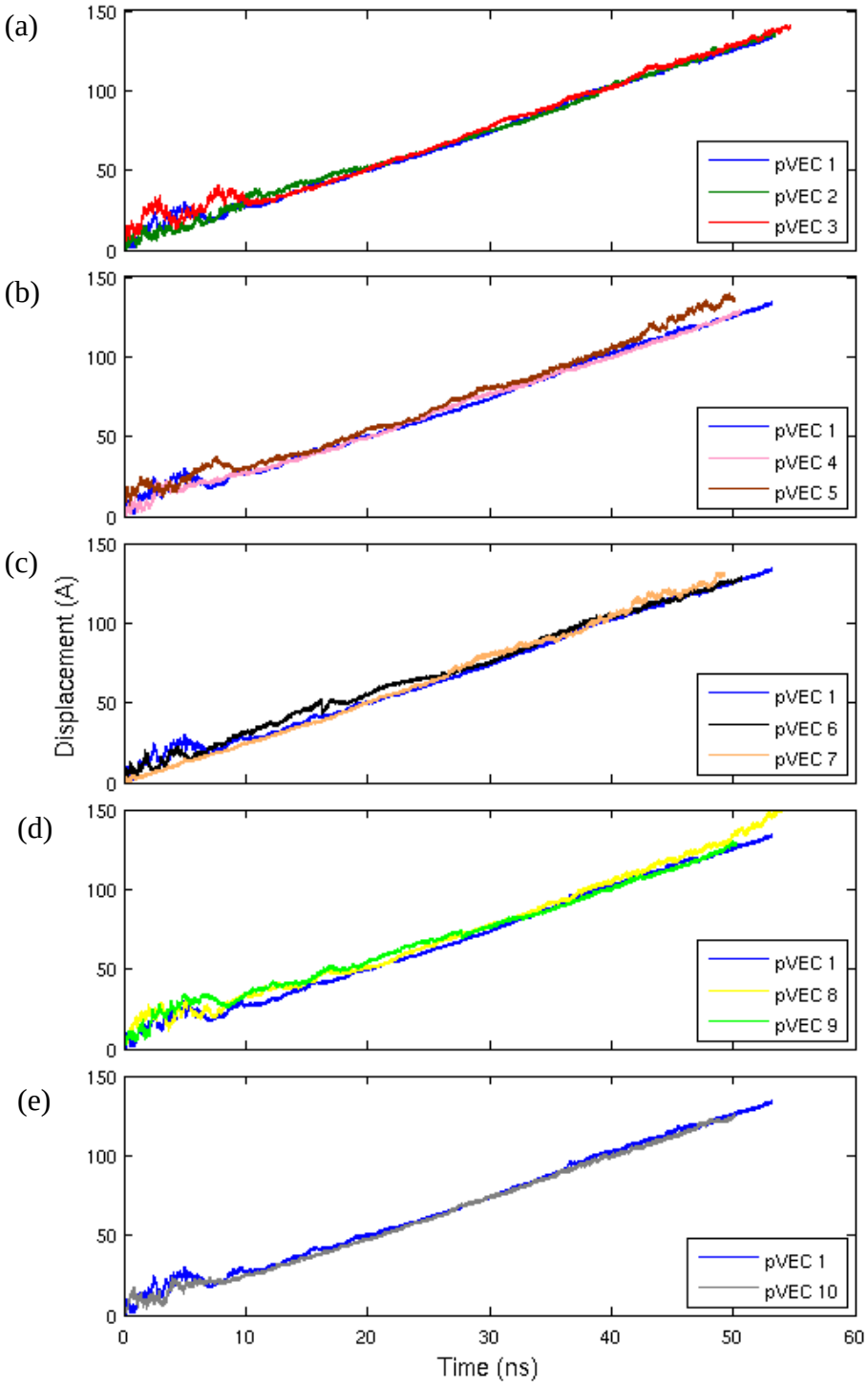

Figure 3.49. The displacements of pVEC 1 (original pVEC), (a) pVEC 2 (L1A) and pVEC 3 (L2A) (b) pVEC 4 (I9A) and pVEC 5 (R10A) (c) pVEC 6 (S17A) and pVEC 7 (K18A) (d) pVEC 8 (retro-pVEC) and pVEC 9 (scramble pVEC) and (e) pVEC 10 (H14A).

In Figure 3.49(a) the displacement profiles of pVEC 1, pVEC 2 and pVEC 3 were plotted. Up to 10 ns, there were fluctuations in the displacement of pVEC 2 and pVEC 3 similar to the fluctuations of pVEC 1. The reasons for these fluctuations were the movements of the peptide in the x-y plane and unfolding of the peptide as same for the original pVEC. All the profiles were linear with the same slope since the peptides were pulled with the same velocity.

Figure 3.49(b) shows the displacement profiles of pVEC 1, pVEC 4 and pVEC 5. Up to 10 ns, there were fluctuations in the displacement of pVEC 2 and pVEC 3 similar to the fluctuations of pVEC 1. The reasons for these fluctuations were the movements of the peptide in the x-y plane and unfolding of the peptide. All the profiles were linear with the same slope since the peptides were pulled with the same velocity. Nevertheless, the displacement profile of pVEC 5 had some fluctuations after 40 ns. The reason for these additional fluctuations was the moving out of some lipid tails with the peptide. Since the lipid tails hanged to the peptide, they affected the movement of the peptide.

In Figure 3.49(c), the displacement of pVEC 1, pVEC 6 and pVEC 7 were plotted. There were fluctuations in the displacement of pVEC 6 and pVEC 7 similar to the fluctuations of pVEC 1. The same reasons for original pVEC (pVEC 1) were valid for these fluctuations of pVEC 6 and pVEC 7: the movements of the peptide in the x-y plane and unfolding of the peptide. There were some more fluctuations in the profile of pVEC 7 after 40 ns since some lipid tails hanged to the peptide and affected its movement.

The displacement profiles of the retro-pVEC and the scramble pVEC did have same fluctuations in the beginning of the simulation (Figure 3.49(d)). The unfolding occurred in every simulation since the peptide was pulled from its only one side. Movements in the x-y plane were addition for these fluctuations. Since no lipid tail hanged to the peptide as it went out of the membrane, no more fluctuation was seen in the end of the simulation.

In Figure 3.49(e), the displacement profile of pVEC 10 had similar behavior of the profile of original pVEC. There were some fluctuations in the first 10 ns period and none for the rest of the simulation. Unfolding and movements in x-y plane were the reasons. Both of the profiles had the same slope since the velocity was same.

The displacement profiles of all 10 pVEC peptides had fluctuations in the first 10 ns period. As previously stated, there were two reasons for these fluctuations: unexpected moves in other directions and unfolding. Apart from that, the profiles were almost linear with the same slope because all the peptides were pulled with same velocity. The initial coordinates of the peptides were not identical and for some of the peptides the simulations were extended so that the peptide completely passed through the membrane.

In Figure 3.50(a), the interaction energy between the membrane and pVEC 1 were plotted as a function of z-coordinate of the SMD atom which was the alpha carbon atom of the first residue in the N terminus of the peptide. The abscissa was the z-coordinate of the N terminal alpha carbon atom of the peptide in the system. In other words, when z = 0 Å, the SMD atom was at the center of the membrane. At the beginning, the peptide was in the water layer above the membrane, so it had positive z coordinate number. The peptide moved in negative z direction; therefore, the plot starts from right and must be read from right to left.

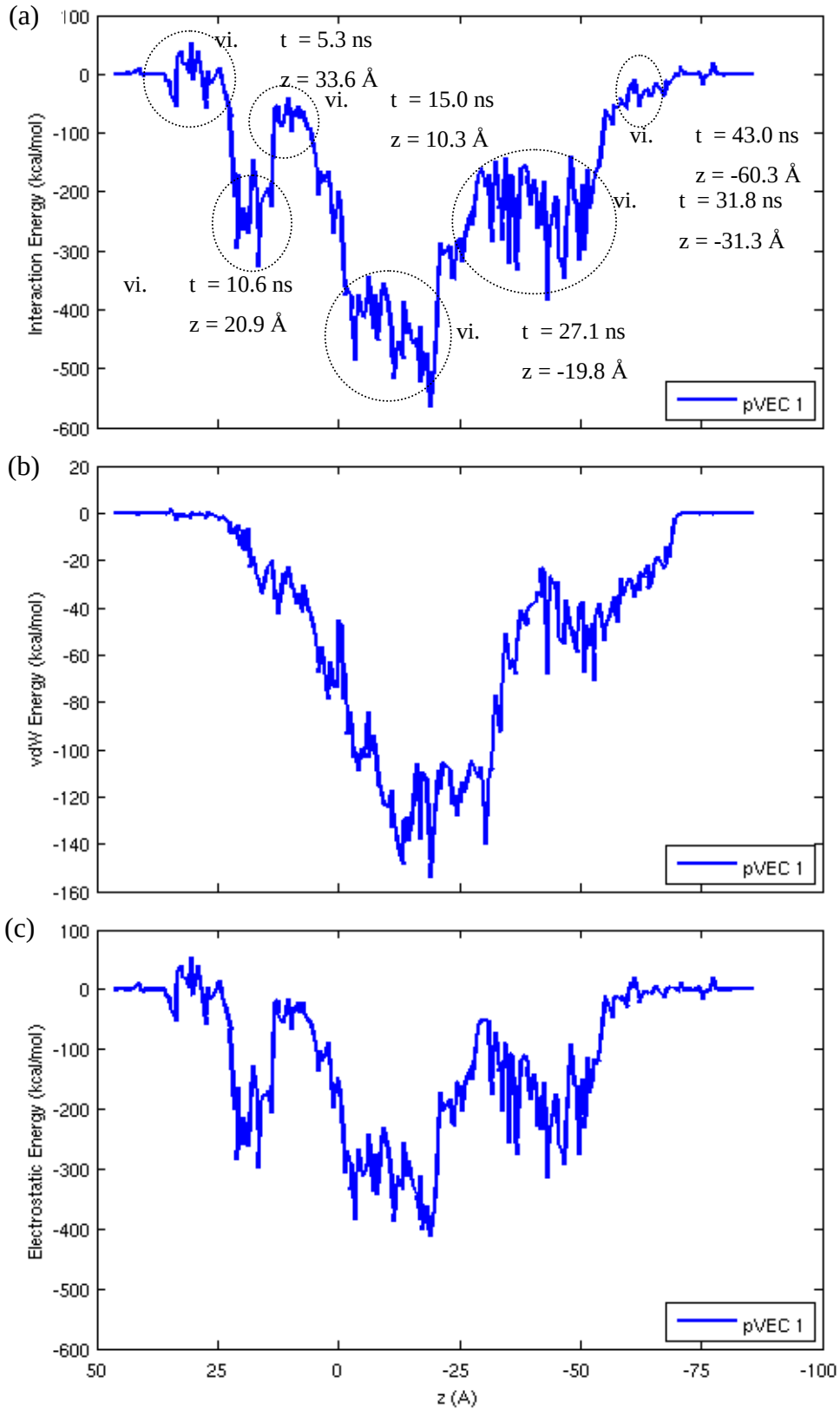

Figure 3.50. (a) The interaction energy profile of pVEC 1 (original pVEC) (b) The van der Waals energy profile of pVEC 1 (c) The electrostatic energy profile of pVEC 1.

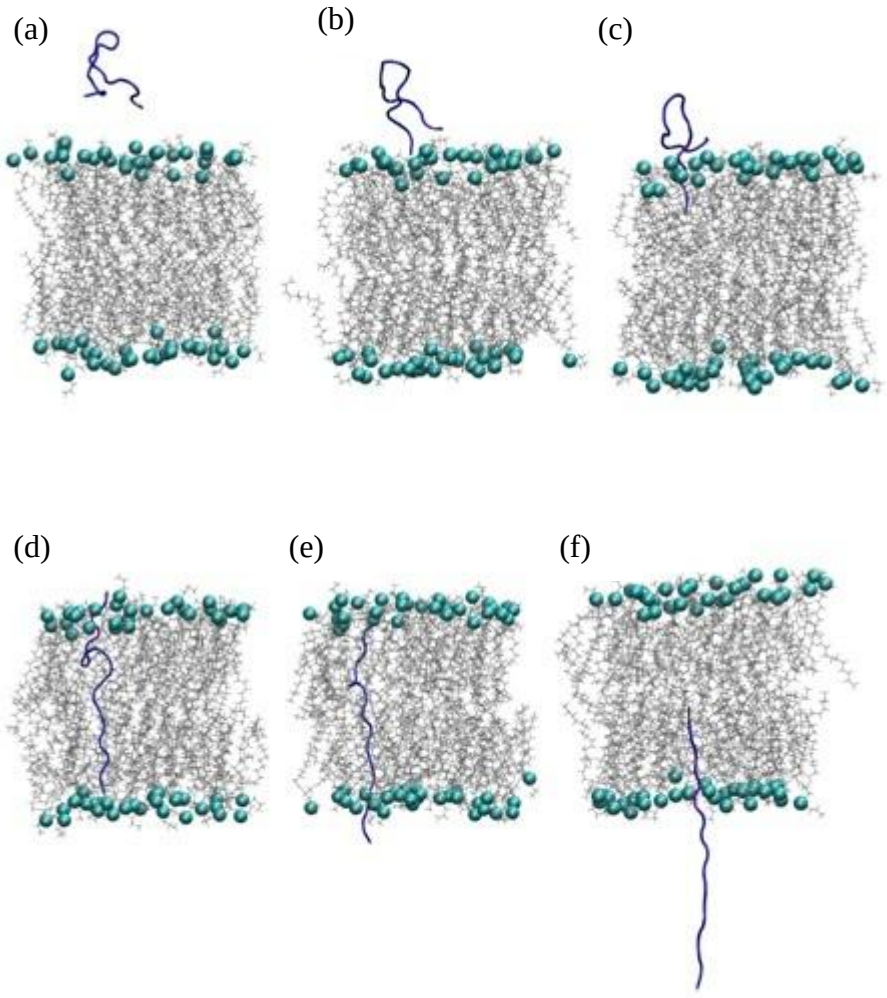

Figure 3.51. The structure of the system of pVEC 1 (original pVEC) at (a) t = 5.3 ns and z = 33.6 Å (b) t = 10.6 ns and z = 20.9 Å (c) t = 15.0 ns and z = 10.3 Å (d) t = 27.1 ns and z = -19.8 Å (e) t = 31.8 ns and z = -31.3 Å (f) t = 43.0 ns and z = -60.0 Å.

Six regions during the interaction energy makes minima or maxima are shown with circles in Figure 3.50(a). The snapshots corresponding to these regions are shown in Figure 3.51. In Figure 3.51(a), the peptide was getting closer to the membrane; however, there was no contact between the peptide and the membrane. Figure 3.51(b) showed the initial touch of the peptide to the membrane. Moreover, the N terminus was immersed in the phosphate heads of the membrane and the C terminus was touching them. Figure 3.51(c) shows that the N terminus had passed the P heads of the membrane and moved through the membrane. The C terminus was still touching the P heads. Figure 3.51(d) is the structure figure when the peptide was totally embedded in the membrane. The N terminus was

touching the lower P heads while the C terminus was in the upper P heads. The rest of the peptide was in the membrane. At this point, the interaction was at maximum. In Figure 3.51(e), the peptide was leaving the membrane. There was still a high interaction but not as much as it was in the previous point. Figure 3.51(e) shows that the peptide kept on leaving the membrane. Initially, when the peptide was away from the membrane, there was no interaction between them. As the peptide approached the membrane, the energy profile started to decrease; in other words, the interaction started to occur. When the peptide was entering and moving along the membrane, the energy decreased even more since they touched each other. Around -19 Å, the peptide was totally unfolded and the peptide was almost inside the membrane. Therefore, the interacting surface area of the peptide and the membrane reached maximum. Because the surface area reached maximum, the van der Waals energy between the peptide and membrane reached its minimum (Figure 3.50). Thus, the interaction between them was at maximum.

As the peptide moved along and the N terminus started to leave the membrane, the energy profile increased since the interacting surface area decreased. In other words, the van der Waals energy increased (Figure 3.50(b)). When the peptide totally left the membrane and was away from the membrane, the interaction energy was back to 0 kcal/mol.

When the hydrophilic residues contacted with the P heads, electrostatic energy became positive (Figure 3.50(c)). This meant that the peptide and the membrane repelled each other at these points. Nevertheless, there was no obvious distance increase is seen.

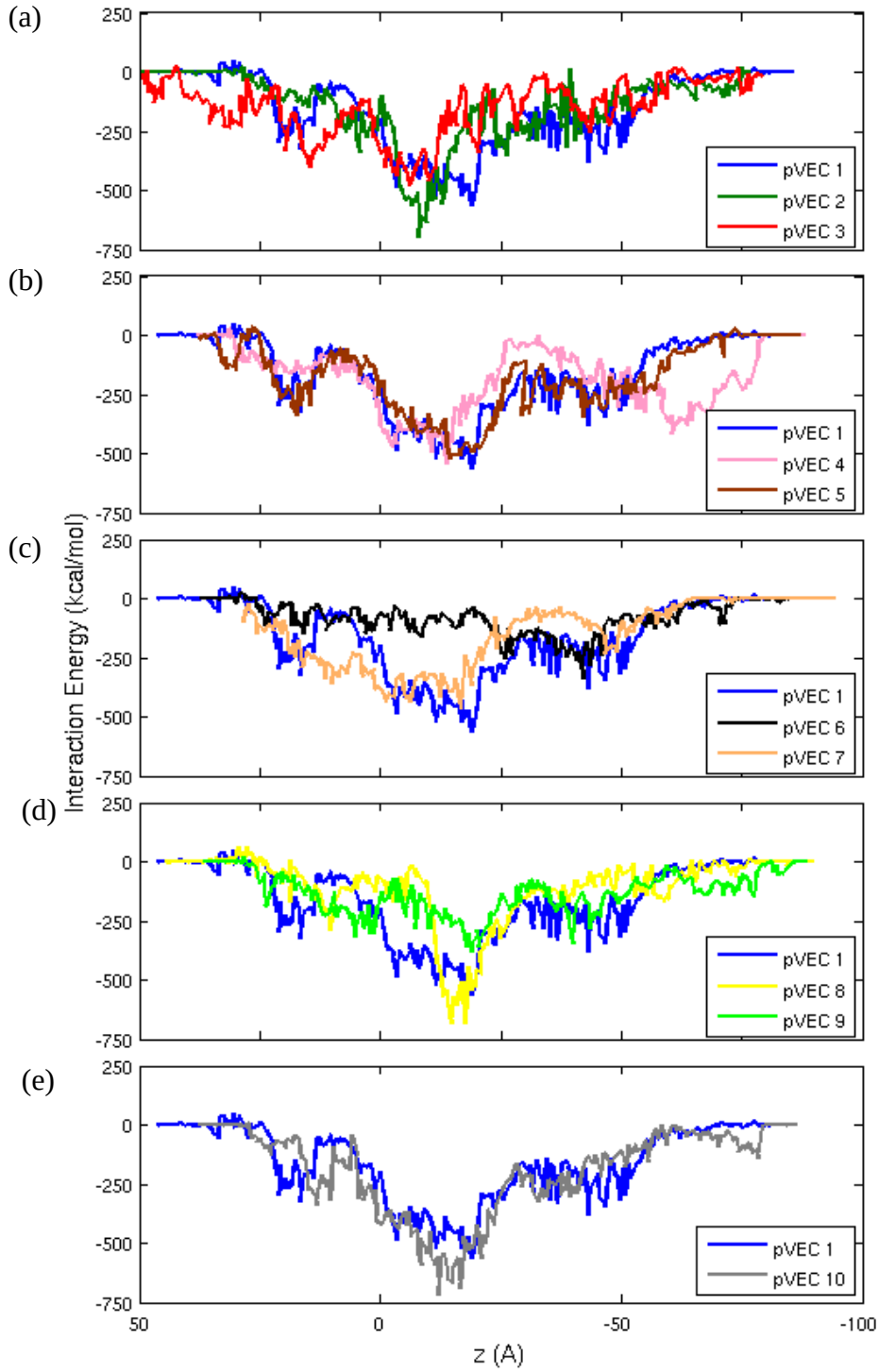

Figure 3.52. The interaction energy of pVEC 1 (original pVEC), (a) pVEC 2 (L1A), pVEC 3 (L2A) (b) pVEC 4 (I9A) and pVEC 5 (R10A) (c) pVEC 6 (S17A) and pVEC 7 (K18A) (d) pVEC 8 (retro-pVEC) and pVEC 9 (scramble pVEC) and (e) pVEC 10 (H14A).

The interaction energy between the peptide and the membrane for pVEC 2 (L1A) and pVEC 3 (L2A) were plotted in Figure 3.52(a). It was seen that the energy profiles followed a similar trend such that as the peptide approached and started to penetrate the membrane, the energy decreased. This meant that interaction was increasing. When the peptide was totally immersed which corresponded to z = -10 Å for both pVEC 2 and pVEC 3, the energy reached its minimum meaning that the interaction was at maximum. Then as the peptide travelled out of the membrane, the energy regressed to zero. When the minimum values of pVEC 2 (-694 kcal/mol) and pVEC 3 (-481 kcal/mol) were compared, the one of pVEC 2 was lower. Moreover, it was lower than the one of pVEC 1 (-565 kcal/mol). Therefore, mutating the first residue into alanine increased the interaction between the peptide and the membrane, while mutation of second residue decreased the interaction.

Figure 3.52(b) shows the interaction energy between the peptide and the membrane for pVEC 4 (I9A) and pVEC 5 (R10A) systems. The energy profile of pVEC 5 coincided with the profile of pVEC 1 which was the original pVEC. Therefore, the mutation on the 10^{th} residue did not affect the interaction between the peptide and the membrane. Up to z = -25 Å, the profile of pVEC 4 coincided with the one for the original pVEC. But after this check point, the interaction was very low when the center of the peptide was in the middle of the membrane. In contrast, when the SMD atom was at z = -60 Å, C terminus was in contact with the lower P heads. This contact caused a high interaction. The minimum energy of pVEC 4 was -540 kcal/mol while it was -521/mol kcal for pVEC 5. The energy at the minimum was -565 kcal/mol for the original one. These minima were very close to each other meaning that the highest interaction was almost equal in these three simulations.

The interaction between the peptide and the membrane of the systems of pVEC 6 (S17A) and pVEC 7 (K18A) was shown in Figure 3.52(c). The energy profile of pVEC 6 system in which the second residue from the C terminus was mutated was very higher than the energy profile of the original pVEC (pVEC 1). Thus, mutation of the 17^{th} residue lowered the interaction of the peptide and the membrane. The energy profile of pVEC 7 in which the first residue in the C terminus was mutated had close values to the values of pVEC 1. The minimum of pVEC 6 is -339 kcal which was much higher and far beyond

than the values of pVEC 1 (-565 kcal/mol) and pVEC 7 (-465 kcal/mol). The minimum of pVEC 7 was greater than the one for pVEC 1; nevertheless, they occurred at z = -12 Å.

The interaction energy profile of pVEC 9 (scramble pVEC) was lower than the profile of pVEC 1 as seen in Figure 3.52(d). This peptide having the same residue composition but different sequence caused less interaction between the peptide and the membrane. Similar to the profile of pVEC 9, the profile of pVEC 8 (retro-pVEC) was higher than the one of pVEC 1 in most of the simulation. However, there was a difference: at the point where the minimum energy was reached the energy of pVEC 8 (-685 kcal/mol) was lower than pVEC 1 (-565 kcal/mol). The minimum of pVEC 9 (-380 kcal/mol) was way higher than both of them. Thus altered sequence disfavored the interaction between the peptide and the membrane. Similarly, changing the sequence into reverse sequence disfavored the interaction except for the point at which the interaction was at maximum.

Figure 3.52(e) shows the interaction energy between pVEC 10 (H14A) and its membrane. Most of the time, the energy profile of pVEC 10 coincided with the one of the original pVEC. When the peptide was totally in the membrane, the interaction was at maximum. These maximum values of pVEC 1 and pVEC 10 were -565 kcal/mol and -715 kcal/mol. The value of pVEC 10 was lower than the other. Thus mutating the 14^{th} residue favored the interaction between the membrane and the peptide.

The total minimum interaction energy between the membrane and the peptide reached was tabulated in Table 3.19 and plotted in Figure 3.53. The tabulated data was sorted in the decreasing order of cellular uptake as reported by Langel [16]. As the cellular uptake values decreased, the minimum energy reached was decreasing. The decreasing cellular uptake value meant that it was harder for the peptide to enter the membrane and the decreasing minimum energy meant that the interaction between the peptide and the membrane was stronger. Therefore, as it got harder for the peptide to enter the membrane, the interaction between the peptide and the membrane got stronger as the slope of Figure 3.53 showed.

Table 3.19. The minimum interaction energy between the peptides and the membranes.

Name	Cellular uptake (pmol/mg protein)	Minimum interaction energy (kcal/mol)
pVEC 6 (S17A)	2219	-339
pVEC 7 (K18A)	2158	-465
pVEC 5 (R10A)	1535	-521
pVEC 1 (original pVEC)	1377	-565
pVEC 4 (I9A)	789	-540
pVEC 9 (scramble pVEC)	702	-380
pVEC 10 (H14A)	570	-715
pVEC 3 (L2A)	526	-481
pVEC 8 (retro-pVEC)	412	-685
pVEC 2 (L1A)	307	-694

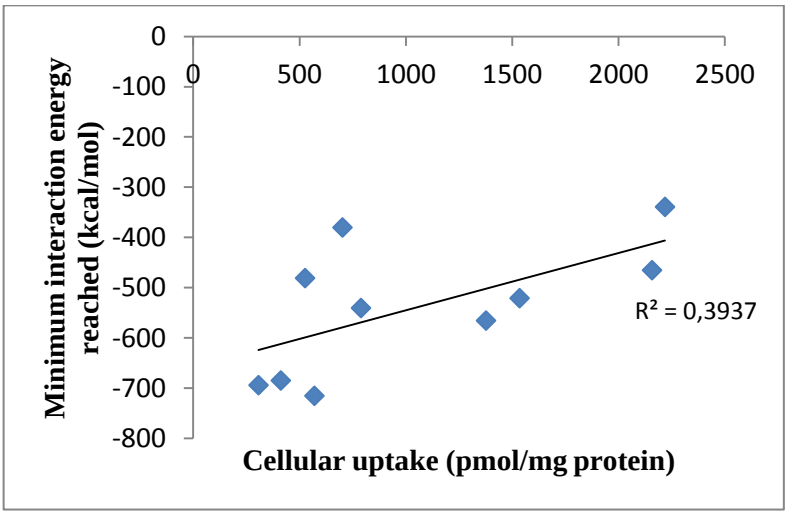

Figure 3.53. The comparison of experimental cellular uptake [16] and minimum interaction energy reached.

When the interactions were analyzed by contribution, there were several moments for pVEC 1 (original pVEC) and its membrane repelling each other. When His14 and ALA15 of the peptide came close to the upper phosphate heads of the membrane, there was a repulsion between those points. When the C terminus of the peptide touched either the upper or the lower phosphate heads of the lipids, repulsions were distinguished. Nevertheless, when the C terminus was in the middle of the peptide and when Arg7 and Arg8 were near the lower phosphate heads at the same time, attraction between the peptide and the membrane was detected. Moreover, strong attraction was shown when the peptide was totally embedded in the membrane.

When pVEC 2 (L1A) was considered, there was an immediate repulsion at the beginning of the simulation. This repulsion corresponded the time at when the N terminus touched the upper phosphate heads and the C terminus was very close to both the N terminus and upper phosphate heads. To be more specific Ala1 led this repulsion with the heads. Moreover, when the C terminus was in the middle of the bilayer and Arg6, Arg7 and Arg8 were in the lower P heads at the same time, there was an obvious repulsion. Nevertheless, when the C terminus of the peptide was in the membrane and stayed close to the upper P heads and the N terminus was next to the lower P heads, a major attraction was detected.

When the interaction between the membrane and pVEC 3 (L2A) was seeked, the only repulsion was detected when the Arg6, Arg7 and Arg8 were touching the lower P heads. There was an obvious attraction while the N terminus was in the middle of the bilayer and the C terminus was touching the upper P heads. And similar attraction was detected when the C terminus was in the middle of the bilayer. This attraction became stronger as the N terminus moved to the lower P heads.

A repulsion was detected for pVEC 4 (I9A) when the residues from 6 to 10 (having the sequence RRRAR) were interacting with the lower P heads. When the N terminus of the peptide was in the lower P heads and the C terminus was in the upper P heads at the

same time, strong attraction between the peptide and the lipid was detected. When the C terminus was in the lower P heads, an attraction was also seen.

The first obvious interaction for pVEC 5 (R10A) was distinguished when the residues 6 to 8 having the sequence RRR were touching the upper P heads. When the following ILE9 and Ala10 residues touched the upper P heads, the attraction became stronger. When the N terminus (residues from 1 to 5 having the sequence LLIIL) was in the lower P heads and the C terminus (residues from 13 to 18 having the sequence HAHSK) was in the upper P heads, the attraction between the peptide and the membrane was at maximum. When the residues from 6 to 10 having the sequence RRRIA were in the lower P heads, there was an attraction detected.

The major attraction between pVEC 6 (S17A) and the bilayer was detected when the C terminus was around the upper P heads and the residues from 6 to 10 having the sequence RRRIR were also in the upper P heads. Then when the N terminus was touching the lower P heads and even Arg6 was touching the lower P heads, an obvious attraction was noticed.

When pVEC 7 (K18A) was considered, there was a major attraction detected for a long period of time. This attraction started when the N terminus was in the upper P heads and the C terminus was near them. Then the N terminus advanced in the upper layer of the membrane and the C terminus was totally embedded in the upper P heads. This attraction reached its maximum when the residues from 8 to 15 having the sequence RIRKQAHA were in the upper P heads. This interaction ended when the C terminus was away from the upper P heads. A second attraction was distinguished when the C terminus residues from 9 to 18 were in the lower P heads. A weak repulsion was detected when the residues from 6 to 10 having the sequence RRRIR were in the lower P heads.

When pVEC 8 (retro-pVEC) was in consideration, the attractions started when the N terminus of the peptide was in the upper P heads. As the middle part (residues from 6 to 10

having the sequence AQKRI) touched the upper P heads, the attraction grew stronger. When the N terminus was in the lower P heads and the C terminus was in the upper P heads, the attraction reached its maximum. However, when the C terminus was in the lower P heads, a repulsion was seen.

The interaction between pVEC 9 (scramble pVEC) and the bilayer started when both of the N and the C terminus touched the upper P heads at the same time. As the C terminus was being embedded in the upper P heads, the attraction grew stronger. The attraction weakened when Arg8 and Ser9 were in the upper P heads; however, as the N terminus was in the lower P heads, the attraction became strong again. When the C terminus was still in the upper P heads and Lys6 and Ile5 were in the lower P heads at the same time, the high attraction was preserved.

When the N terminus of pVEC 10 (H14A) was in the upper P heads and the C terminus was very close to them at the same time, an attraction was seen. When the residues from 12 to 18 having the sequence QAAAHSK were in the upper P heads, the attraction became stronger. As the residues from 7 to 18 having the sequence RRIRKQAAAHSK were in the upper P heads, the attraction reached its maximum. However, as the residue from 11 to 14 having the sequence KQAA were touching the lower P heads, repulsion was detected.

Figure 3.54 shows the force applied to the pVEC 1 peptide in negative z direction. The force profile must be read from right to left since the pulling direction of peptide was negative z direction. Initially the force applied to the peptide was 0 pN because the peptide moved through the water layer. At around z = 20 Å there was a sudden increase in the force value when the peptide contacted the membrane. Since the peptide was penetrating the membrane, the membrane resisted in return. To overcome this resistance, force was being applied to the peptide.

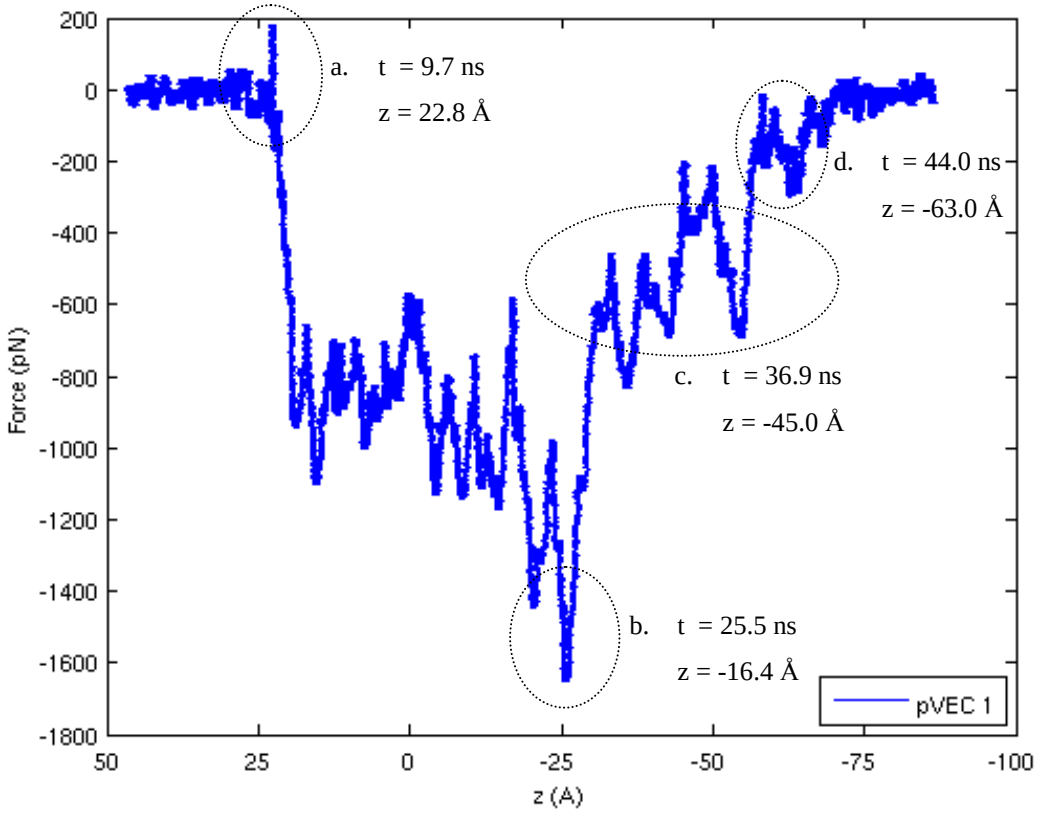

Figure 3.54. The force applied to the pVEC 1 (original pVEC) in negative z direction.

The force value reached a maximum at around z = 20 Å when the peptide was totally immersed in the membrane. After this checkpoint, the peptide started to leave the membrane. Since the membrane wanted to expel the peptide and the peptide started to go out of the membrane, less force was required to pull the peptide. Thus the applied force decreased. After the peptide was out of the membrane and moving through water, the force applied was 0 pN again.

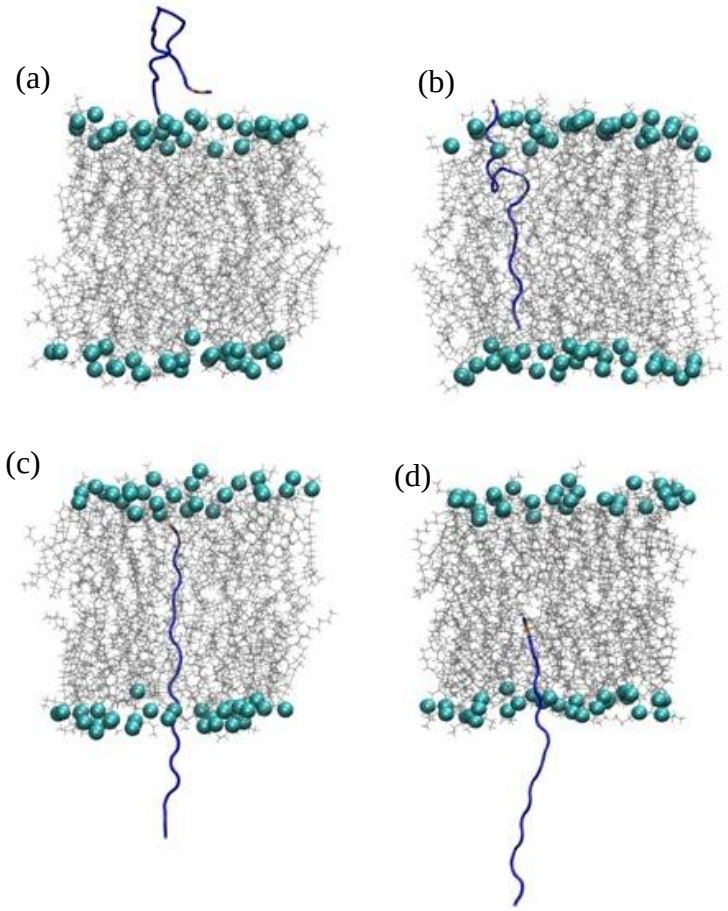

Figure 3.55. The structure of the system of pVEC 1 (original pVEC) at (a) t = 9.7 ns and z = 22.8 Å (b) t = 25.5 ns and z = -16.4 Å (c) t = 36.9 ns and z = -45.0 Å (d) t = 44.0 ns and z = -63.0 Å.

In Figure 3.54, there were four critical points on the force curve. These critical points were circulated and the structures of the peptide and the membrane system corresponding to these points were shown in Figure 3.55. In Figure 3.55(a), the peptide had the initial contact with the membrane. The N terminus of the peptide was immersed in the upper P heads of the membrane while the C terminus was very close to them. The peptide had a hairpin conformation so it was not unfolded. Figure 3.55(b) shows that the peptide was almost totally embedded in the membrane. The N terminus of the peptide was touching the lower P heads while the C terminus (residues 15 to 18) was in the upper P heads. The rest of the peptide was in the membrane. In Figure 3.55(c), the peptide was totally unfolded. The N terminus was out of the membrane while the C terminus was still touching to the upper P heads. The residues 7 to 10 were in interaction with the lower P heads. Figure

3.55(d) shows that two thirds of the peptide had left the membrane. The residues from 12 to 15 had contact with the lower P heads.

When the critical points of Figure 3.54 were compared with the ones in Figure 3.50, they corresponded to each other. The point a of Figure 3.54 (force curve) corresponded to the point b of Figure 3.50 (interaction energy curve). There was a high energy between the both termini and the upper P heads. The point b of Figure 3.54 corresponded to the point b of Figure 3.50 where there was interaction with the residues from 15 to 18 and the upper P heads. Moreover, the N terminus was touching to the lower P heads. Thus, the interaction was at maximum and maximum force (-565 pN) was required to pull the peptide and to overcome this interaction. The point c of Figure 3.54 and the point e of Figure 3.50 corresponded to the condition when there was an interaction between the C terminus and the upper P heads. Finally, the point d of Figure 3.54 and the point f of Figure 3.50 were the condition when the peptide was out of the membrane and there was small interaction left between the residues 12 to 15 with the lower P heads. Thus, -200 pN force was sufficient to overcome this interaction.

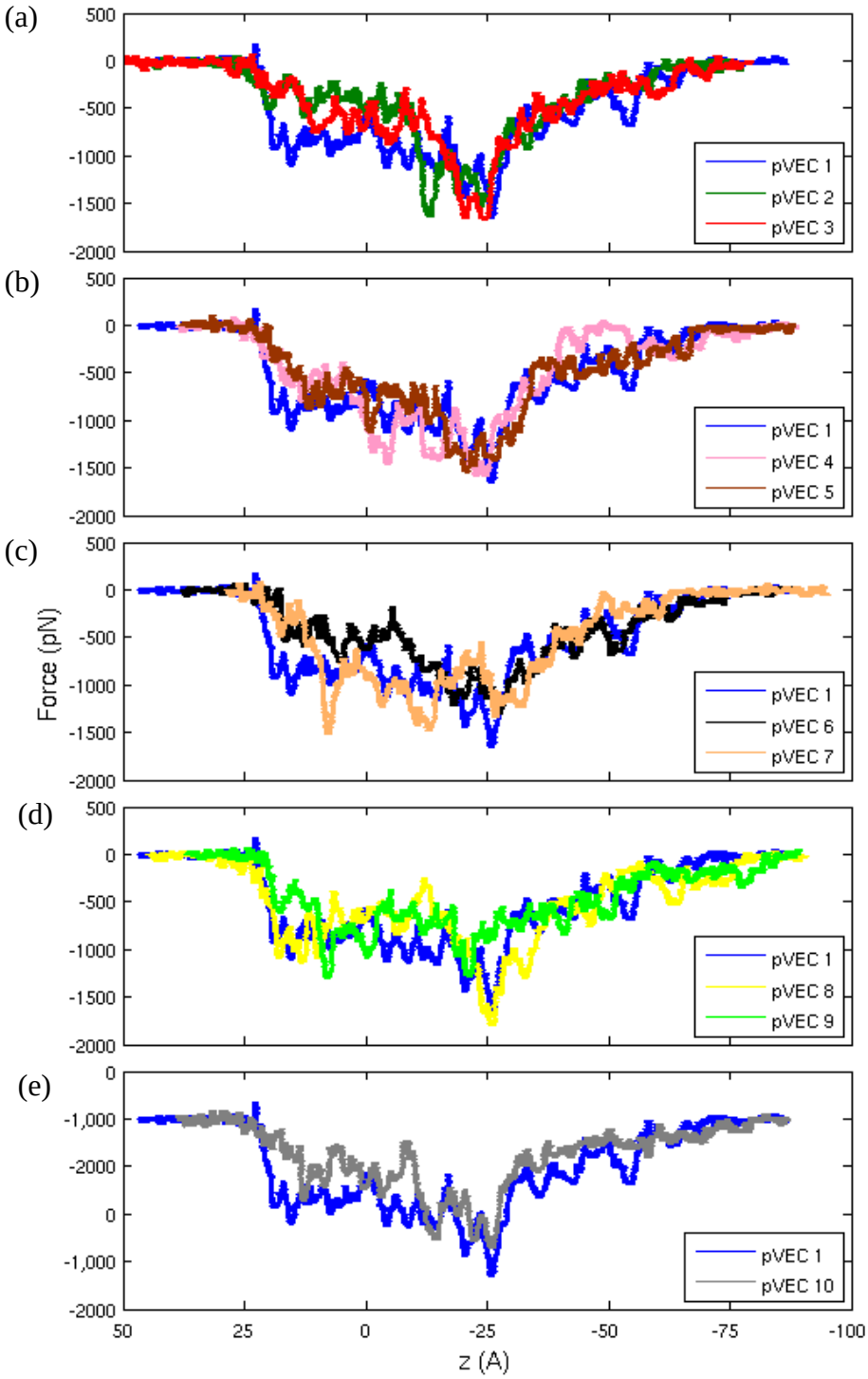

Figure 3.56. The force applied to pVEC 1 (original pVEC), (a) pVEC 2 (L1A) and pVEC 3 (L2A) (b) pVEC 4 (I9A) and pVEC 5 (R10A) (c) pVEC 6 (S17A) and pVEC 7 (K18A) (d) pVEC 8 (retro-pVEC) and pVEC 9 (scramble pVEC) and (e) pVEC 10 (H14A).

In Figure 3.56(a), the force applied to the peptide in negative z direction in pVEC 1, pVEC 2 and pVEC 3 systems were shown. The force curves of pVEC 2 (L1A) and pVEC 3 (L2A) almost coincided. Thus, mutating the first two residues in the N terminus had almost the same affects. Except the small shift from z = 20 Å to z = 0 Å, the force curves of the mutated peptides coincided with the force curve of the original pVEC (pVEC 1). The maximum force in negative z direction applied to the original pVEC was 1653 pN, while the force applied to pVEC 2 was 1641 pN and the one applied to pVEC 3 was 1675 pN. The maximum force values were very close to each other. Therefore, mutating the first two residues into alanine did not affect the required force to pull the peptide. The resistance of the membrane was almost same for these two mutants.

Figure 3.56(b) shows the forces applied to the pVEC 4 (I9A) and pVEC 5 (R10A). Until z = -50 Å, the force curves applied in the negative z direction coincided. The main mismatch occurred at around z = -50 Å. The C terminus of pVEC 4 contacted and interacted with the lower P heads of its membrane. Since when the hydrophilic residues interacted with the P heads, the peptide and the membrane repelled each other, less force in negative z direction was sufficient to continue the simulation. The maximum force applied to pVEC 4 (1587 pN) was close to the force applied to the original pVEC (1653 pN). Therefore, mutating the 9^{th} residue did not have much effect on the required force. However, the maximum force applied to pVEC 5 (1547 pN) was little lower than the maximum force applied to the original pVEC. Thus mutating the 10^{th} residue into alanine favored the simulation since less force was required.

In Figure 3.56(c), the force applied to the pVEC 6 (S17A) and pVEC 7 (K18A) in negative z direction are plotted. Until z = -50 Å, there were difference in force curves. The force curve of pVEC 6 followed the same trend with the curve of the original pVEC; however, it had lower values. The force curve of pVEC 7 was close to the one of the original pVEC; however; at z = 8 Å, the force applied to pVEC 7 in negative z direction made a maximum (1514 pN). The reason was the interaction of the residues from 9 to 14 (IRKQAH) with the upper P heads. A high force must have been applied to the peptide to overcome this interaction. After z = -50 Å, the force curves coincided and decreased back to zero. The maximum force required to pull the original pVEC was 1653 pN. The

maximum force in pVEC 7 was close to it. However, the maximum force applied to pVEC 6 (1308 pN) was lower than the force in the original pVEC. Therefore, mutating the 18th residue into alanine made the simulation perform more easily.

The force applied to the retro-pVEC (pVEC 8) and scramble pVEC (pVEC 9) in negative z direction was shown in Figure 3.56(d). The force curve of the retro-pVEC mostly coincided with the curve of the original pVEC except for the maximum value. The maximum force applied to it was 1803 pN which exceeded the maximum force applied to the original pVEC (1653 pN). The force curve of the scramble pVEC had lower values than the one of pVEC 1. Its maximum was 1305 pN which was quite low. Thus, it was easier for the scramble pVEC to pass through the membrane than the original pVEC did. It was harder for the retro-pVEC to pass through the membrane.

The force applied to pVEC 10 (H14A) in negative z direction followed the same path with the force of the original pVEC (Figure 3.56(e)). The curve of pVEC 10 was lower than the one of the original pVEC as shown in Figure 3.56(e). The maximum force values were 1653 pN and 1357 pN in pVEC 1 system and pVEC 10 system, respectively. This big gap said that mutating the 14th residue into alanine made the simulation require less force.

The maximum force values were tabulated in Table 3.20 and shown in Figure 3.57 in decreasing order of the cellular uptake values. If the experimental cellular uptake value of a peptide was low, there was higher resistance to be overcome in order to move. It was harder for a peptide to move through a membrane in which the resistance was higher. Thus, greater force was expected to be applied to the peptide. The minimum interaction energy vs. experimental cellular uptake graph (Figure 3.53) shows that if the cellular uptake was low, the interaction between the peptide and the membrane was high. Therefore, high force should have been applied to overcome this interaction. Thus there should have been an inverse proportionality that higher force needed to be applied for peptide with low uptake potential. The results agreed with this expectation but not very obviously. The slope in Figure 3.57 satisfied the expectation but since it was small, there was no clear conclusion.

Table 3.20. The maximum force applied to all pVEC peptides in negative z direction.

Name	Cellular uptake (pmol/mg protein)	Maximum force applied in negative z direction (pN)
pVEC 6 (S17A)	2219	1308
pVEC 7 (K18A)	2158	1514
pVEC 5 (R10A)	1535	1547
pVEC 1 (original pVEC)	1377	1653
pVEC 4 (I9A)	789	1587
pVEC 9 (scramble pVEC)	702	1308
pVEC 10 (H14A)	570	1357
pVEC 3 (L2A)	526	1675
pVEC 8 (retro-pVEC)	412	1803
pVEC 2 (L1A)	307	1641

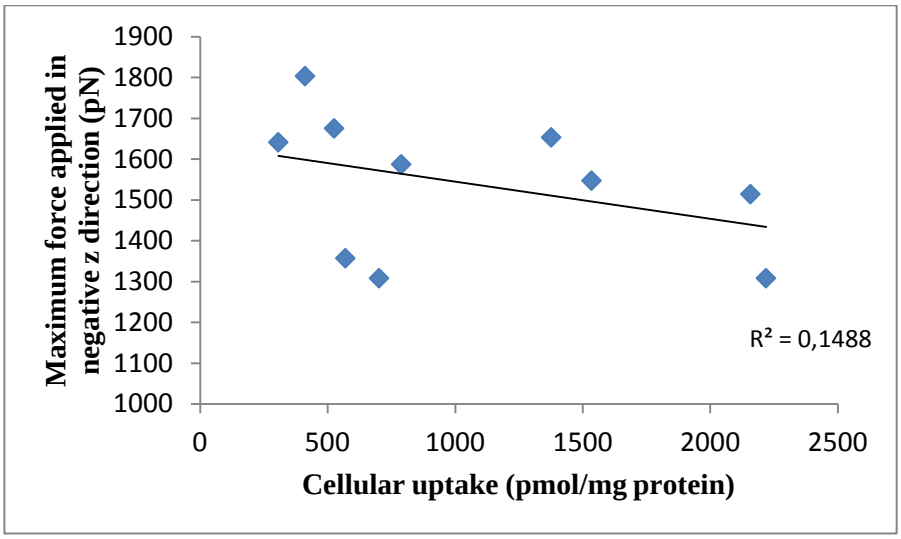

Figure 3.57. The comparison of the maximum force applied in negative z direction and the experimental cellular uptake values [16].

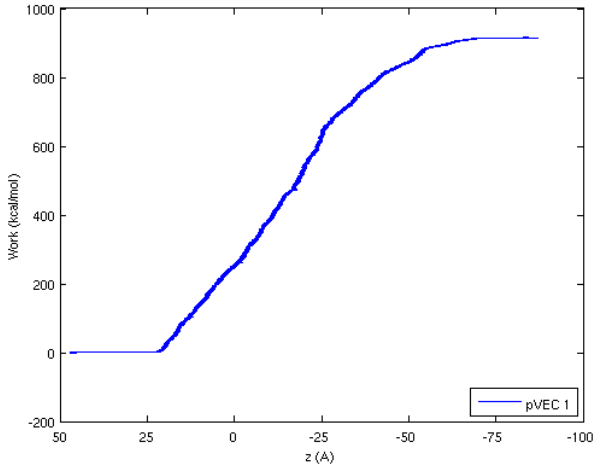

Figure 3.58. The work done on pVEC 1 (original pVEC).

In Figure 3.58, the work done on pVEC1 during the SMD simulation was plotted. Similarly, this graph must be read from right to left. Initially the SMD atom, the N terminal alpha carbon atom, was located at z = 50 Å. The work was stable up to about z = 20 Å at which point the SMD atom contacted the membrane. The peptide moved without accumulating any work in the z = 50 Å to z = 20 Å region because it moved easily through the water layer and no force was applied (Figure 3.54).

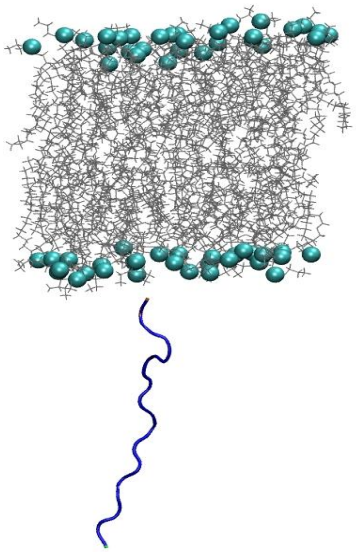

Figure 3.59. The snapshot of the system of pVEC 1 (original pVEC) at t = 48.7 ns and z = -75 Å.

At the z = 20 Å checkpoint, the work performed on the peptide started to increase as the peptide started to penetrate the membrane. The work done by pulling the peptide through the membrane continued to increase until z = -75 Å (Figure 3.59). This location was critical since the peptide was out of the membrane when the N terminus was at this point as shown in Figure 3.59. When the SMD atom was at this location, the force became zero again (Figure 3.54). There was no more force necessary to be applied to the peptide. Therefore, no more work was required and done.

In Figure 3.60(a), the work performed on pVEC 2 (L1A) and pVEC 3 (L2A) were plotted as a function of z-coordinate of the SMD atom which was the alpha carbon of the N terminal residue. The work curves of pVEC 2 and pVEC 3 coincided most of the time meaning that mutating first two residues of the peptide had the same effect on the work done. The maximum work values attained in the pVEC 2 (716 kcal/mol) system and pVEC 3 (762 kcal.mol) system were very close to each other. When the work done on the original pVEC (pVEC 1) was compared to the works done on the mutants, it was seen that the mutation yielded less work requirement. The maximum work done on pVEC 1 (916 kcal/mol) also satisfied this conclusion. Even though the applied force curves coincided in Figure 3.56, since the work was calculated cumulatively and there was higher force value applied on pVEC 1 at z = 20 Å and z = 0 Å, the final work done on pVEC 1 was greater than the mutants.

Figure 3.60(b) shows the work done on pVEC 4 (I9A) and pVEC 5 (R10A) throughout SMD simulations. The work curve of pVEC 1 (original pVEC) and the curve of pVEC 5 had a discrete difference throughout the simulation. This difference was also seen in the maximum work done values. 843 kcal/mol was the maximum work done on pVEC 5 where it was 916 kcal/mol for pVEC 1.

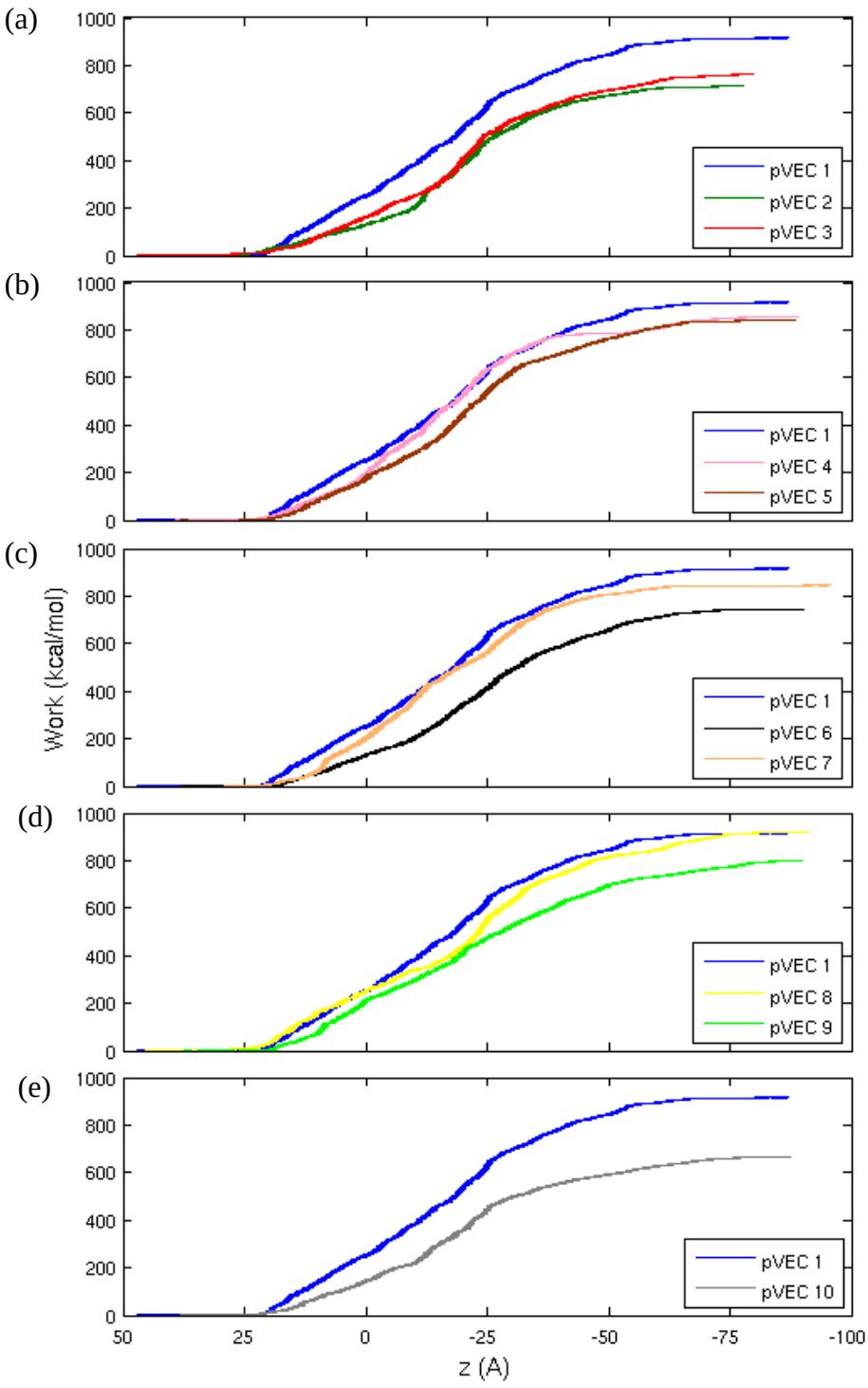

Figure 3.60. The work done on pVEC 1 (original pVEC), (a) pVEC 2 (L1A) and pVEC 3 (L2A) (b) pVEC 4 (I9A) and pVEC 5 (R10A) (c) pVEC 6 (S17A) and pVEC 7 (K18A) (d) pVEC 8 (retro-pVEC) and pVEC 9 (scramble pVEC) and (e) pVEC 10 (H14A).

The work curve of pVEC 4 oscillated between the curves of pVEC 1 and pVEC 5. In fact, after z = -14 Å, the work curve of pVEC 4 coincided with the one of the original pVEC. However, since there was a decrease in the force profile of pVEC 4 at around z = -50 Å (Figure 3.60(b)), the cumulative work curve continued to increase but with a smaller slope which brought it close to the curve of pVEC5. The maximum work done in pVEC 4 is 857 kcal/mol which was very close to the one of pVEC 5 (916 kcal/mol). Thus mutating residues which were in the middle of the pVEC led to less work values than the work done on the original pVEC.

The work done on pVEC 6 (S17A) and pVEC 7 (K18A) was shown in Figure 3.60(c). Since the force profile of pVEC 6 was lower than the force profile of pVEC 1 (original pVEC) as shown in Figure 3.60(c), the work done was also lower than the work done in both pVEC 1 and pVEC 7. The work curve of pVEC 7 was very close to the curve of pVEC 1 except for the final work attained. The maximum work done in pVEC 7 was 846 kcal/mol which was lower than 916 kcal/mol of pVEC 1. pVEC 6 had a much lower work done value (746 kcal/mol).

Figure 3.60(d) shows the work done on pVEC 8 (retro-pVEC) and pVEC 9 (scramble pVEC. The work curve of pVEC 8 was very close to the curve of pVEC 1 which was the original pVEC. The reason was the coinciding force profiles in Figure 3.56(d). Moreover, the maximum work values were almost equal since it was 916 kcal/mol in pVEC 1 system and 919 kcal/mol in pVEC 8 system. Thus, changing the sequence of the peptide in reverse direction did not affect the work done. When the sequence of the peptide was scrambled (pVEC 9), less work was done on the peptide throughout the simulation. This was also valid in the maximum work value of pVEC 9 which was 797 kcal/mol.

The work done on pVEC 10 (H14A) was quite lower than the work done on pVEC 1 (Figure 3.60(e)). The reason was the lower force profile which was shown in Figure 3.56(e). When the maximum values were compared, 666 kcal/mol of pVEC 10 was very low than 916 kcal/mol of pVEC 1.

The maximum work performed on each pVEC peptide was tabulated in

Table 3.21 and plotted in Figure 3.61. The values were sorted in decreasing order of cellular uptake values. The correlation observed for maximum force applied in negative z direction and cellular uptake might be expected for the maximum work done and uptake values. However, a similar correlation was not observed for cellular uptake and maximum work values. The slope of the trendline of Figure 3.61 was almost zero meaning that it is hard to make a correlation.

Table 3.21. The maximum work done on the peptides.

Name	**Cellular uptake (pmol/mg protein)**	**Maximum work done (kcal/mol)**
pVEC 6 (S17A)	2219	746
pVEC 7 (K18A)	2158	846
pVEC 5 (R10A)	1535	843
pVEC 1 (original pVEC)	1377	916
pVEC 4 (I9A)	789	857
pVEC 9 (scramble pVEC)	702	797
pVEC 10 (H14A)	570	666
pVEC 3 (L2A)	526	762
pVEC 8 (retro-pVEC)	412	919
pVEC 2 (L1A)	307	716

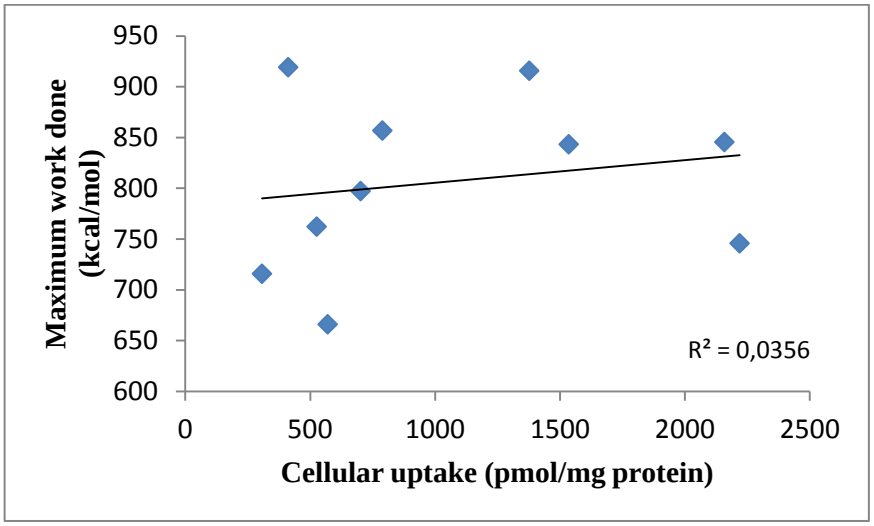

Figure 3.61. The comparison of the maximum work done on the peptide and the experimental cellular uptake values [16].

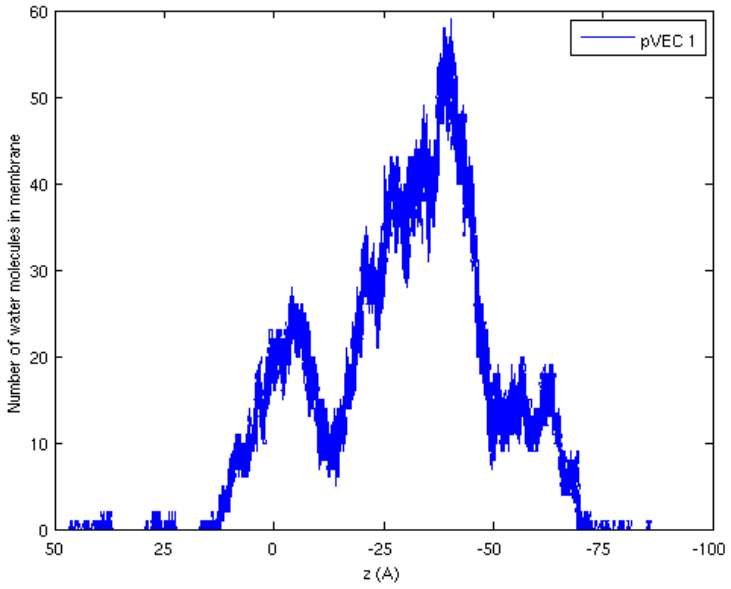

Figure 3.62. The number of water molecules present in the membrane in pVEC 1 system.

In Figure 3.62 the number of water that entered the membrane bilayer was plotted as a function of z-coordinate of the SMD atom which was the alpha carbon atom of the first residue in the N terminus of the peptide. While the ordinate was the number of water molecules, the abscissa was the z-coordinate of the first residue of the N terminus of the

peptide in the system. In other words, when z = 0 Å, the SMD atom had reached the center of the membrane (Figure 3.63). At the beginning, the peptide was in the water layer above the membrane, so it had positive z coordinate number. The peptide moved in negative z direction; therefore, the plot starts from right and must be read from right to left.

At the beginning of the simulation, there were no water molecules in the membrane. When the peptide started to enter the membrane, the water molecules also started to follow the peptide and enter the membrane. As the peptide was totally immersed, the water amount made a maximum reaching 59 molecules at z = -40 Å (Figure 3.63(a)). Then as peptide moved along, the water molecule number decreased. And finally when the peptide was far away from the membrane, there was no water left in the membrane.

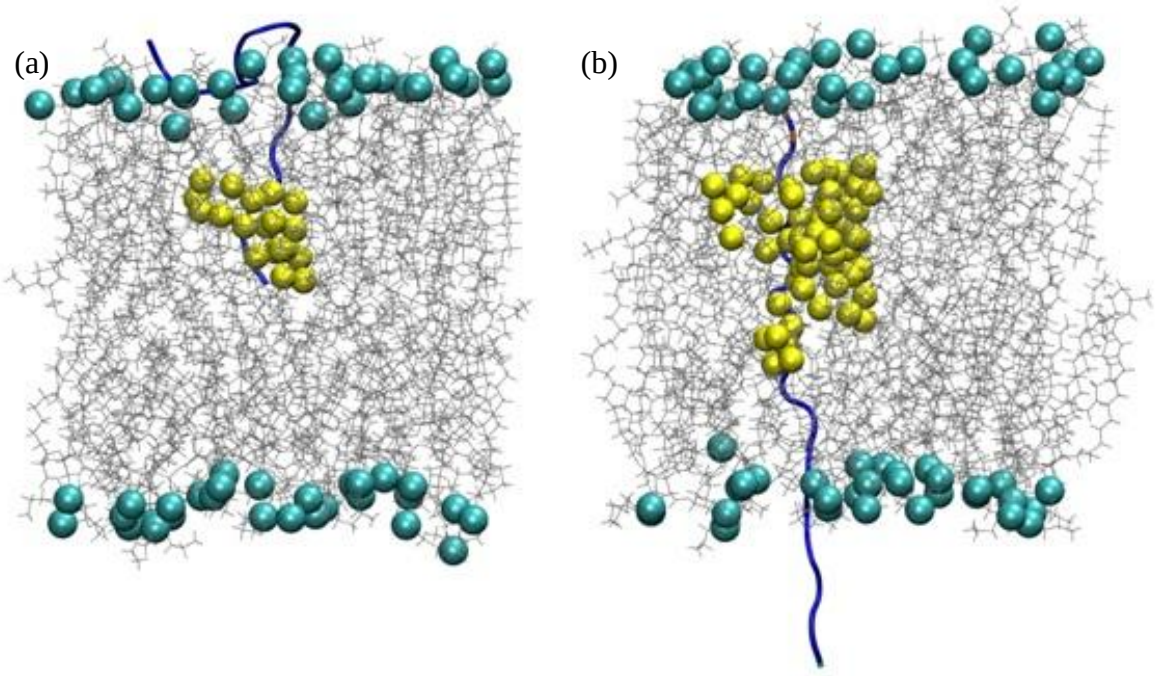

Figure 3.63. The system of water, membrane and peptide of pVEC 1 (original pVEC) at (a) z = 0 Å and t = 7.0 ns (b) z = -40 Å and t = 35.0 ns.

When the water profile was analyzed (Figure 3.62), there was a smaller maximum at around z = 0 Å. The reason for this small maximum was that as the peptide entered the membrane, the N terminus had a hairpin form, which extended out as the peptide moved

through the membrane as shown in Figure 3.63(b). The peptide was shown in NewCartoon representation and in blue color. The lipid tails of the membrane were shown in color grey and the phosphate heads were shown in cyan VDW representation. The water molecules in the membrane were shown in yellow color and VDW representation. The hairpin structure of the peptide created a cavity in the membrane. When the peptide completed unfolding, the smaller maximum diminished.

In Figure 3.64(a), the number of water molecules that enter the membrane as the peptide moved through the membrane in pVEC 1, pVEC 2 and pVEC 3 systems were plotted as a function of z-coordinate of the N terminus residue. The number of water molecules increased from zero to a small maximum in pVEC 2 and pVEC 3 systems similar to the system of the original pVEC. The cause of this small maximum was the cavity that the peptide created because of expansion of its hairpin conformation as it entered the membrane. Then there was a greater maximum when the center of the peptide was in the membrane. After the peptide left the membrane, there was no water left in the membrane. All the three profiles coincided and the maximum numbers of water molecules were almost equal for the systems of pVEC 2 (51 molecules) and pVEC 3 (49 molecules).

Figure 3.64(b) shows the number of water molecules that entered the membrane as the peptide moved through the membrane in pVEC 1, pVEC 4 and pVEC 5 systems. The plots were prepared as a function of z-coordinate of the N terminus residue. The number of water molecules was zero initially. Then it increased from zero to a small maximum in pVEC 4 and pVEC 5 systems similar to the system of the original pVEC. The cavity that the peptide created because of expansion of its hairpin conformation as it entered the membrane was the reason for this small maximum. Then there was a greater maximum when the center of the peptide was in the membrane. After the peptide left the membrane, there was no water left in the membrane. The profiles of pVEC 1 and pVEC 4 almost coincided; however, the profile of pVEC 5 reached greater values. The maximum numbers of water molecules were 54 and 73 for pVEC 4 and pVEC 5, respectively.

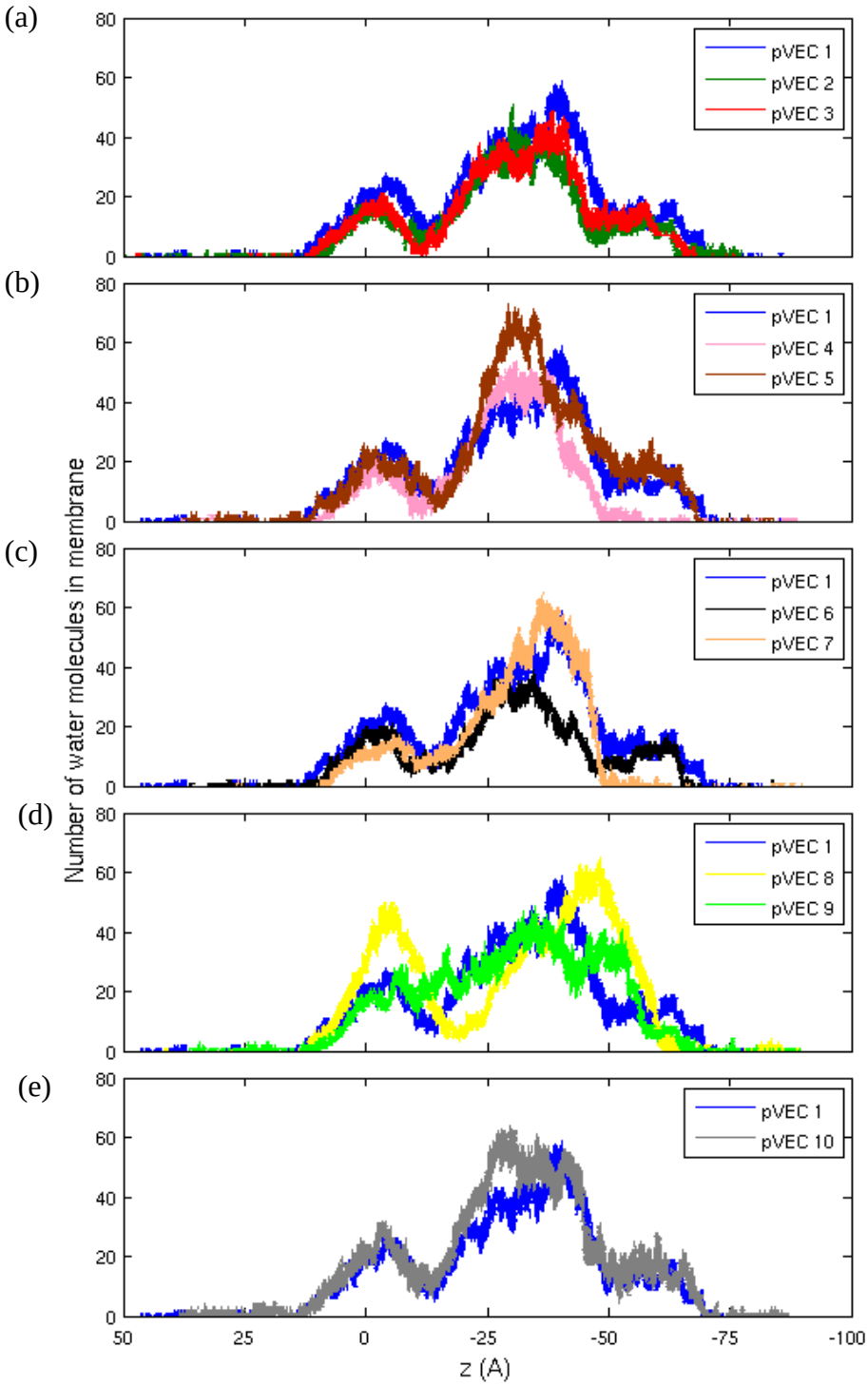

Figure 3.64. The water molecules in the membranes pVEC 1 (original pVEC), (a) pVEC 2 (L1A) and pVEC 3 (L2A) (b) pVEC 4 (I9A), pVEC 5 (R10A) (c) pVEC 6 (S17A), pVEC 7 (K18A) (d) pVEC 8 (retro-pVEC), pVEC 9 (scramble pVEC) (e) pVEC 10 (H14A).

The number of water molecules which entered the membrane when the peptide entered the membrane was shown in Figure 3.64(c) for the systems of pVEC 1, pVEC 6 and pVEC 7. These profiles were plotted as a function of z-coordinate of the N terminus residue. There was a small maximum in the number of water molecules for systems of pVEC 6 and pVEC 7. The reason of this small maximum was the cavity that the peptide created because of expansion of its hairpin conformation as it entered the membrane. Despite that these small maxima of pVEC 4 and pVEC 5 almost coincided, they were lower than the small maximum of the original pVEC. When the main maxima were compared, there were 65 water molecules in the membrane of pVEC 7, while there were 39 molecules for the system of pVEC 6.

The water molecules in pVEC 8 increased with same slope; however, the small maximum in its membrane was almost as high as the main maxima of pVEC 1 and pVEC 9 (Figure 3.64(d)). The main maximum of pVEC 8 (65 molecules) exceeded the one for pVEC 1 (59 molecules). In contrast, the main maximum of pVEC 9 was lower than the pVEC 1 with 49 molecules.

The profiles of number of water molecules entering the membrane of pVEC 1 and pVEC 10 shown in Figure 3.64(e) almost coincided. The small maximum values were equal. The only differences were the peaks of the main maximum. The maximum number of water in the membrane of pVEC 10 was 64 while it was 59 for the pVEC 1 case. The z-coordinates at which the maxima were reached differ 5 ns.

Table 3.22 and Figure 3.65 showed the maximum number of water molecules present in the each pVEC-membrane system sorted according to the decreasing experimental cellular uptake values [16]. A higher cellular uptake value meant that the peptide spontaneously entered the membrane more easily and a smaller value meant that it was harder for the peptide to immerse in the membrane. One could expect that if it was harder for a peptide to enter the membrane, more disorder might result in the membrane. Thus, as the cellular uptake decreased, higher distortion of the membrane; in other words, higher number of water molecules in the membrane might have been expected. However, when

the data in Table 3.22 and Figure 3.65 were analyzed, a correlation between the cellular uptake values and the number of water molecules could not be observed. The maximum number of water molecules was all around 39-65 except for pVEC 5, which carried 73 water molecules with it.

Table 3.22. The maximum number of water molecules.

Name	**Cellular uptake (pmol/mg protein)**	**Maximum number of water molecules in the membrane**
pVEC 6 (S17A)	2219	39
pVEC 7 (K18A)	2158	65
pVEC 5 (R10A)	1535	73
pVEC 1 (original pVEC)	1377	59
pVEC 4 (I9A)	789	54
pVEC 9 (scramble pVEC)	702	49
pVEC 10 (H14A)	570	64
pVEC 3 (L2A)	526	49
pVEC 8 (retro-pVEC)	412	65
pVEC 2 (L1A)	307	51

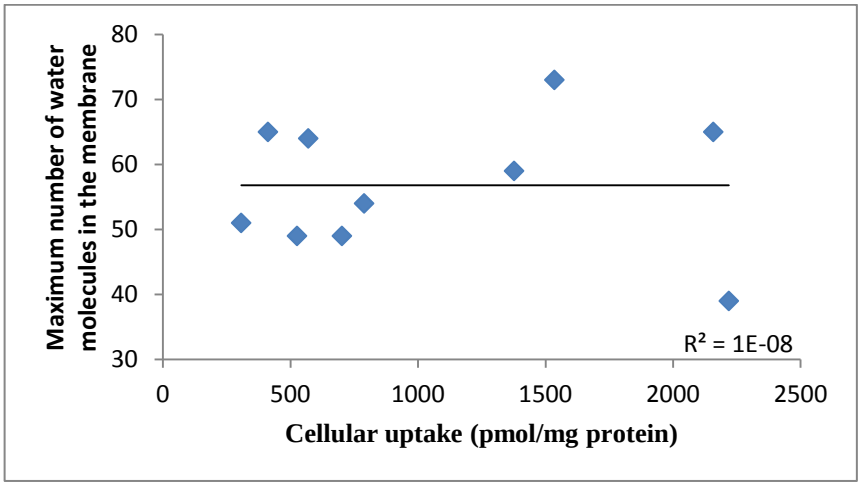

Figure 3.65. The comparison of the experimental cellular uptake values [16] and the maximum number of water molecules.

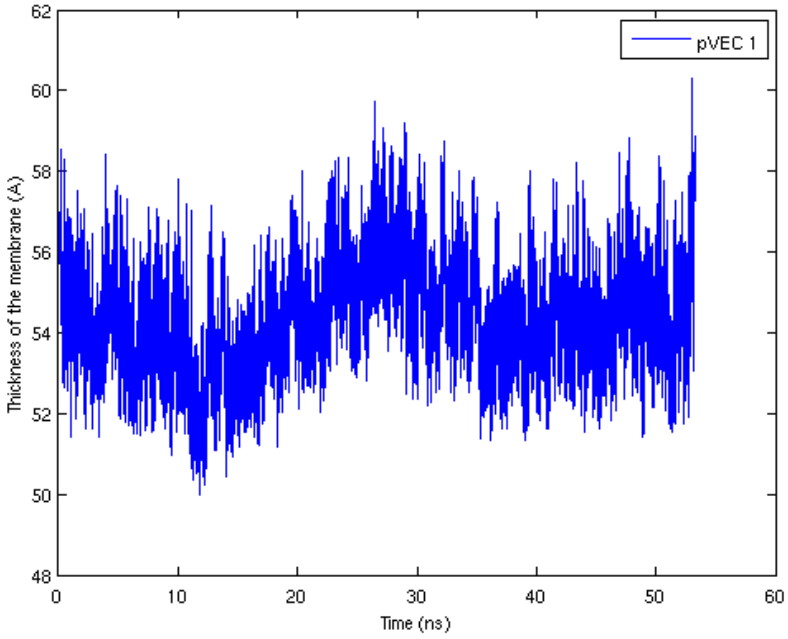

Figure 3.66. The thickness of the membrane of pVEC 1 (original pVEC).

Figure 3.66 shows how the thickness of the membrane of pVEC 1 changed throughout the simulation. The thickness of the membrane was another way of observing the disorder of the membrane. The membrane thickness stayed between 52 Å and 58 Å during the pVEC 1 simulation and the membrane did not undergo any major change in thickness.

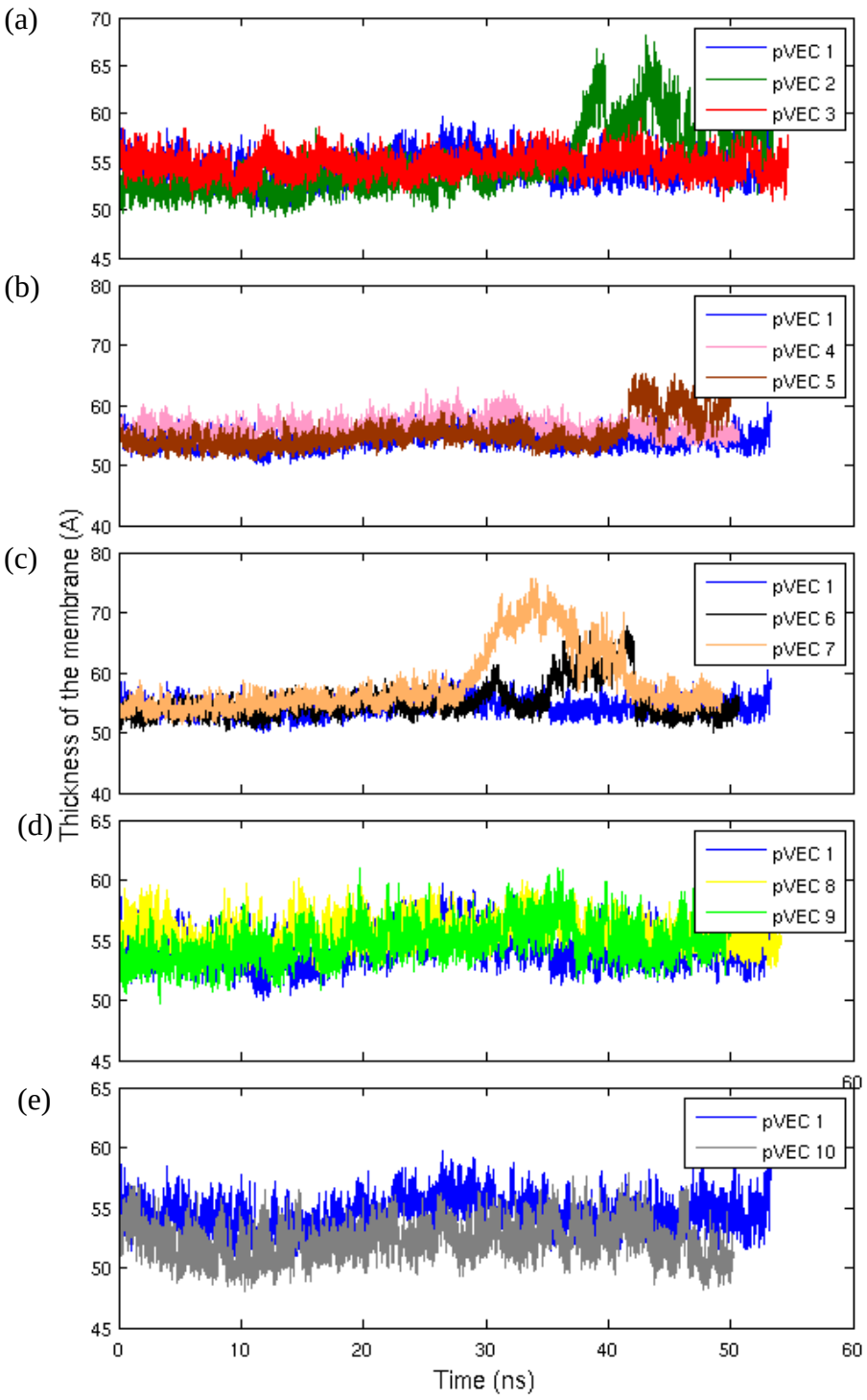

Figure 3.67. The thickness of the membrane of pVEC 1 (original pVEC), (a) pVEC 2 (L1A), pVEC 3 (L2A) (b) pVEC 4 (I9A), pVEC 5 (R10A) (c) pVEC 6 (S17A), pVEC 7 (K18A) (d) pVEC 8 (retro-pVEC), pVEC 9 (scramble pVEC) and (e) pVEC 10 (H14A).

The thicknesses of pVEC 2 (L1A) and pVEC 3 (L2A) were plotted in Figure 3.67(a). There was no change in the thickness of pVEC 3 through the whole simulation, while the thickness of pVEC 2 increased after t = 38 ns to 68.2 Å. The mean of the thickness of three membranes were very close to each other (pVEC 1: 54.3 Å, pVEC 2: 55.0 Å, pVEC 3: 54.7 Å) However, the standard deviation of pVEC 2 (3.49 Å) showed the difference of thickening when compared with the standard deviation of pVEC 1 (1.36 Å) and pVEC 3 (1.13 Å). This increment was caused by some lipid tails which go out of the membrane.

Figure 3.67(b) shows the thickness variation of pVEC 4 (I9A) and pVEC 5 (R10A) during the simulations. Thicknesses of membranes of both pVEC 4 (mean: 56.3 Å) and pVEC 5 (mean: 55.3 Å) were higher than the one of pVEC 1 (mean: 54.3 Å). Thickness of pVEC 4 membrane was also higher than the thickness of pVEC 5 membrane. The thickness of the membrane of pVEC 5 increased after t = 42 ns to 66.8 Å thickness. This increment was also seen in standard deviation values. The standard deviation of pVEC 4 was 1.42 Å while it was 2.63 Å for pVEC 5. This increment was caused by some lipid tails which go out of the membrane.

The thicknesses of membranes of both pVEC 6 and pVEC 7 were close to the one of pVEC 1 up to t = 30 ns (Figure 3.67(c)). After this point, both the thicknesses of pVEC 6 (maximum: 67.8 Å) and pVEC 7 (maximum: 75.68) increased because of hanging out of some lipid tails. In fact, the thickness of pVEC 7 membrane increased very much. The mean of the thickness of pVEC 6 (55.2 Å) was close to the mean of the thickness of pVEC 1 (54.3 Å); however, the mean of pVEC 7 (58.2 Å) was higher. The standard deviations supported these increments in the thickness. The standard deviation of pVEC 6 was 2.98 Å while it was 5.20 Å for pVEC 7.

The thicknesses of pVEC 8 (retro-pVEC) and pVEC 9 (scramble pVEC) were shown in Figure 3.67(d). Thicknesses of both peptides had stable values and they were close to the pVEC 1 membrane thickness. The mean of the thickness of pVEC 8 was 55.6 Å while it was 54.8 Å for pVEC 9. These values were close to 54.3 Å of pVEC 1. The standard

deviation values of pVEC 8 (1.24 Å) and pVEC 9 (1.56 Å) agreed with the stability conclusion.

Figure 3.67(e) shows that the membrane of pVEC 10 (H14A) was thinner than the membrane of pVEC 1 (original pVEC). The mean values agreed with this: mean of pVEC 1 membrane was 54.3 Å while the mean of pVEC 10 was 52.3 Å. The thickness of pVEC 10 membrane stayed steady as its standard deviation says (1.47 Å).

Table 3.23. Summary of the cellular uptake, the minimum interaction energy reached and the maximum force applied in negative z direction for all pVEC simulation.

Name	**Cellular uptake (pmol/mg protein)**	**Minimum interaction energy (kcal/mol)**	**Maximum force applied in negative z direction (pN)**
pVEC 1 (original pVEC)	1377	-565	1653
pVEC 2 (L1A)	307	-694	1641
pVEC 3 (L2A)	526	-481	1675
pVEC 4 (I9A)	789	-540	1587
pVEC 5 (R10A)	1535	-521	1547
pVEC 10 (H14A)	570	-715	1357
pVEC 6 (S17A)	2219	-339	1308
pVEC 7 (K18A)	2158	-465	1514
pVEC 8 (retro-pVEC)	412	-685	1803
pVEC 9 (scramble pVEC)	702	-380	1308

Table 3.24. Summary of the cellular uptake, the maximum work pone on the peptide and the maximum number of water molecules in the membrane.

Name	**Cellular uptake (pmol/mg protein)**	**Maximum work done (kcal/mol)**	**Maximum number of water molecules in the membrane**
pVEC 1 (original pVEC)	1377	916	59
pVEC 2 (L1A)	307	716	51
pVEC 3 (L2A)	526	762	49
pVEC 4 (I9A)	789	857	54
pVEC 5 (R10A)	1535	843	73
pVEC 10 (H14A)	570	666	64
pVEC 6 (S17A)	2219	746	39
pVEC 7 (K18A)	2158	846	65
pVEC 8 (retro-pVEC)	412	919	65
pVEC 9 (scramble pVEC)	702	797	49

In order to summarize the effect of the mutations and the sequence variation, mutating the 2^{nd} (L2A), 17^{th} (S17A) and 18^{th} (K18A) residues to alanine and scrambling the sequence (scramble pVEC) decreased the interaction between the peptide and the membrane (Table 3.23). In contrast, mutating the 1^{st} (L1A), 14^{th} (H14A) residues to alanine and reversing the sequence (retro-pVEC) enhanced the interaction. Mutating the residues from the middle part of the pVEC which are 9^{th} (I9A) and 10^{th} (R10A) residues did not have any effect on the interaction when they were compared with the interaction of the original pVEC and the membrane.

When the force required to move the peptides were compared, it was seen that mutations on the N terminus (L1A and L2A) and the middle part (I9A and R10A) had almost no effect on the force necessary (Table 3.23). The mutation on the 14^{th} residue (H14A) and the residues on the C terminus (S17A and K18A) favored the simulation since they required less force to be applied. Reversing the sequence (retro-pVEC) had to be

pulled with a higher force than the original sequence while scrambling the sequence (scramble pVEC) required less force.

When the work applied on the peptides were in consideration, it was seen that less work was done on the mutants and the scramble pVEC except the retro-pVEC on which equal work to the original one was done (Table 3.24). The least work was done on mutant H14A while it was followed by the N terminal mutants (L1A and L2A), mutant S17A and scramble pVEC. The work done on the middle part mutants (I9A and R10A) and mutant K18A were close to the value of the original pVEC but still smaller.

In order to examine the deformation on the membrane, number of water molecules entering the membrane (Table 3.24) and the thickness of the membrane were the parameters. The membrane of mutant S17A had the least number of water molecules. The N terminal mutants (L1A and L2A) and the scramble pVEC assisted lower number of water molecules than the original one did to enter the membrane. The mutant I9A caused a similar result to the original one. The mutants H14A and K18A, and the retro-pVEC systems had higher number of waters while the system of the mutant R10A had the greatest.

When the thicknesses of the membranes were compared (except for the parts where the lipid tails move out of the membrane), the N terminal mutant L2A, the middle part mutant R10A, the C terminal mutants S17A and K18A, scramble pVEC and the retro-pVEC systems had the same thickness values with the original pVEC. The mutant L1A and H14A thinned their membranes while the mutant I9A thickened its membrane.

In order to sum up and suggest which alteration is preferable, the mutation H14A seemed to favor the simulation by its less force requirement and less work done on it. To scramble the sequence (scramble pVEC) and mutating the C terminal residues (S17A and K18A) into alanine enhanced the simulations following H14A. The N terminal mutations (L1A and L2A) also favored the simulations but not as much as the previously stated ones

did. The middle part mutations (I9A and R10A) did not have almost any effect while reversing the sequence (retro-pVEC) disfavored the simulation.

Table 3.25. The mean and standard deviation values of highest interaction energies, maximum forces applied, work done on peptide and number of water molecules in membrane for all 3 sections.

Interaction energy (kcal/mol):		
	mean	**standard deviation**
BLIP based peptide (vel = 5.0 Å/ns)	-272,7	58,76
modified BLIP based peptide (vel = 5.0 Å/ns)	-454,6	47,46
pVEC (vel = 2.5 Å/ns)	-538,5	129,72
Force (pN):		
	mean	**standard deviation**
BLIP based peptide (vel = 5.0 Å/ns)	755,0	92,65
modified BLIP based peptide (vel = 5.0 Å/ns)	1097,3	212,63
pVEC (vel = 2.5 Å/ns)	1539,3	168,14
Work (kcal/mol):		
	mean	**standard deviation**
BLIP based peptide (vel = 5.0 Å/ns)	316,8	25,06
modified BLIP based peptide (vel = 5.0 Å/ns)	579,9	99,71
pVEC (vel = 2.5 Å/ns)	806,8	84,16
Number of water molecules in membrane:		
	mean	**standard deviation**
BLIP based peptide (vel = 5.0 Å/ns)	55,5	12,77
modified BLIP based peptide (vel = 5.0 Å/ns)	86,9	28,56
pVEC (vel = 2.5 Å/ns)	56,8	10,18

In Table 3.25, the mean and standard deviation values of highest interaction energies between the peptide and the membrane, maximum forces applied to the peptide in negative z direction, the work done on the peptide and the number of water molecules in membrane

for all 3 sections were tabulated. For the first two sections, only the values of the simulations in which the peptide was pulled with 5.0 Å/ns velocity are chosen.

When the means of the interaction energies for the BLIP based and the modified BLIP based peptides were compared, it was seen that addition of the cargo carrying part (LLIIL) increased the interaction energy from -272.7 kcal/mol to -454.6 kcal/mol. This increase was expected since LLIIL part was extracted from the N terminus of the pVEC peptide of which N terminus was crucial for the spontaneous cellular uptake. Since there was higher interaction between the modified BLIP based peptide and its membrane, higher force was necessary to move the peptide against this higher resistance. This situation was also seen in the force part of Table 3.25. Thus, higher work must have been done on the peptide in order to pull it as it was also seen in the work values of BLIP based peptide (316.8 kcal/mol) and the modified BLIP based peptide (579.9 kcal/mol). Moreover, it was seen that addition of the cargo carrying LLIIL part increased the deformation of the membrane by increasing the number of water molecules entering the membrane.

When the mean values of the pVEC peptide systems were compared with the values of others, it was seen that except the water numbers, the values of the pVEC system reached higher values than the first two systems. This higher interaction energy could have two reasons. First, the peptide was pulled with a slower velocity. Thus the peptide had more time to interact with the membrane. Moreover, the sequences of the pVEC systems could have enhanced the interaction, too. Since the interaction was highest of all, highest force was required to pull the pVEC peptides. Even though the pulling velocities decreased, the higher forces applied yielded higher work values than the both previous cases did. Although interaction, force and work values of the pVEC systems were the highest of all, the deformation on the membranes of the pVEC systems were almost same with the deformation on the membranes of the BLIP based peptide systems.

4 CONCLUSION

In the current study, steered molecular dynamics simulations were performed to identify the optimum parameters such as spring constant, pulling velocity and place of pulling, to study the uptake potential of the BLIP based peptides and to determine the important residues of the pVEC peptide in cellular uptake. The simulation systems of all the BLIP based, pVEC and mutant pVEC peptides were composed of POPE type lipid which represents the model bacterial membrane, the peptide and water molecules in the either side of the membrane.

The first BLIP based peptide has the sequence HAAGDYYA. When the work done on the peptide, force required to pull the peptide and the interaction energy between the peptide and the membrane were analyzed, it showed that no clear distinction could be made in the different spring constant values which were 7 kcal/mol/Å^2 and 10 kcal/mol/Å^2. When the peptide was pulled faster which was 5.0 Å/ns, the peptide passed through the membrane more easily. The peptide was pulled with highest force and work when it was pulled from its N terminus. The first 5 residues of pVEC peptide with the sequence LLIILRRRIRKQAHAHSK were stated to be important in the cellular uptake in the literature; therefore, the LLIIL part of the pVEC was extracted and added to the N terminus of the first BLIP based peptide. Thus, the second BLIP based peptide had the sequence LLIILHAAGDYYA. The peptide moved through the membrane easily when it was pulled with small spring constant which was 7 kcal/mol/Å^2. There was no difference in the results of the pulling velocities which were 2.5 Å/ns and 5.0 Å/ns. The peptide was pulled with highest force and work when it was pulled from its N terminus. Finally, the important residues of the pVEC were found to be 14, 17, 18, 1 and 2 in descending order. Moreover, scrambling the sequence enhanced the uptake as high as the mutation on the 14th residue did.

When the spring constant values were compared for both of the BLIP based peptides, there was no obvious distinction for the first peptide, while the simulations having the

second peptide showed that it was easier to pass with the soft spring. Before the addition of the LLIIL part, there was more interaction between the peptide and the membrane when the spring constant was smaller. However, addition altered this observation to more interaction when the spring constant was greater. The forces applied to the both peptides in the negative z direction showed that greater force was necessary for the greater spring constant. The work values calculated for both peptides showed that there was no difference for any spring constant. In the membranes of both peptides, water molecules entered the membrane if the spring constant was stiffer; nevertheless, if the peptide was pulled with softer spring, the water molecules spent more time in the membrane. The thickness of the membrane of the first BLIP based peptide was thicker when the spring constant was smaller; however, addition of the LLIIL part yielded the results that there was no difference between the thicknesses of the membrane with different spring constants.

The first peptide moved through the membrane more easily when it was pulled faster even though pulling faster and slower had the same effect on the simulation with the second BLIP based peptide. The interaction between the first peptide and the membrane was lower when the peptide was pulled faster; however, addition of LLIIL equated the interaction between the peptide and the membrane for different velocities. The force was higher when the first BLIP based peptide was pulled slowly, but addition of LLIIL again equated the force values for different velocities. The calculated work values were opposite of each other for the first and the second peptide. In the simulation having the first peptide, slower peptide reached higher work values. In contrast, the faster modified peptide reached higher work values. The water molecules in the membrane were equal when the first peptide was used and pulled with any velocity. However, it LLIIL was added to the peptide, more water molecules entered when the peptide was pulled slowly. The thicknesses of the membranes of both peptides were all equal for different velocities.

When the places of pulling were considered, it was seen that the interaction between the first peptide was equal when it was pulled from either C terminus or its center of mass. This interaction was stronger when it was pulled from N terminus. Addition of the cargo carrying part did not change the order of these interactions. For both of the peptides, when the peptides were pulled from their N terminus, it required the highest force. Similarly, the

work done on the both peptides was highest when the peptides were pulled from their N terminus. Additionally, the number of water molecules in the membranes of both peptides was highest when they were pulled from their center of mass.

The N terminus of pVEC peptide was previously found to be significant in the cellular uptake. Addition of the N terminal hydrophobic residues LLIIL to the BLIP based peptide increased the interaction between the peptide and the membrane. Thus, higher force was required and more work had to be done to move the peptide in the membrane.

When the importance of the mutations on the residues of pVEC was investigated, the mutation of 14^{th} residue and scrambling the residues favored the uptake across the membrane at most. Reduction in the cellular uptake of the mutation of the 14^{th} residue and scramble pVEC was previously stated to be highest by experiments in literature. Therefore, the SMD results for these two peptides were not in agreement with the experimental results. The mutations on the first and the second residues were also previously stated to reduce the cellular uptake; however, SMD results showed that these mutations enhanced the cellular uptake. This was the second contradiction. In contrast, the experimental and SMD results of the mutations of the 17^{th} and 18^{th} residues into alanine were in agreement with each other that these mutations favored the uptake. The second main satisfaction was the retro-pVEC since retro-pVEC had one of the highest reduction in its cellular uptake and it passed the membrane hardly since the maximum force and work values of its simulations yielded high values.

The mean of the interaction energy between the peptide and the membrane, the maximum force and work values of the pVEC system reached higher values than the first two systems because either the peptide was pulled with a slower velocity or the sequences of the pVEC systems could have enhanced the interaction. Although interaction, force and work values of the pVEC systems were the highest of all, the deformation on the membranes of the pVEC systems were almost same with the deformation on the membranes of the BLIP based peptide systems.

APPENDIX A: THE PROFILES OF THE FORCE APPLIED TO THE PEPTIDE IN NEGATIVE Z-DIRECTION WITH RUNNING AVERAGE

A.1. Membrane Uptake of a BLIP Based Peptide

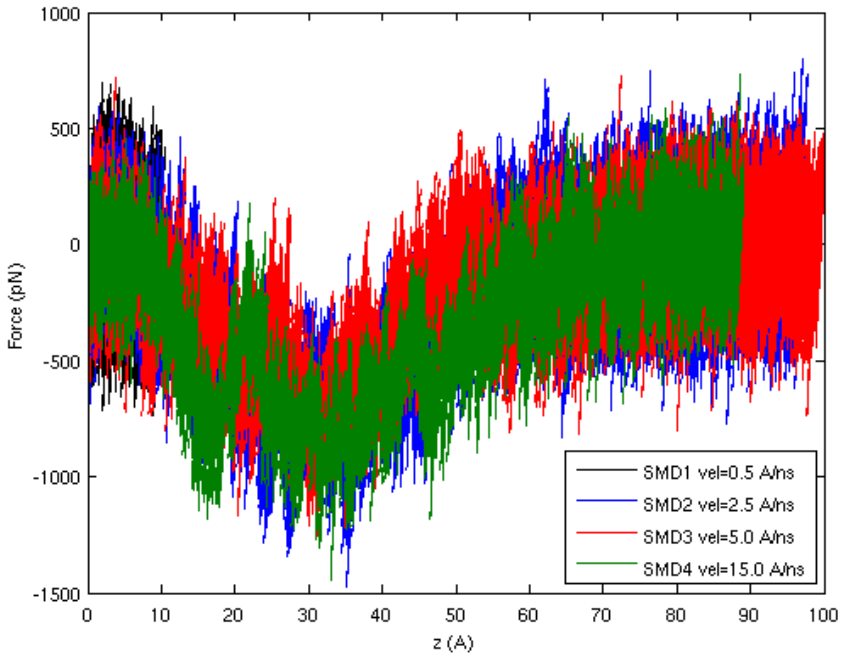

Figure A.1. The force applied in simulations SMD1 (v = 0.5 Å/ns) (black), SMD2 (v = 2.5 Å/ns) (blue), SMD3 (v = 5.0 Å/ns) (red), and SMD4 (v = 15.0 Å/ns) (green) on the peptides.

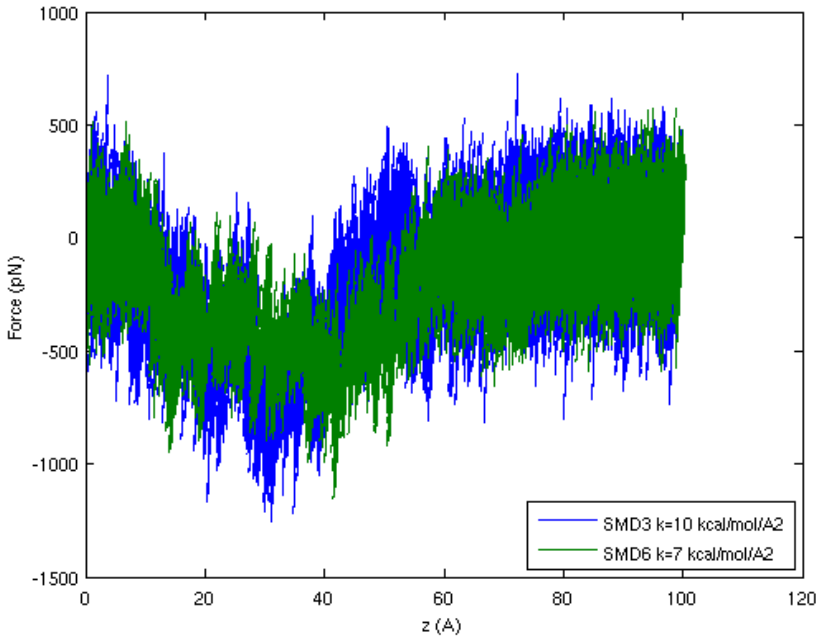

Figure A.2. The force applied to the peptides in SMD3 (blue) and SMD6 (green) as a function of change in z-coordinates of the SMD atom.

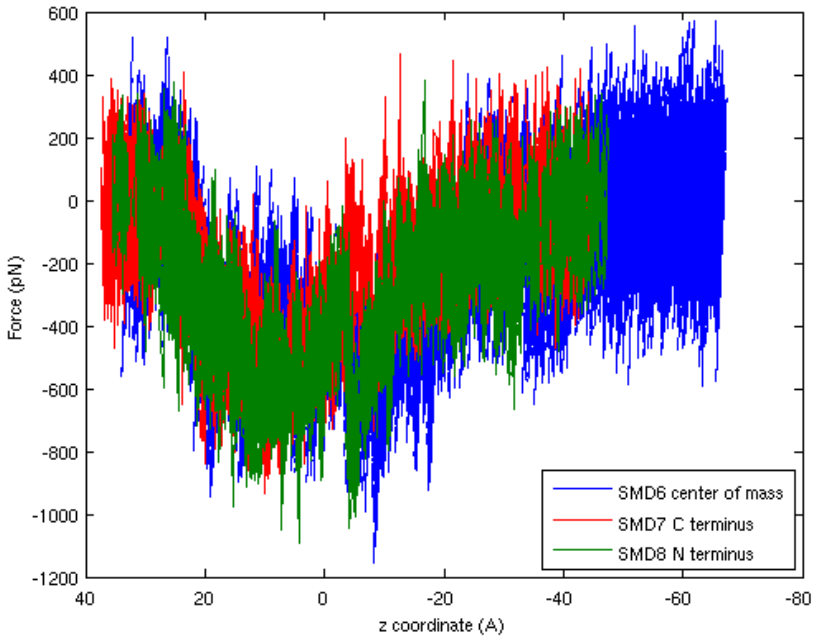

Figure A.3. The force applied to the peptides in the simulations SMD6 (center of mass, blue), SMD7 (C terminus, red), SMD8 (N terminus, green).

A.2. Membrane Uptake of a Modified BLIP Based Peptide

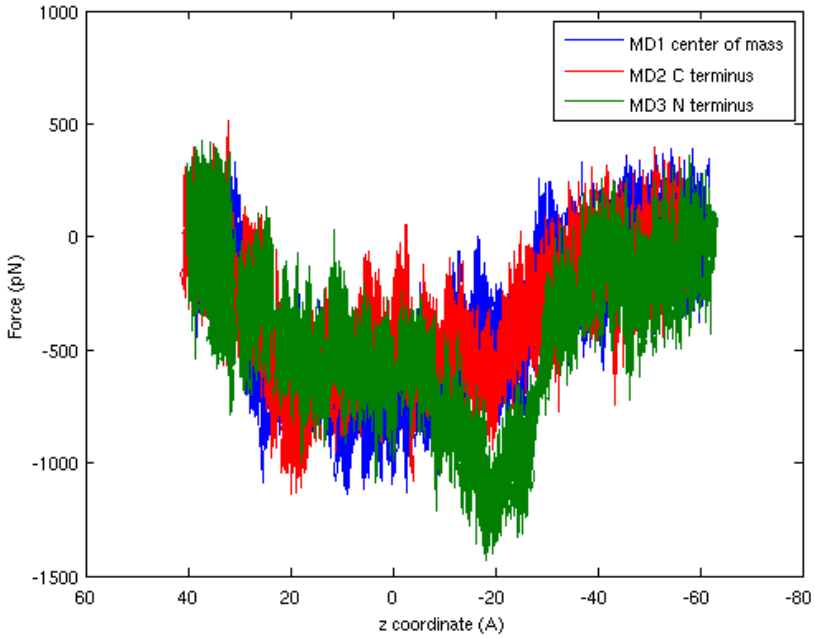

Figure A.4. The force applied to the peptides in the simulations MD1 (center of mass, blue), MD2 (C terminus, red), MD3 (N terminus, green).

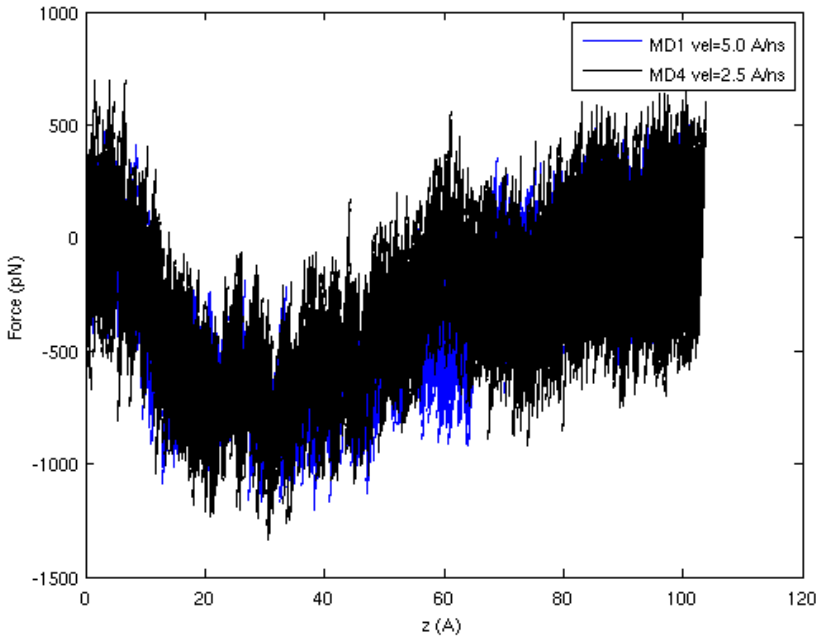

Figure A.5. The force applied in simulations MD1 (v = 5.0 Å/ns) (blue) and MD4 (v = 2.5 Å/ns) (black) on the peptides.

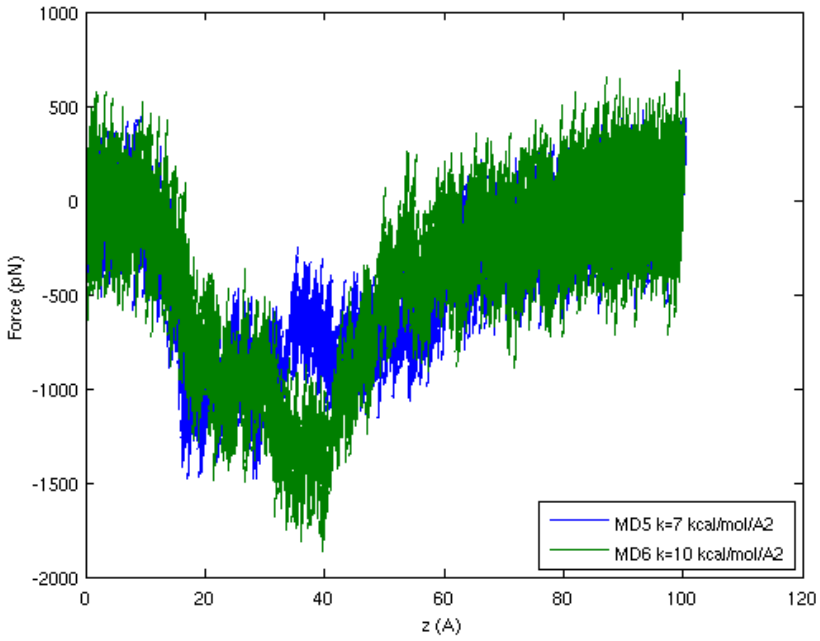

Figure A.6. The force applied to the peptides in MD5 (7 kcal/mol/Å^2) (blue) and MD6 (10 kcal/mol/Å^2) (green) as a function of change in z-coordinates of the SMD atom.

A.3. pVEC Results

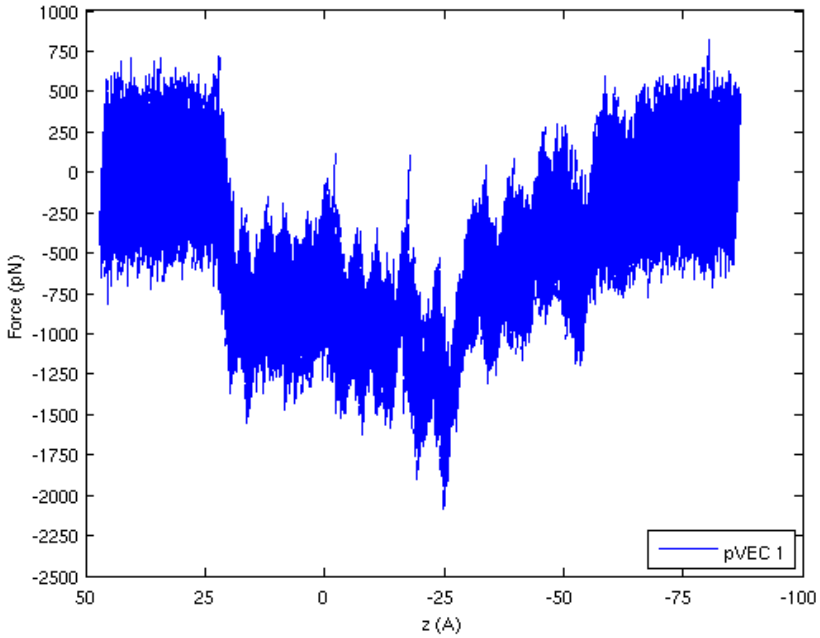

Figure A.7. The force applied to the pVEC 1 (original pVEC) in negative z direction.

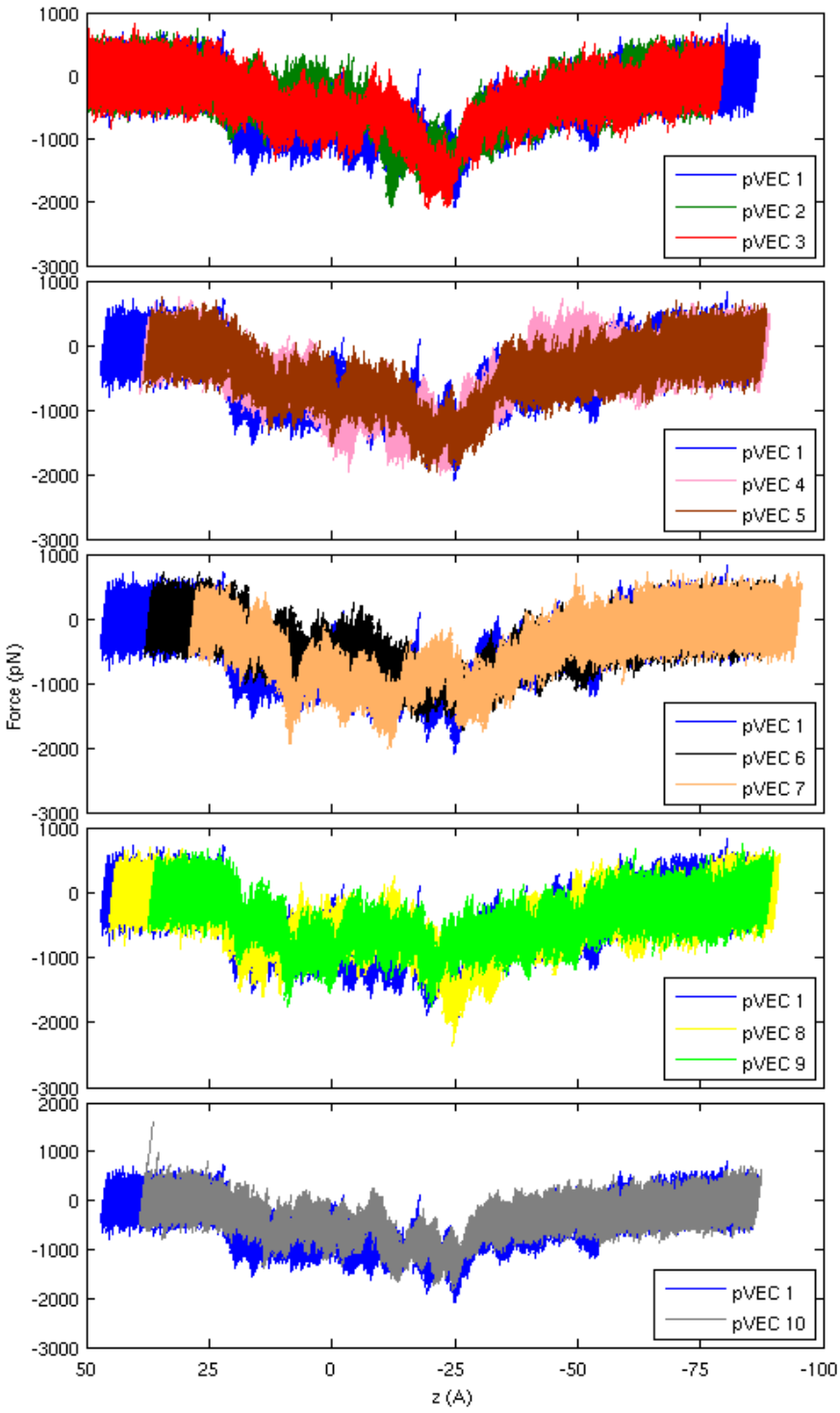

Figure A.8. The force applied to pVEC 1 (original pVEC), (a) pVEC 2 (L1A) and pVEC 3 (L2A) (b) pVEC 4 (I9A) and pVEC 5 (R10A) (c) pVEC 6 (S17A) and pVEC 7 (K18A) (d) pVEC 8 (retro-pVEC) and pVEC 9 (scramble pVEC) and (e) pVEC 10 (H14A).

APPENDIX B: THE VMD SCRIPTS

B.1. trial.tcl

```
resetpsf

package require psfgen

topology
/home/omur/Applications/toppar/top_all27_prot_lipid.inp

pdbalias residue HIS HSE

pdbalias atom ILE CD1 CD

segment A {

residue 1 LEU

residue 2 LEU

residue 3 ILE

residue 4 ILE

residue 5 LEU

residue 6 ARG

residue 7 ARG

residue 8 ARG

residue 9 ILE

residue 10 ARG

residue 11 LYS

residue 12 GLN
```

```
residue 13 ALA

residue 14 HSE

residue 15 ALA

residue 16 HSE

residue 17 SER

residue 18 LYS

}

coordpdb peptide.pdb A

writepsf newpeptide.psf

guesscoord

writepdb newpeptide.pdb
```

B.2. code.tcl

```
mol delete all

package require solvate

solvate newpeptide.psf newpeptide.pdb -o new_pep_sol -t 10

mol load psf new_pep_sol.psf pdb new_pep_sol.pdb

set all [atomselect top all]

$all set beta 0

set clash [atomselect top "resname TIP3 and same residue as
(within 2.8 of protein)"]

$clash set beta 1
```

```
set clashwater [atomselect top "name OH2 and beta > 0"]
set seglist [$clashwater get segid]
set reslist [$clashwater get resid]
mol delete all
package require psfgen
readpsf new_pep_sol.psf
coordpdb new_pep_sol.pdb
foreach segid $seglist resid $reslist {
delatom $segid $resid
}
writepdb pep_VdW.pdb
writepsf pep_VdW.psf
mol delete all
mol load psf pep_VdW.psf pdb pep_VdW.pdb
```

B.3. membrane_equilibrate.tcl

```
mol delete all
resetpsf
package require membrane
membrane -l POPE -x 50 -y 50
set all [atomselect top all]
$all moveby [vecinvert [measure center $all]]
```

```
$all writepdb centered.pdb

mol delete all

package require solvate

solvate membrane.psf centered.pdb -o membrane_water_TEMP -
minmax {{-24 -24 -80} {24 24 80}}

set all [atomselect top all]

$all set beta 0

set seltext "segid WT1 to WT99 and same residue as abs(z)
<10"

set sel [atomselect top $seltext]

$sel set beta 1

set badwater [atomselect top "name OH2 and beta > 0"]

set seglist [$badwater get segid]

set reslist [$badwater get resid]

mol delete all

#mol load psf membrane_water.psf pdb membrane_water.pdb

package require psfgen

readpsf membrane_water_TEMP.psf

coordpdb membrane_water_TEMP.pdb

foreach segid $seglist resid $reslist {

delatom $segid $resid

}

writepdb membrane_water.pdb
```

```
writepsf membrane_water.psf

#file delete membrane_water_TEMP.psf

#file delete membrane_water_TEMP.pdb

mol load psf membrane_water.psf pdb membrane_water.pdb
```

B.4. manipulation.tcl

```
mol load pdb finalsnapshot.pdb

mol load pdb created.pdb

package require psfgen

readpsf membrane_water.psf

coordpdb finalsnapshot.pdb

## created manually by save coordinates

readpsf created.psf

coordpdb peptidemanipulated.pdb

## created manually by save coordinates

writepdb manipulated.pdb

writepsf manipulated.psf

mol load pdb manipulated.pdb

set all [atomselect top all]

$all set beta 0

set clash [atomselect top "resname TIP3 and same residue as
(within 2.8 of protein)"]
```

```
$clash set beta 1

set clashwater [atomselect top "name OH2 and beta > 0"]

set seglist [$clashwater get segid]

set reslist [$clashwater get resid]

foreach segid $seglist resid $reslist {

delatom $segid $resid

}

writepdb memb_wat_pep.pdb

writepsf memb_wat_pep.psf

mol delete all

mol load pdb memb_wat_pep.pdb
```

B.5. count_water_in_membrane.tcl

```
puts "count_water_in_active_site {{molid top} {outputfile count_water_in_membrane.out}}"

puts "For Example"

puts "count_water_in_membrane top count_water_in_membrane.out \n"

proc count_water_in_membrane {{molid top} {outputfile count_water_in_membrane.out}} {

set selection ""

set selection "abs(z)<10 and water and name OH2"

set fid [open $outputfile "w"]
```

```
set total_frame [molinfo $molid get numframes]

for {set frame 0} {$frame < $total_frame} {incr frame} {

set sel1 [atomselect top $selection frame $frame]

set a [$sel1 get resid]

puts $fid [llength $a]

set a ""

}

close $fid

}
```

B.6. thickness_of_memb.tcl

```
puts "thickness_of_memb {{molid top} {outputfile thickness_of_memb.out}}"

puts "For Example"

puts "thickness_of_memb top  thickness_of_memb.out \n"

proc thickness_of_memb {{molid top} {outputfile thickness_of_memb.out}} {

set fid [open $outputfile "w"]

set total_frame [molinfo $molid get numframes]

for {set frame 0} {$frame < $total_frame} {incr frame} {

set sel [atomselect top lipid frame $frame]

set m [measure minmax $sel]

set z1 [lindex $m 0 2]
```

```
set z2 [lindex $m 1 2]

set r [expr $z2 - $z1]

puts $fid $r

}

close $fid

}
```

B.7. z_center_of_mass.tcl

```
puts "z_center_of_mass {{molid top} {outputfile
z_center_of_mass.out}}"

puts "For Example"

puts "z_center_of_mass top  z_center_of_mass.out \n"

proc z_center_of_mass {{molid top} {outputfile
z_center_of_mass.out}} {

set fid [open $outputfile "w"]

set total_frame [molinfo $molid get numframes]

for {set frame 0} {$frame < $total_frame} {incr frame} {

set sel [atomselect top "name CA" frame $frame]

set m [measure center $sel]

puts $fid $m

}

close $fid

}
```

APPENDIX C: THE MATLAB SCRIPTS

C.1. displacement_time.m

```
A=load('smdforces.out');
for i=1:length(A(:,1))
    B(i,1)          =          sqrt((A(i,2)-A(1,2))^2+(A(i,3)-
A(1,3))^2+(A(i,4)-A(1,4))^2);
end
plot((A(:,1)*2*10^(-6)),B(:,1))
xlabel('Time (ns)')
ylabel('Displacement (A)')
```

C.2. energy_coor.m

```
x=load('energy_profile');
Nonbond=x(:,5);
Total=x(:,6);
z=load('smdforces.out');
plot(abs(z(1:50.0050:end,4)),Total)
xlabel('z coordinate (A)')
ylabel('Interaction Energy')
```

C.3. energy_z.m

```
x=load('energy_profile');
Nonbond=x(:,5);
Total=x(:,6);
```

```
z=load('smdforces.out');
for i=1:length(z(:,1))
    B(i,1) = z(i,4)-z(1,4);
end
plot(abs(B(1:50.0050:end,1)),Total)
xlabel('z (A)')
ylabel('Interaction Energy')
```

C.4. energy_z_com.m

```
x=load('energy_profile');
Nonbond=x(:,5);
Total=x(:,6);
z=load('z_center_of_mass.out');
plot(z(:,3),Total)
xlabel('z coordinate (A)')
ylabel('Interaction Energy')
```

C.5. force_coor.m

```
x=load('smdforces.out');
plot(x(:,4),x(:,7));
xlabel('z coordinate (A)');
ylabel('Force (pN)');
```

C.6. force_coor_av.m

```
x=load('smdforces.out');
windowsize = 5000;
runningavgF=filter(ones(1,windowsize)/windowsize,1,x(:,7));
plot(x(:,4),runningavgF(:,1));
xlabel('z coordinate (A)');
ylabel('Force (pN)');
```

C.7. force_z.m

```
load smdforces.out;
A = smdforces;
for i=1:length(smdforces(:,1))
    B(i,1) = A(i,4)-A(1,4);
end
plot(abs(B(:,1)),A(:,7))
xlabel('z (A)')
ylabel('Force (pN)')
```

C.8. force_z_av.m

```
x=load('smdforces.out');
for i=1:length(x(:,1))
    B(i,1) = x(i,4)-x(1,4);
end;
windowsize = 5000;
runningavgF=filter(ones(1,windowsize)/windowsize,1,x(:,7));
plot(abs(B(:,1)),runningavgF(:,1));
xlabel('z (A)');
```

```
ylabel('Force (pN)');
```

C.9. force_z_com.m

```
x=load('smdforces.out');
z=load('z_center_of_mass.out');
plot(z(:,3),x(1:50.0001:end,7))
xlabel('z coordinate (A)');
ylabel('Force (pN)');
```

C.10. force_z_av_com.m

```
x=load('smdforces.out');
z=load('z_center_of_mass.out');
windowsize = 5000;
runningavgF=filter(ones(1,windowsize)/windowsize,1,x(:,7));
plot(z(:,3),runningavgF(1:50.0001:end,1));
xlabel('z coordinate (A)');
ylabel('Force (pN)');
```

C.11. thickness_of_memb.m

```
x=load('thickness_of_memb.out');
plot(((1:1:length(x))/1000*2),x)
xlabel('Time (ns)')
ylabel('Thickness of the membrane (A)')
```

C.12. water_coor.m

```
x=load('count_water_in_membrane.out');
y=load('smdforces.out');
plot(y(1:50.0007:end,4),x)
xlabel('z coordinate(A)')
ylabel('Number of water molecules in membrane')
```

C.13. water_z.m

```
x=load('count_water_in_membrane.out');
y=load('smdforces.out');
for i=1:length(smdforces(:,1))
    B(i,1) = y(i,4)-y(1,4);
end
plot(y(1:50.0007:end,1),x)
xlabel('z (A)')
ylabel('Number of water molecules in membrane')
```

C.14. water_z_com.m

```
y=load('count_water_in_membrane.out');
z=load('z_center_of_mass.out');
plot(z(:,3),y)
xlabel('z coordinate (A)')
ylabel('Number of water molecules in membrane')
```

C.15. work_coor.m

```
load smdforces.out;
ftemp = smdforces(:,7)/69.479;
fsum = 0;
v = -1*0.0000100;
dt = 20;
for i = 1:length(smdforces)
    fsum(i+1) = fsum(i) + ftemp(i)*v*dt;
    w(i) = fsum(i);
end
plot(abs(smdforces(:,4)),w)
xlabel('z coordinate (A)')
ylabel('Work (kcal/mol)')
```

C.16. work_z.m

```
load smdforces.out;
ftemp = smdforces(:,7)/69.479;
fsum = 0;
v = -1*0.0000100;
dt = 20;
for i = 1:length(smdforces)
    fsum(i+1) = fsum(i) + ftemp(i)*v*dt;
    w(i) = fsum(i);
end
A = smdforces;
for i=1:length(smdforces(:,1))
    B(i,1) = A(i,4)-A(1,4);
end
plot(abs(B(:,1)),w)
```

```
xlabel('z (A)')
ylabel('Work (kcal/mol)')
```

C.17. work_z_com.m

```
load smdforces.out;
ftemp = smdforces(:,7)/69.479;
fsum = 0;
v = -1*0.0000100;
dt = 20;
for i = 1:length(smdforces)
    fsum(i+1) = fsum(i) + ftemp(i)*v*dt;
    w(i) = fsum(i);
end
z=load('z_center_of_mass.out');
plot(z(:,3),w(1:50.0001:end))
xlabel('z coordinate (A)')
ylabel('Work (kcal/mol)')
```

REFERENCES

1. Wilke, M.S., A.L. Lovering, and N.C.J. Strynadka, "Beta-Lactam Antibiotic Resistance: A Current Structural Perspective", *Current Opinion in Microbiology*, Vol. 8, No. 5, pp. 525-533, 2005.

2. Babic, M., A.M. Hujer, and R.A. Bonomo, "What's New In Antibiotic Resistance? Focus On Beta-Lactamases", *Drug Resistance Updates*, Vol. 9, No. 3, pp. 142-156, 2006.

3. Ambler, R.P., "The Structure Of Beta-Lactamases", *Philosophical Transactions of the Royal Society of London Series B-Biological Sciences*, Vol. 289, No. 1036, pp. 321-331, 1980.

4. Bush, K., G.A. Jacoby, and A.A. Medeiros, "A Functional Classification Scheme For Beta-Lactamases And Its Correlation With Molecular-Structure", *Antimicrobial Agents and Chemotherapy*, Vol. 39, No. 6, pp. 1211-1233, 1995.

5. Lim, D., H.U. Park, L. De Castro, S.G. Kang, H.S. Lee, S. Jensen, K.J. Lee, and N.C.J. Strynadka, "Crystal Structure And Kinetic Analysis Of Beta-Lactamase Inhibitor Protein-II In Complex With TEM-1 Beta-Lactamase", *Nature Structural Biology*, Vol. 8, No. 10, pp. 848-852, 2001.

6. Henriques, S.T., M.N. Melo, and M.A.R.B. Castanho, "Cell-Penetrating Peptides And Antimicrobial Peptides: How Different Are They?", *Biochemical Journal*, Vol. 399, No. 1, pp. 1-7, 2006.

7. Yesylevskyy, S., S.-J. Marrink, and A.E. Mark, "Alternative Mechanisms for the Interaction of the Cell-Penetrating Peptides Penetratin and the TAT Peptide with Lipid Bilayers", *Biophysical Journal*, Vol. 97, No. 1, pp. 40-49, 2009.

8. Herce, H.D. and A.E. Garcia, "Molecular Dynamics Simulations Suggest A Mechanism For Translocation Of The HIV-1 TAT Peptide Across Lipid Membranes", *Proceedings of the National Academy of Sciences of the United States of America*, Vol. 104, No. 52, pp. 20805-20810, 2007.

9. Gupta, B., T.S. Levchenko, and V.P. Torchilin, "Intracellular Delivery Of Large Molecules And Small Particles By Cell-Penetrating Proteins And Peptides", *Advanced Drug Delivery Reviews*, Vol. 57, No. 4, pp. 637-651, 2005.

10. Morris, M.C., S. Deshayes, F. Heitz, and G. Divita, "Cell-Penetrating Peptides: From Molecular Mechanisms To Therapeutics", *Biology of the Cell*, Vol. 100, No. 4, pp. 201-217, 2008.

11. Eiriksdottir, E., K. Konate, U. Langel, G. Divita, and S. Deshayes, "Secondary Structure Of Cell-Penetrating Peptides Controls Membrane Interaction And Insertion", *Biochimica Et Biophysica Acta-Biomembranes*, Vol. 1798, No. 6, pp. 1119-1128, 2010.

12. Liu, L., Y. Fang, Q. Huang, and J. Wu, "A Rigidity-Enhanced Antimicrobial Activity: A Case For Linear Cationic Alpha-Helical Peptide HP(2-20) And Its Four Analogues", *Plos One*, Vol. 6, No. 1, pp. 714-719, 2011.

13. Mager, I., E. Eiriksdottir, K. Langel, S.E.L. Andaloussi, and U. Langel, "Assessing The Uptake Kinetics And Internalization Mechanisms Of Cell-Penetrating Peptides Using A Quenched Fluorescence Assay", *Biochimica Et Biophysica Acta-Biomembranes*, Vol. 1798, No. 3, pp. 338-343, 2010.

14. Magzoub, M., A. Pramanik, and A. Graslund, "Modeling The Endosomal Escape Of Cell-Penetrating Peptides: Transmembrane Ph Gradient Driven Translocation Across Phospholipid Bilayers", *Biochemistry*, Vol. 44, No. 45, pp. 14890-14897, 2005.

15. Jarver, P., I. Mager, and U. Langel, "In Vivo Biodistribution And Efficacy Of Peptide Mediated Delivery", *Trends in Pharmacological Sciences*, Vol. 31, No. 11, pp. 528-535, 2010.

16. Elmquist, A., M. Hansen, and U. Langel, "Structure-Activity Relationship Study Of The Cell-Penetrating Peptide pVEC", *Biochimica Et Biophysica Acta-Biomembranes*, Vol. 1758, No. 6, pp. 721-729, 2006.

17. Epand, R.M. and R.F. Epand, "Lipid Domains In Bacterial Membranes And The Action Of Antimicrobial Agents", *Biochimica Et Biophysica Acta-Biomembranes*, Vol. 1788, No. 1, pp. 289-294, 2009.

18. Joanne, P., C. Galanth, N. Goasdoue, P. Nicolas, S. Sagan, S. Lavielle, G. Chassaing, C. El Amri, and I.D. Alves, "Lipid Reorganization Induced By Membrane-Active Peptides Probed Using Differential Scanning Calorimetry", *Biochimica Et Biophysica Acta-Biomembranes*, Vol. 1788, No. 9, pp. 1772-1781, 2009.

19. Epand, R.M., S. Rotem, A. Mor, B. Berno, and R.F. Epand, "Bacterial Membranes as Predictors of Antimicrobial Potency", *Journal of the American Chemical Society*, Vol. 130, No. 43, pp. 14346-14352, 2008.

20. Soliman, W., S. Bhattacharjee, and K. Kaur, "Interaction of an Antimicrobial Peptide with a Model Lipid Bilayer Using Molecular Dynamics Simulation", *Langmuir*, Vol. 25, No. 12, pp. 6591-6595, 2009.

21. Davis, C.H. and M.L. Berkowitz, "Structure Of The Amyloid-Beta (1-42) Monomer Absorbed To Model Phospholipid Bilayers: A Molecular Dynamics Study", *Journal of Physical Chemistry B*, Vol. 113, No. 43, pp. 14480-14486, 2009.

22. de Planque, M.R.R., E. Goormaghtigh, D.V. Greathouse, R.E. Koeppe, J.A.W. Kruijtzer, R.M.J. Liskamp, B. de Kruijff, and J.A. Killian, "Sensitivity Of Single Membrane-Spanning Alpha-Helical Peptides To Hydrophobic Mismatch With A

Lipid Bilayer: Effects On Backbone Structure, Orientation, And Extent Of Membrane Incorporation", *Biochemistry*, Vol. 40, No. 16, pp. 5000-5010, 2001.

23. Wimley, W.C. and S.H. White, "Designing Transmembrane Alpha-Helices That Insert Spontaneously", *Biochemistry*, Vol. 39, No. 15, pp. 4432-4442, 2000.

24. Im, W. and C.L. Brooks, "Interfacial Folding And Membrane Insertion Of Designed Peptides Studied By Molecular Dynamics Simulations", *Proceedings of the National Academy of Sciences of the United States of America*, Vol. 102, No. 19, pp. 6771-6776, 2005.

25. Babakhani, A., A.A. Gorfe, J. Gullingsrud, J.E. Kim, and J.A. McCammon, "Peptide Insertion, Positioning, And Stabilization In A Membrane: Insight From An All-Atom Molecular Dynamics Simulation", *Biopolymers*, Vol. 85, No. 5-6, pp. 490-497, 2007.

26. Stepaniants, S., S. Izrailev, and K. Schulten, "Extraction Of Lipids From Phospholipid Membranes By Steered Molecular Dynamics", *Journal of Molecular Modeling*, Vol. 3, No. 12, pp. 473-475, 1997.

27. Kelkar, D.A. and A. Chattopadhyay, "Membrane Interfacial Localization Of Aromatic Amino Acids And Membrane Protein Function", *Journal of Biosciences*, Vol. 31, No. 3, pp. 297-302, 2006.

28. Tsai, C.-W., N.-Y. Hsu, C.-H. Wang, C.-Y. Lu, Y. Chang, H.-H.G. Tsai, and R.-C. Ruaan, "Coupling Molecular Dynamics Simulations With Experiments For The Rational Design Of Indolicidin-Analogous Antimicrobial Peptides", *Journal of Molecular Biology*, Vol. 392, No. 3, pp. 837-854, 2009.

29. Subbalakshmi, C., V. Krishnakumari, R. Nagaraj, and N. Sitaram, "Requirements For Antibacterial And Hemolytic Activities In The Bovine Neutrophil Derived 13-Residue Peptide Indolicidin", *Febs Letters*, Vol. 395, No. 1, pp. 48-52, 1996.

30. Falla, T.J., D.N. Karunaratne, and R.E.W. Hancock, "Mode Of Action Of The Antimicrobial Peptide Indolicidin", *Journal of Biological Chemistry*, Vol. 271, No. 32, pp. 19298-19303, 1996.

31. Wu, M.H., E. Maier, R. Benz, and R.E.W. Hancock, "Mechanism Of Interaction Of Different Classes Of Cationic Antimicrobial Peptides With Planar Bilayers And With The Cytoplasmic Membrane Of Escherichia Coli", *Biochemistry*, Vol. 38, No. 22, pp. 7235-7242, 1999.

32. Pimthon, J., R. Willumeit, A. Lendlein, and D. Hofmann, "Membrane Association And Selectivity Of The Antimicrobial Peptide NK-2: A Molecular Dynamics Simulation Study", *Journal of Peptide Science*, Vol. 15, No. 10, pp. 654-667, 2009.

33. Olak, C., A. Muenter, J. Andrae, and G. Brezesinskia, "Interfacial Properties And Structural Analysis Of The Antimicrobial Peptide NK-2", *Journal of Peptide Science*, Vol. 14, No. 4, pp. 510-517, 2008.

34. Lorenzo, A.C. and P.M. Bisch, "Analyzing Different Parameters Of Steered Molecular Dynamics For Small Membrane Interacting Molecules", *Journal of Molecular Graphics & Modelling*, Vol. 24, No. 1, pp. 59-71, 2005.

35. Levtsova, O.V., M.Y. Antonov, D.Y. Mordvintsev, Y.N. Utkin, K.V. Shaitan, and M.P. Kirpichnikov, "Steered Molecular Dynamics Simulations Of Cobra Cytotoxin Interaction With Zwitterionic Lipid Bilayer: No Penetration Of Loop Tips Into Membranes", *Computational Biology and Chemistry*, Vol. 33, No. 1, pp. 29-32, 2009.

36. Pal, S., G. Milano, and D. Roccatano, "Synthetic Polymers And Biomembranes. How Do They Interact?: Atomistic Molecular Dynamics Simulation Study Of PEO In Contact With A DMPC Lipid Bilayer", *Journal of Physical Chemistry B*, Vol. 110, No. 51, pp. 26170-26179, 2006.

37. Allen, W.J. and D.R. Bevan, "Steered Molecular Dynamics Simulations Reveal Important Mechanisms in Reversible Monoamine Oxidase B Inhibition", *Biochemistry*, Vol. 50, No. 29, pp. 6441-6454, 2011.

38. Wei, C. and A. Pohorile, "Permeation Of Nucleosides Through Lipid Bilayers", *Journal of Physical Chemistry B*, Vol. 115, No. 13, pp. 3681-3688, 2011.

39. Crooks, G.E., "Entropy Production Fluctuation Theorem And The Nonequilibrium Work Relation For Free Energy Differences", *Physical Review E*, Vol. 60, No. 3, pp. 2721-2726, 1999.

40. De Fabritiis, G., P.V. Coveney, and J. Villa-Freixa, "Energetics Of K+ Permeability Through Gramicidin A By Forward-Reverse Steered Molecular Dynamics", *Proteins-Structure Function and Bioinformatics*, Vol. 73, No. 1, pp. 185-194, 2008.

41. Karplus, M. and J.A. McCammon, "Molecular Dynamics Simulations Of Biomolecules ", *Nature Structural Biology*, Vol. 9, No. 10, pp. 788-798, 2002.

42. Foloppe, N. and A.D. MacKerell, "All-Atom Empirical Force Field For Nucleic Acids: I. Parameter Optimization Based On Small Molecule And Condensed Phase Macromolecular Target Data", *Journal of Computational Chemistry*, Vol. 21, No. 2, pp. 86-104, 2000.

43. Kale, L., R. Skeel, M. Bhandarkar, R. Brunner, A. Gursoy, N. Krawetz, J. Phillips, A. Shinozaki, K. Varadarajan, and K. Schulten, "NAMD2: Greater Scalability For Parallel Molecular Dynamics", *Journal of Computational Physics*, Vol. 151, No. 1, pp. 283-312, 1999.

44. Phillips, J.C., R. Braun, W. Wang, J. Gumbart, E. Tajkhorshid, E. Villa, C. Chipot, R.D. Skeel, L. Kale, and K. Schulten, "Scalable Molecular Dynamics With NAMD", *Journal of Computational Chemistry*, Vol. 26, No. 16, pp. 1781-1802, 2005.